1. ***To supplement Attachment B, please explain how SROG will monitor the pipeline between the Little Willow Facility and well DJS 2-14 to prevent leaks and/or spills.***
    a. ***Pipeline monitoring measures have been provided in Attachment K (pg. 44) and attachment P (pg. 52).***
        i. ***Pressure relief valve installation to protect injection Flowline ("FL") from over-pressuring.***
        ii. ***Portions of the injection FL that will be above ground will be dressed with insulation and heat tracing components to help avoid line freezing during winter months.***
        iii. ***The entire FL easement and wellhead will be visually inspected daily.***
    b. ***Additional monitoring measures (Supplemental):***
        i. ***Installation of a 2nd flow meter at the DJS 2-14 well site, just upstream of the wellhead. This will be a redundant check meter that will be compared to the master flow meter at the Little Willow Facility on a daily basis. If significant rate/volume discrepancies exist, various system diagnostics will be performed in order to determine the issue(s). Flow meters will be calibrated on a monthly basis.***
        ii. ***Routine static pressure tests will be performed on the injection FL to ensure integrity (test frequency, test duration, and maximum test pressure TBD).***

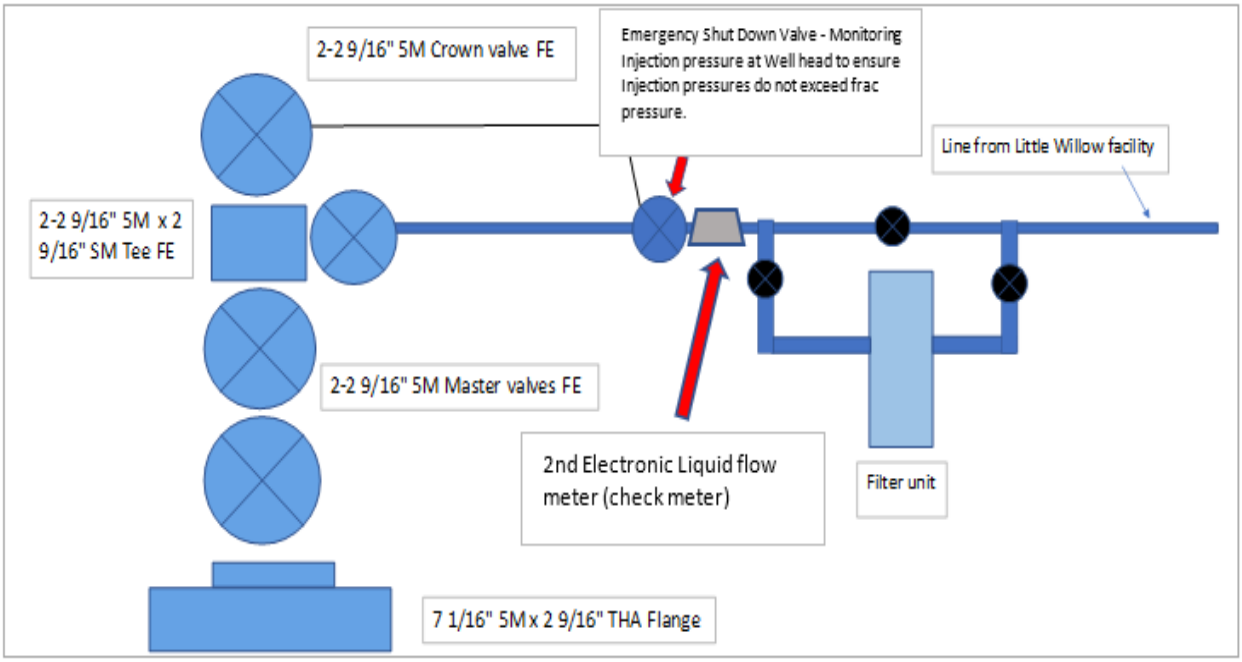

2. ***The application states on page 10 that a complete water flow testing and water analysis was done for two existing wells prior to developing the Willow Field. Data are presented for one of these two wells. To supplement Attachment E, provide the name, location, or value of Total Dissolved Solids for this other well.***
   The statement referenced above is on page 12 of the application. The other shallow water well tested prior to developing the Willow Field is the Semon water well, it was originally drilled for Ralph Crawford in November of 1992. It is located in T 8N- R 4W section 3, SW/4 of NE/4. It has Total Dissolved Solids measured at 288 mg/L. The location and ground water chemistry analysis for this well are shown below in Figure 2-1 and Table 2:

Figure 2-1

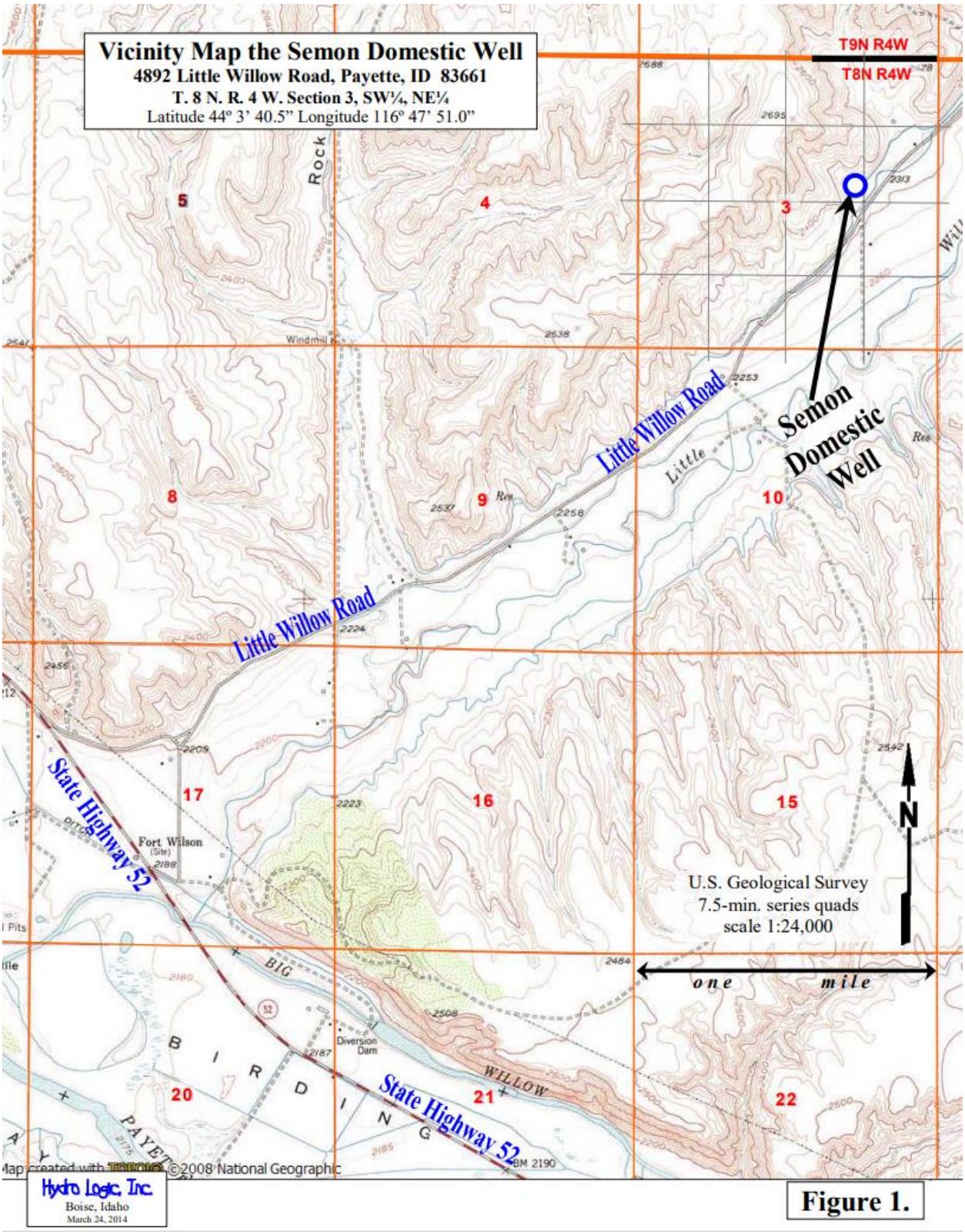
Vicinity Map the Semon Domestic Well
4892 Little Willow Road, Payette, ID 83661
T. 8 N. R. 4 W. Section 3, SW¼, NE¼
Latitude 44° 3' 40.5" Longitude 116° 47' 51.0"
T9N R4W
T8N R4W
Little Willow Road
Semon Domestic Well
State Highway 52
Fort Wilson
BIG
BIRDING
WILLOW
Diversion Dam
U.S. Geological Survey
7.5-min. series quads
scale 1:24,000
one mile
N
©2008 National Geographic
Hydro Logic, Inc.
Boise, Idaho
March 24, 2014
Figure 1.

Table 2 - Ground Water Chemistry of Semon Domestic Well

Laboratory Analyses	Results (in mg/L unless noted) Sampled at a flow rate of 23 gallons / minute
Alkalinity	228
Aluminum (total)	<0.10
Arsenic	<0.003
Barium	<0.05
Boron	<0.10
Calcium	41.9
Chloride	9
Fluoride	0.31
Iron (dissolved)	0.09
Iron (total)	0.09
Magnesium	22.1
Manganese (dissolved)	0.11
Methane	0.0041
Nitrate (as N)	<0.2
Potassium	4.3
Selenium	<0.005
Silica	42.6
Sodium	36.3
Sulfate	42
Total Dissolved Solids	288
VOC's	none detected
Radiology (in pCi/L unless noted)	
Gross Alpha	<3
Gross Beta	12 ± 2.3
Uranium pCi/L (µg/L)	<0.67 (<1)
Adjusted Gross Alpha	<2.33
Field Measured (by Hydro Logic, Inc.) **Parameters**	
Field Conductivity (µS)	493.5
Field Dissolved Oxygen	+0.02
Field Odor (describe)	medium H_2S
Field O.R.P. (mV)	-169.6
Field pH (S.U.)	8.06
Field Sand Production (describe)	none
Field Taste (describe)	minor sulfur taste
Field Temperature (°F)	64.8
Field Visible Gas (describe)	none
Samples collected by Hydro Logic, Inc. on February 19, 2014 Analyses by Analytical Laboratories, Boise, ID.	

3. ***To clarify Attachment E, explain whether field blanks, laboratory duplicates, or other QA samples were taken for the water quality analysis performed at the "Auxier well.".***

   Duplicate water samples were taken in the field during the sampling of both the Auxier and Semon domestic water wells. All samples were collected near the end of the flow testing phases. All chain of custody, filtering, and preservation protocols were observed and the original set of samples for each well were analyzed for a suite of analytes recommended by the Idaho Department of Environmental Quality. The original samples were transported directly from the field to Analytical Laboratories, Inc., which company performed the chemical analyses. The duplicate samples were maintained in refrigerated storage at Hydro Logic, Inc. until the laboratory analyses were successfully completed and reviewed.

4. ***To clarify Attachment E (regarding the identification of USDWs), share any available information regarding the use of the aquifer in the turbidite sands situated below the Pierce Gulch Aquifer. If applicable, provide information on how this water is or has been used, and whether there are any wells located within the project area.***

   The only wells in the project area that have been drilled deep enough to see the sands below the Pierce Gulch Aquifer have been oil and gas exploration wells. <u>None</u> of these wells have been utilized for fresh water or irrigation. Some of these wells have perforated and tested those sands for potential oil and gas production. Those results are addressed in #5 below.

5. ***To supplement Attachment E, provide any previously-available water quality information on groundwater held within the turbidite sands situated between the Pierce Gulch Aquifer and the Willow Sands.***

   There are six known wells in the greater project area that have sampled water from the sands between the Pierce Gulch Aquifer and the Willow Sands, found typically between 1500' and 2000' below ground level. All these wells were drilled as exploratory oil and gas tests. The water analyses for these wells are provided in the electronic folder in folder 5. An Index Map (Figure 5-1) showing the location of these wells and a Summary Table (Figure 5-2) listing the wells sampled are below:

Figure 5-1: ***Index Map for Wells Sampling Water from Turbidite Sands at 1500'-2000' BGL***

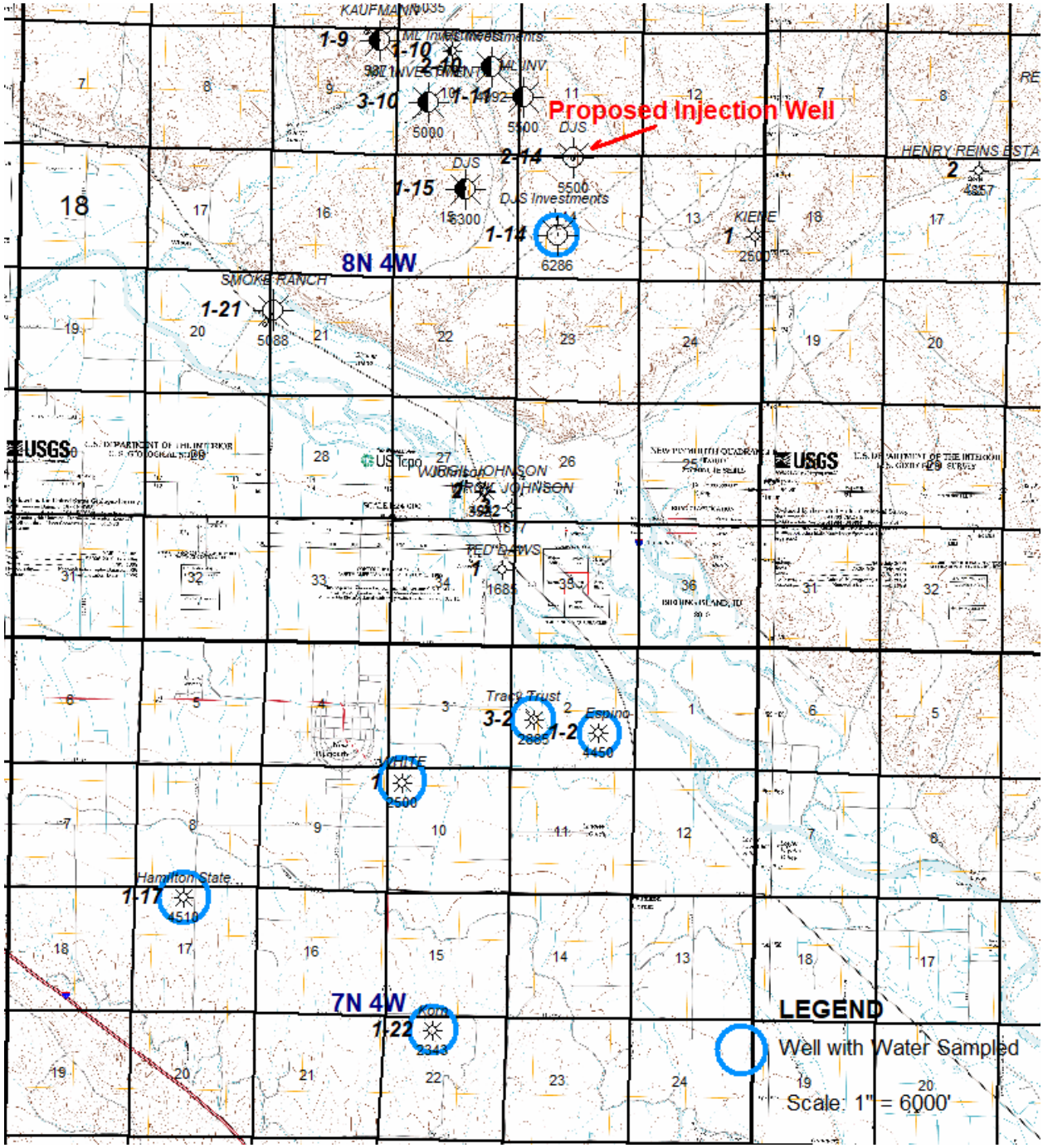

Water Test Analysis Table – Turbidite sands (approx 1,500' – 2,000')

Location (T-R-S)	Well Name	Date Sampled	Zone	Sample Depth	Chlorides (mg/L)	TDS (mg/L)	Comments
7N-4W-17	Hamilton State 1-17	5/20/10	3	1875' – 1,880'	50	1,008	Zone 3 flow tested gas at 200 – 1,380 MCFD. The measured chlorides of 50 are significantly less than the typical chloride range that is seen in the area. Suspect that the water produced during this test is essentially the condensation of water from the gas stream. See flow test reports.
7N-4W-17	Hamilton State 1-17	5/15/10	2	1,926'-1,934'; 1,937'-1,947'	500	1,550	Zone 2 would not flow, but had gas shows during swabbing operations. See work report showing swab activity.
7N-4W-17	Hamilton State 1-17	5/14/10	1	1,964'-1972'	500	1,789	Zone 1 would not flow, but had traces of gas during swabbing operations. See work reports showing swab activity.
7N-4W-17	Hamilton State 1-17	5/14/10	1	1,964'-1972'	350	1,427	Zone 1 would not flow, but had traces of gas during swabbing operations. See work reports showing swab activity. *Note: This is 1 of 2 water samples taken from this completion in zone 1.*
7N-4W-22	Korn 1-22	10/7/10	2	1,878' – 1900'; 2,078' – 2100'	450	1,192	Zone 1 was completed at 2,113' – 2,120' but did not flow and was not swab tested. No fluid samples were taken, and the well was plugged back to zone 2. Zone 2 flow tested gas but appeared to be a limited reservoir size or was damaged, etc. Initial test rates ranged from 10 MCFD – 469 MCFD. See flow test report.
7N-4W-2	Tracy-Trust 3-2	08/17/10	2	2,275' – 2,297'	850	2,149	Subsequent flow test with commingled perfs (1,496' – 2,297') tested gas at 10 MCFD – 500 MCFD.
7N-4W-2	Espino 1-2	5/12/10	3	1,608' – 1,614'	250	679	Flow test well at 50 MCFD – 300 MCFD.
7N-4W-2	Espino 1-2	5/12/10	3	1,608' – 1,614'	1,500	3,301	Flow test well at 50 MCFD – 300 MCFD. *Note: This is 1 of 2 water samples taken from this completion in zone 3.*
7N-4W-2	Espino 1-2	5/6/10	2	1,766' – 1787'	700	2,133	Swab test well with good gas shows. See work report showing swab activity.
8N-4W-14	DJS 1-14	11/21/10	1	1,530' – 1,539'	370	897	No flow test data available. Core data taken from this interval describes several cores exhibiting bright yellow-green fluorescence.
7N-4W-10	White 1-10	10/02/10	2	1,880' – 2,012'	1,550	5,998	Zone 2 flow tested at 10 MCFD – 500 MCFD.

Fig. 5-2: Summary Table of Wells that Sampled Water from Turbidite Sands

6. ***To Supplement Attachment G, provide calculated or estimated porosity and permeability data for the Chalk Hills claystone.***

   a. ***The Chalk Hills Formation section in the DJS 2-14 wellbore, extends from 2,380' – 4,910' TVD. The most reliable data source that is available to determine both porosity and permeability within this shale/claystone section can be evaluated by viewing the core data that was obtained on 9/24/14 during the drilling of the DJS 2-14. Although core data can be adequate for determining various rock characteristics, SWC's , in general can often give slightly inflated results due to the nature in which they are recovered. At times, some shattering can occur while extracting the core and higher than normal permeability and porosity values are recorded.***

      A 3rd party service company was hired and extracted side wall cores (SWC's) at various depths within the lower portion of the Chalk Hills Formation just above the Basalt section. Cores were also taken within the Willow Sands between 5,200' and 5,400' respectively. A core analysis was performed which provided several rock and fluid characteristics for each sample including the lithology description, probable production, a calculation of rock permeability (K), porosity (POR), and fluid saturations for each sample. The claystone/shale samples exhibit permeability values that are considered to be very "tight" and virtually non-permeable (low perm denoted by analysis) compared to the sandstone sampled within the Willow sand members. See Fig. 6-1 and Fig. 6-2 below comparing core data from the Chalk Hills Claystone section as well as the Willow sand sections (Full SWC Analysis attached – Folder #6 in Electronic files .) It is imperative to note that the core data in Fig.1 are cores that were taken in a silty shale section above the Basalt and do have some slight values of porosity and permeability. Qualitatively, open hole log characteristics above 4,299' to 2,380' exhibit classic non-permeable, low porosity shale responses (see Fig.4). For example: The Gamma Ray curve in the Chalk Hills section compared to the Willow Sand sections clearly show a lithology change (1-2 division shift). Typically, nonlaminated and non dispersed shales will read higher gamma counts (gAPI) than clean sandstones. Also, it is evident that there is virtually no invasion profile or mud cake filtrate throughout the Chalk Hills Formation within this depth range, which can be used to infer permeability (qualitative). The caliper readings throughout this section suggest that the hole is consistently in gauge or slightly washed out. Compared to the Willow Sand member, where there are multiple areas of strong invasion as well as mud cake (See Fig.6-3). See log sections below, comparing the invasion profiles and mud cake between the two sections (Chalk Hills and Willow Sands).

Core Data

Chalk Hills Formation - Shale / Claystone Porosity and Permeability data

Fig.6-1

Depth	Porosity %	Permeability (md)
4,303’	11.6	0.012
4,304’	11.5	0.013
4,307’	11.5	0.012
4,316’	10.9	0.011

Note: A total of 61 SWC’s were taken. The table above represents a small sample size (4) of core data within the Chalk Hills Formation just above the Basalt section.

Willow Sand Formation – Sandstone Porosity and Permeability data

Fig.6-2

Depth	Porosity %	Permeability (md)
5,213’	31.7	3,250
5,335’	30.8	2,500
5,337’	31.0	3,100
5,339’	31.0	3,500

Willow Sand- Log Section Example

Fig.6-3

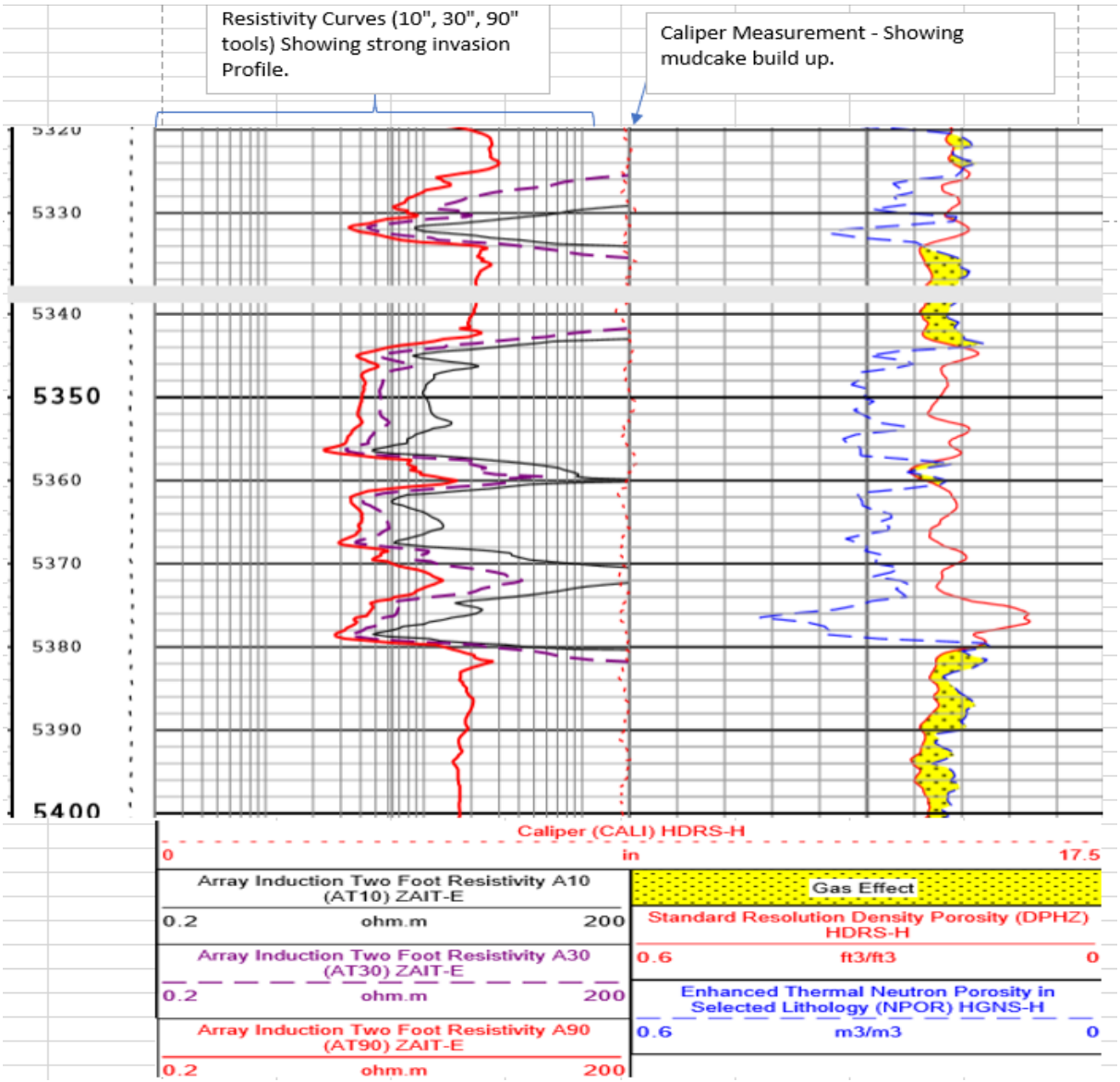

Chalk Hills Formation – Log Section Example

Fig.6-4

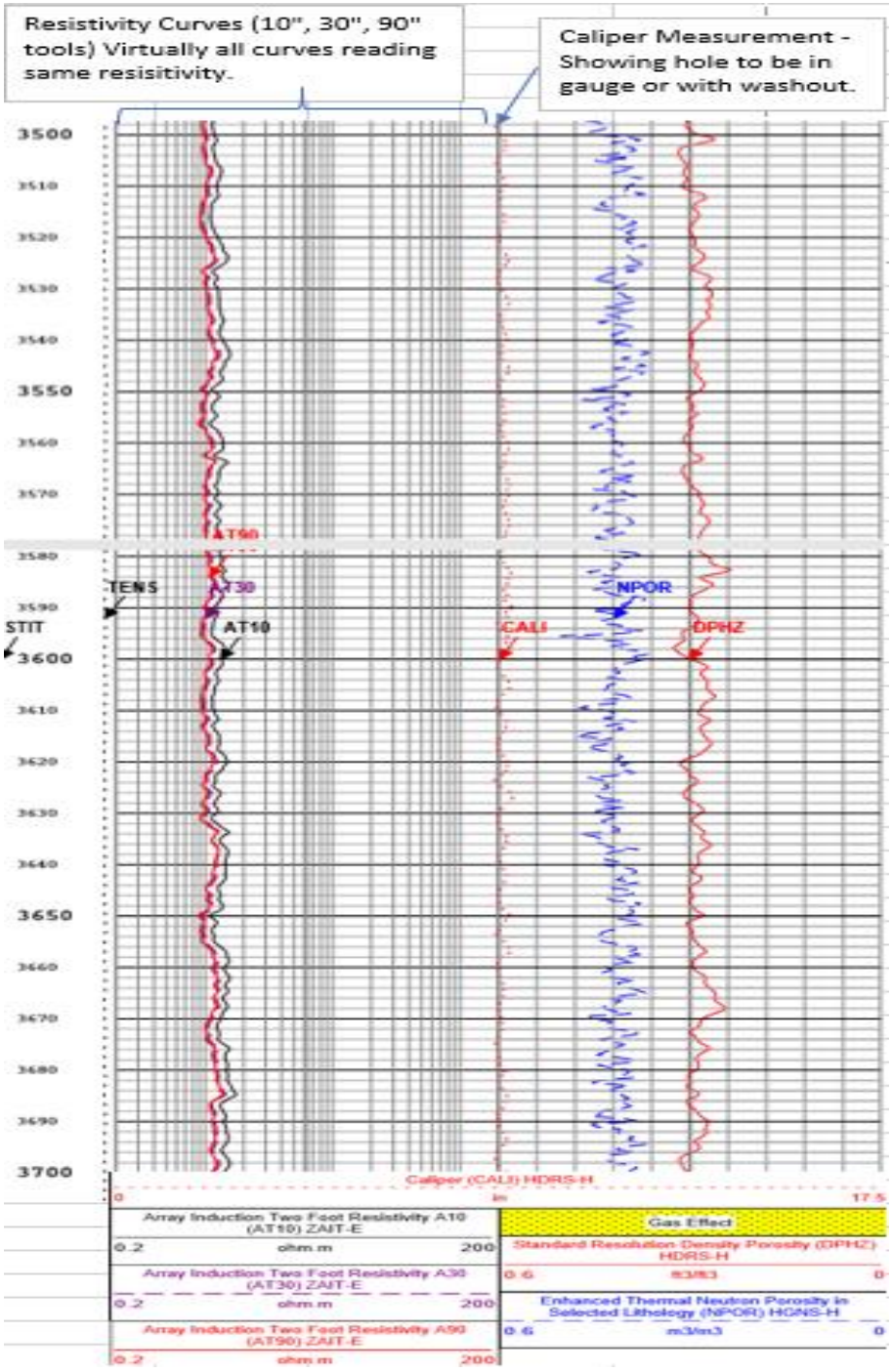

NOTE: The Chalk Hills log section above (200') should be fairly representative of the entire section itself. There is a minimum of 2,000' of shale/claystone above the Willow Sands that have the same consistent log characteristics in terms of the lithology nature, invasion profile, and mud cake.

7. ***To supplement Attachment G, compare the sealing nature of faults across the region to the faults identified near the proposed injection zone. For example, are there faults with similar lithologies, ages, or degrees of offset in the general vicinity? Is there known information regarding possible diagenetic sealing? If this information is not available, please indicate as such.***

   Small-scale syn-depositional faults as observed at the Willow Field are extremely common in the local area and throughout the basin. They can be observed in the subsurface with 3-D seismic and in outcrop locally and throughout the basin. There are literally hundreds of these small faults in the subsurface of the Western Snake River Plain of SW Idaho and SE Oregon. It is important to note that these are not Faults of Concern as defined in the UIC-NTW Final Work Product.

   A very large number of these types of faults observable in outcrops exhibit sealing behavior. Two of the most common sealing mechanisms are clay smear and silica cementation. Examples of both types are presented below, with outcrop photographs and discussion.

   a. ***Clay Smear: Clays are the dominant minerals in the widespread claystones found throughout the basin, above, below and often interbedded within the sandstones. They are very ductile minerals and are often drug along these extremely slow-moving, creeping type of sedimentary normal faults. They often form an extensive, relatively uniform sheet along a fault surface from a few inches to a few feet thick.***

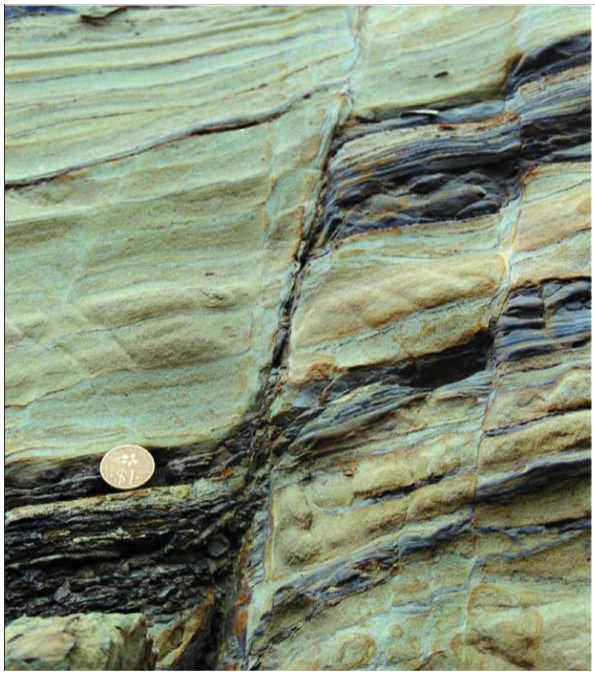

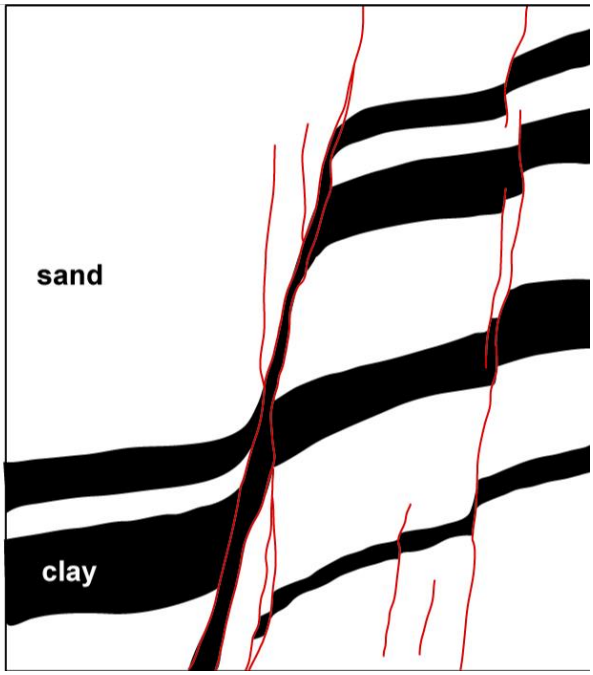

Fig. 7-1: Very small-scale example showing dark clay smearing along normally faulted sandstones, downthrown block on left
Fig. 7-2: Outcrop Along Little Willow Creek, Idaho - showing clay smear in normal fault

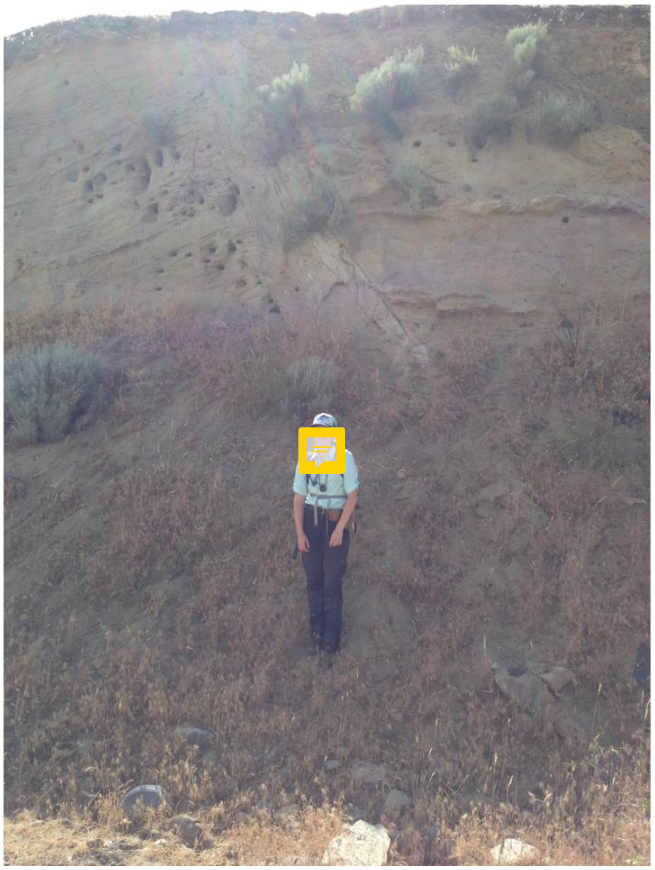

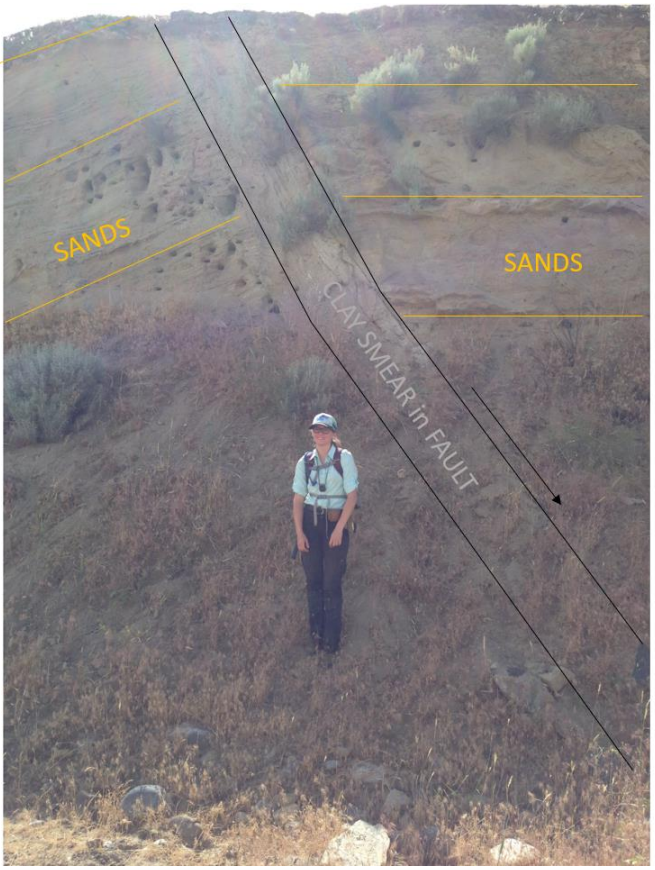

This picture shows a normal fault with the downthrown block on the left, graduate student provides scale. The fault zone is occupied by a clay smear approximately 2.5 feet thick. Sands on the upthrown block on the left are dipping to the left at approximately 20 degrees, the sandstones in the downthrown block on the right are flat lying. (photograph courtesy of Dr. Spencer Wood, Emeritus professor of geology and geophysics, Boise State University, personal communication 2020).

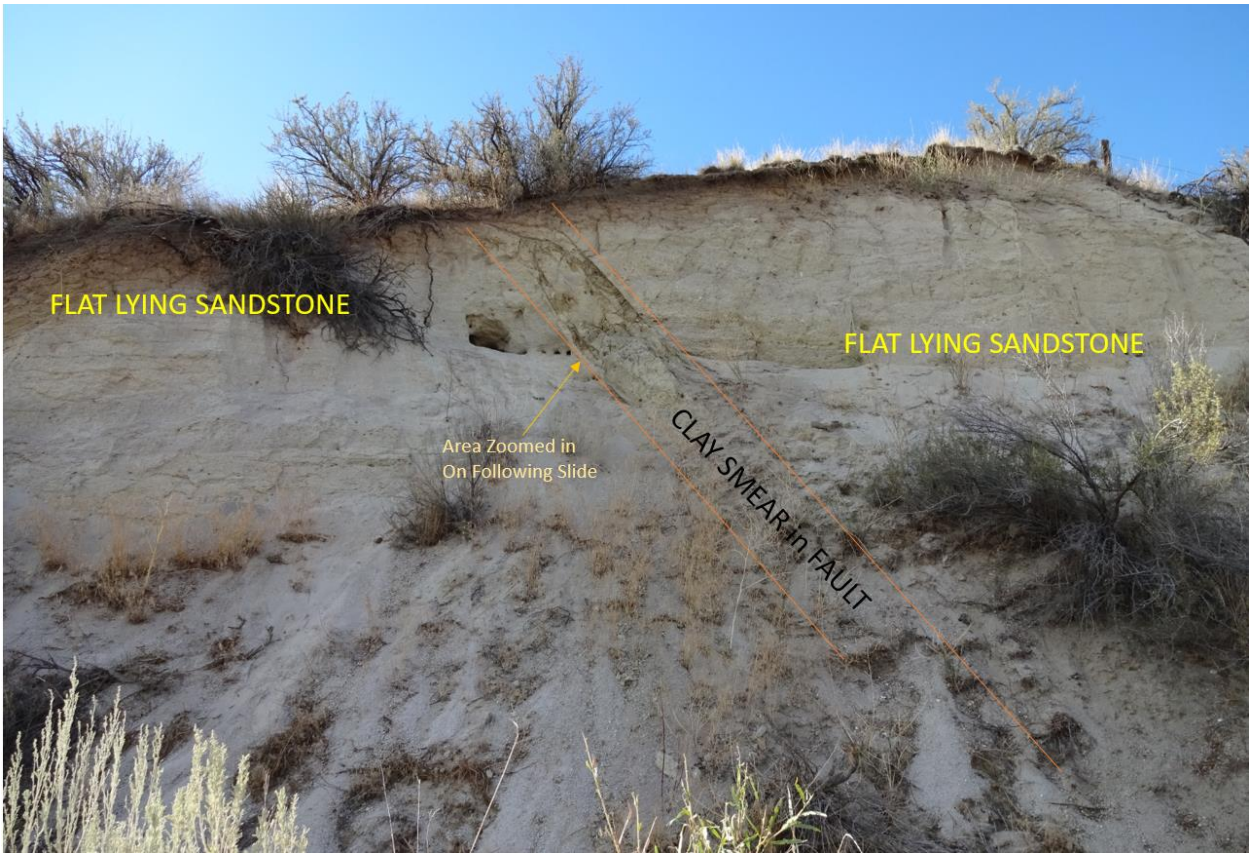

Fig. 7-3: Outcrop SE of Willow Field, Idaho, Showing Clay Smear in Normal Fault (Photograph by D. Smith, on field trip led by Dr. Wood, 2015)

Another example of clay smear occupying a normal fault. In this instance the sands are flat lying on both sides of the fault, which is downthrown to the right. The clay smear is approximately 2 feet thick. Note the arrow in the center of the photograph, a closeup view of the clay smear within the fault is shown in the next figure. Note that some layers of the high porosity sands on either side of the fault are very friable, enough that birds have excavated small nest holes. However, the sands are competent and consolidated enough to form a small but sheer cliff face. This is a physical example that the sand beds are disposed to shear when exposed to a gradual extensional force, and that underlying claystones will bend and smear along the fault plane.

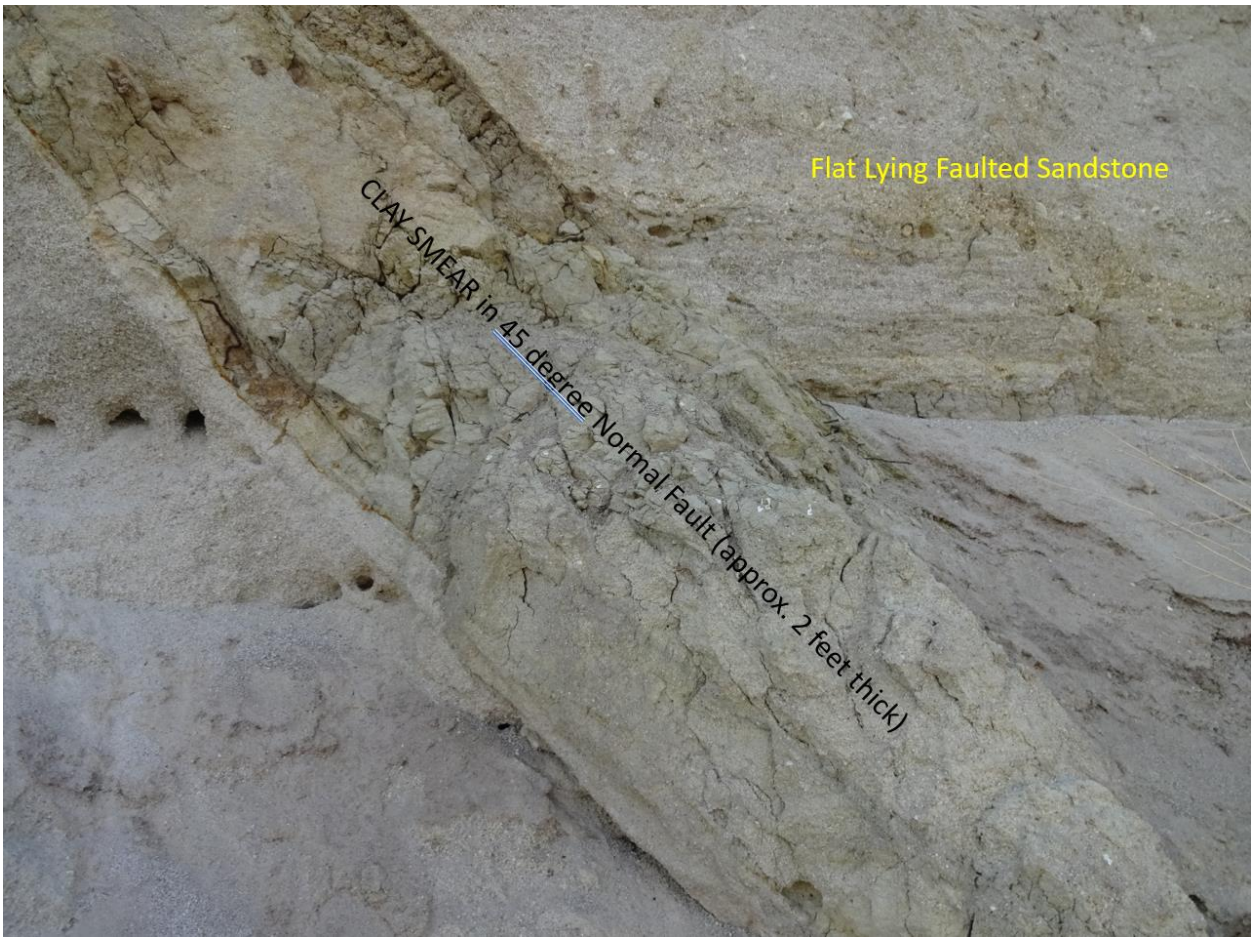

Fig. 7-4: Closeup view of the Clay Smear shown in outcrop on Fig 7-3 (Photograph by D. Smith, on field trip led by Dr. Wood, 2015)

Note that the weakly consolidated sandstones on either side of the fault are flat lying. The clay layers composing the clay smear are aligned parallel with the fault plane at 45 degrees.

One of the most logical explanations for this phenomenon is discussed in a paper provided in the digital folder 7 (Egholm et al, GEOLOGY, 2008). Simply expressed, in normal faults the sandstones tend to shear and the claystones tend to bend, as they are ductile. Over geologic time, as the downthrown block very gradually slides into the basin, the clays bend and become entrained within the plane of the fault.

More specifically, from Egholm et al, GEOLOGY, 2008, pages 787-788:

A MOHR-COULOMB FRAMEWORK

The Mohr-Coulomb criterion for failure of granular material relates the failure plane shear stress, σ_s, to normal stress, σ_n:

$$\sigma_s = \tan(\varphi)\sigma_n + c, \quad (2)$$

where φ is the angle of internal friction and c is cohesion. For any critical stress precisely satisfying the Mohr-Coulomb criterion, shear failure occurs on planes parallel to the failure plane angle (Mandl, 2000) (Fig. 2D):

$$\theta = 45° + \varphi/2. \quad (3)$$

Generally, $\varphi > 30°$ in sands, and consequently, for normal faults (where σ_3 is horizontal), $\theta > 60°$. Shale and clay generally have smaller friction angles than sands (e.g., Wood, 1990). Thus, under conditions of normal faulting, failure plane angles of sand and shale differ by as much as 25°, particularly when bedding-induced fabric is considered (Arch et al., 1988).

According to Mohr-Coulomb theory, a fault intersecting a bed of lower friction angle will refract to a shallower orientation with respect to σ_3, creating a "contractional" bend. Movement on a surface with a contractional bend leads to an increase in mean stress along the fault plane within the low-friction-angle material, and a decrease in the high-friction-angle material. For the case of a layered clay-sand package, stress gradients produced by progressive fault slip will promote granular flow of the clay into the low-mean-stress fault segments between bridging sands. Because of the requirement for flow along failure planes set

b. Silica Cementation: Another phenomenon commonly observed near faults in southern Idaho is silica cementation of sandstones proximal to and within fault zones. Several examples are presented below.

Boise Sandstone – Boise, Idaho sits near the eastern margin of the WSRP. Numerous northwest to southeast trending older inactive down to the basin normal faults are exposed at the surface in the Boise area (Wood, 2004 USGS Open File report 2004-1222, map on pg. 102). The local Boise Sandstone is heavily cemented by silica proximal to and extending several hundred feet away from faults.
As Burnham, USGS (1985) explains on page 8 discussing these sands: "These silica cemented sandstones in the Boise foothills area always occur within 2000 ft (700 m) of the major fault zones. Cementation is attributed to the percolation of geothermal water, bearing dissolved silica, into the permeable sand layers when they were still confined as aquifers within the less permeable siltstone section. As thermal ground waters migrated away from the faults, they cooled and precipitated silica in the voids of the arkosic sands."
(Copies of the papers referenced are included in digital folder 7)

Figure 7-5: Silica cemented Chalk Hills sandstones adjacent to fault, 2 mi. SW of Adrian, OR on west flank of WSRP. Photo courtesy of Mark Barton, Idaho Geological Survey, 2020.

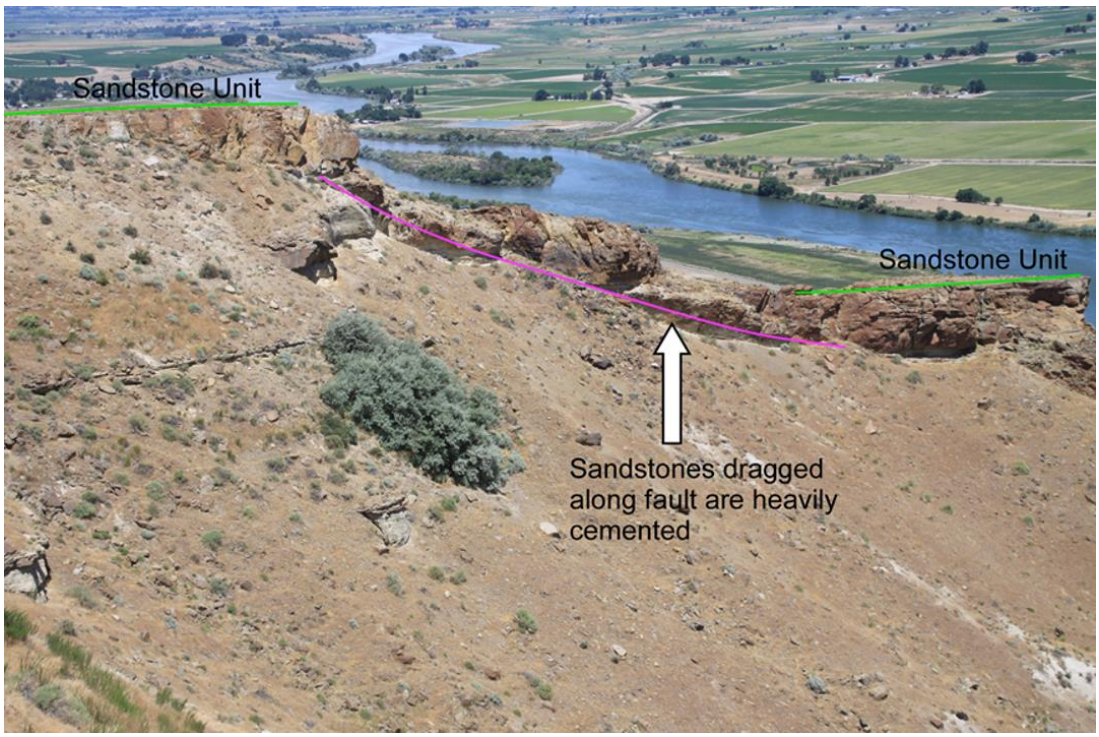

Figure 7-6: Photograph of silica cemented very small throw fault near Marsing Idaho. Note that the silica in the fault is more resistant to weathering, and stands out in relief relative to the wind eroded sands on either side of the fault. D. Smith, 2013 on field trip led by Dr. Wood.

On the following page are two pictures of silica cemented sandstones along a fault trace in the Lower Chalk Hills Fm. (Fig. 7-7 & 7-8) Location is near the confluence of Little Willow Creek and Alkali Creek, about 10 miles due east of the proposed injection well. The sands a short distance away from the fault are friable and erode easily forming a slope, the silica cemented sands adjacent to and along the fault are resistant to erosion and form an extended ridge marking the trace of the fault (fig. 7-7). Figure 7-8 is an outcrop view of the dipping silica cemented sands, notebook for scale. (Dr. S. Wood, 2020, personal communication)

***Figure 7-7**: (above, looking SW) Ridge in middle distance is fault trace with silica cemented Lwr. Chalk Hills sandstones forming ridge. **Figure 7-8**: (below) is outcrop view of the SW dipping cemented Lwr. Chalk Hills sandstones.*

References:

Burnham, WL, USGS: Wood, S.W. , Geology of the Boise Geothermal System, Rocky Mountain Section Meeting of the Geological Society of America, 1985

D.L. Egholm , O.R. Clausen , M. Sandiford , M.B. Kristensen , J.A. Korstgård, The mechanics of clay smearing along faults, Geology, October 2008; v. 36; no. 10; p. 787–790

Haller KM, Wood SW, Geological Field Trips in Southern Idaho, Eastern Oregon, and Northern Nevada, Open-File Report 2004-1222, U.S. Department of the Interior U.S. Geological Survey, 2004

8. ***To supplement Attachment G, provide information regarding the stability of the faults identified in the permit application. If possible, provide a fault slip analysis supported by fault geometry, downhole stresses, and other relevant factors.***

Fault Slip Analysis

A probabilistic fault-slip potential analysis was performed on the faults that create the boundary of the proposed Fault Block E and the results indicated that no slip will occur, based on the maximum proposed reservoir pressure increase of 616 psi as proposed when calculating injection capacity. Details of the analysis are discussed below.

Prior to diving into the details of discussing the fault-slip potential analysis, it should be noted that fault slip is usually an issue where large volumes are injected and usually where the faults being evaluated extend into the deep basement layers of the crust. The daily volumes proposed here are relatively small, 5000 bwpd or less. In this case, very good seismic data exists and the faults are mapped in the seismic to be limited in scope and neither extend to the basement nor to the surface. In addition, another general consideration is the lack of seismicity in this area. Shown below as **Exhibit 8-1** is a map from the USGS website (https://earthquake.usgs.gov/earthquakes/map) that shows this area with history going back to 1900. There is very little activity in this area. The closest activity is questionable data and was

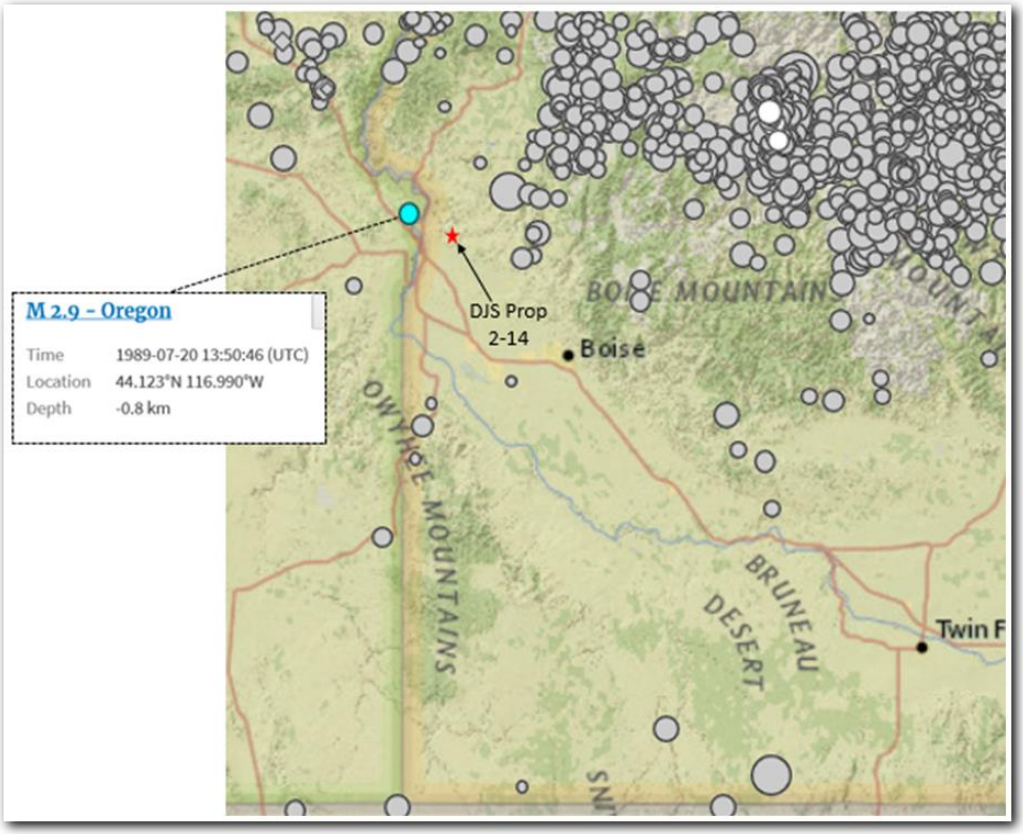

Exhibit 8-1 Map from USGS Earthquake Map Website showing historic seismic activity

recorded in 1989 and shows to be activity very near the ground level surface, as it shows an event at -0.8 km.

A fault-slip-analysis was performed on the faults that create the boundary of Fault Block E using a software program named **Fault Slip Potential vFSP2.0: A Program for Probabilistic Estimation of Fault Slip Potential Resulting From Fluid Injection** (Walsh, 2018).

The method used for this analysis is to calculate the Mohr-Coulomb slip criteria based on the reservoir pressure increase as a result of fluid injection. Each fault location, well location, injection rates, hydrologic parameters, and mechanical stress state parameters are input to create the model and to perform the analysis. The program assumes the faults are not sealing and are exposed to the pressure field in which they are located. The pressure field in the matrix can also be entered manually, rather than using the pressure field estimated from the program's radial flow assumption. The probabilistic estimation portion of this approach is performed by Monte Carlo simulations of multiple combinations of variations of the expected input geomechanical and hydrologic data.

To generate the model 2-D matrix, the isopach map of Fault Block E (see **Exhibit 8-2)** was utilized to create a two-dimensional grid of the fault placement and the well placement relative to the faults. This isopach map was derived from 3D seismic data over this area. Consequently, the accuracy of the position and dip of these faults has very high confidence. These faults were approximated using 4 linear faults. The southwest fault was simulated as 2 separate faults due to the curvature and length of that fault. The FSP software only allows linear fault segments to be input. The fault dip for each fault is 45 degrees.

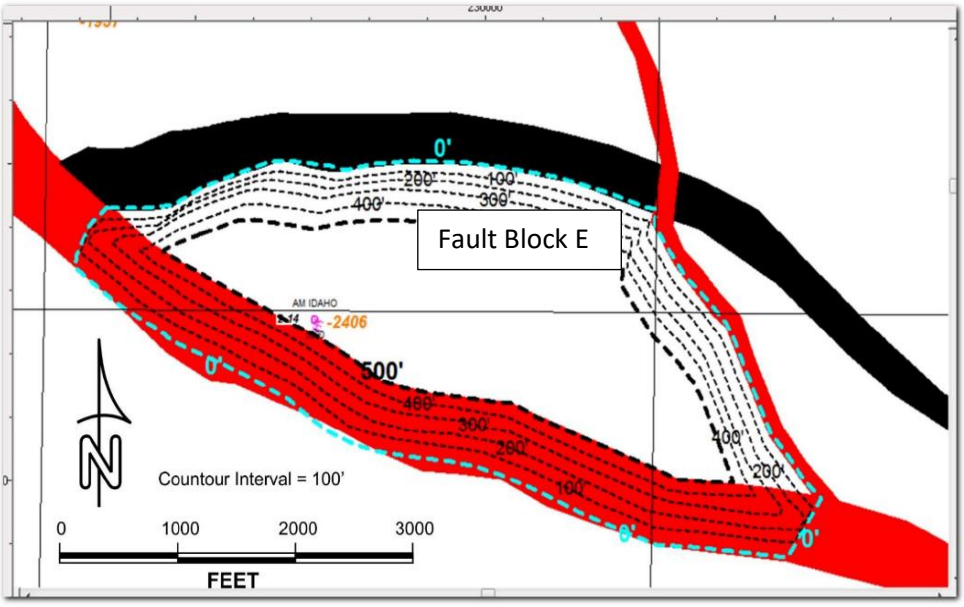

Exhibit 8-2 - Fault Block E Gross Sand Isopach

Exhibit 8-3 shows the output from FSP of the resultant fault orientation utilized for the analysis. The numbers by each fault segment are the Fault #'s associated with each fault in the FSP software.

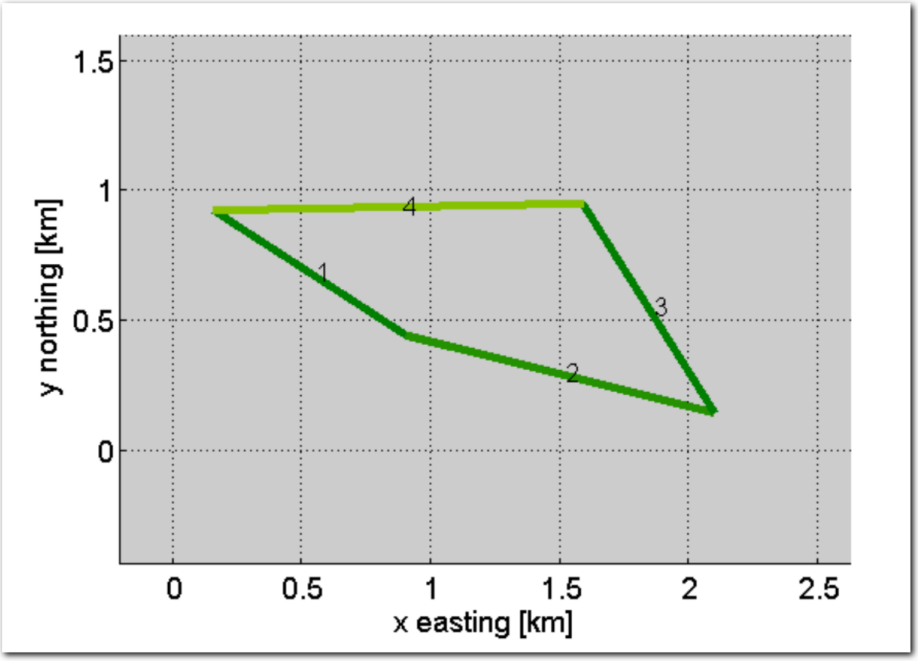

Exhibit 8-3 – Fault Block E Boundary Faults Visualization in FSP Model

Exhibit 8-4 is a table showing the resultant fault data required by the program. Note that the X and Y values are the midpoints of the faults.

Number of faults (max 500)	4
Friction Coefficient mu	0.6

○ Random Faults
◉ Enter Faults

	X [East km]	Y [North km]	Strike [Deg]	Dip [Deg]	Length [km]
1	0.5270	0.6815	122.8000	45	0.8873
2	1.4943	0.2926	104.0030	45	1.2251
3	1.8384	0.5462	147.5950	45	0.9519
4	0.8687	0.9351	88.9584	45	1.4296

Exhibit 8-4 – Fault Slip Potential VFSP2.0 - Fault Data Entry Table

Stress data input for the fracture slip potential analysis is shown in **Exhibit 8-5** below.

Stress Data

○ Specify All Three Stress Gradients [psi/ft]	
◉ Use A-Phi Model	
Vertical Stress Gradient [psi/ft]	0.91
A-Phi Parameter	0.75
☑ Min Horiz Stress Grad Available [psi/ft]	0.77688
Max Hor Stress Direction [deg N CW]	45
Initial Res. Pressure Gradient [psi/ft]	0.46
Reference Depth for Calculations [ft]	5150

Exhibit 8-5 – Fault Slip Potential vFSP 2.0 – Stress Data Entry Table

A vertical stress gradient of 0.91 psi/ft was determined from analysis of the bulk density data recorded in the DJS 2-14 Well. A graph of the bulk density data and the resultant overburden or vertical stress and stress gradient is shown below in **Exhibit 8-6**.

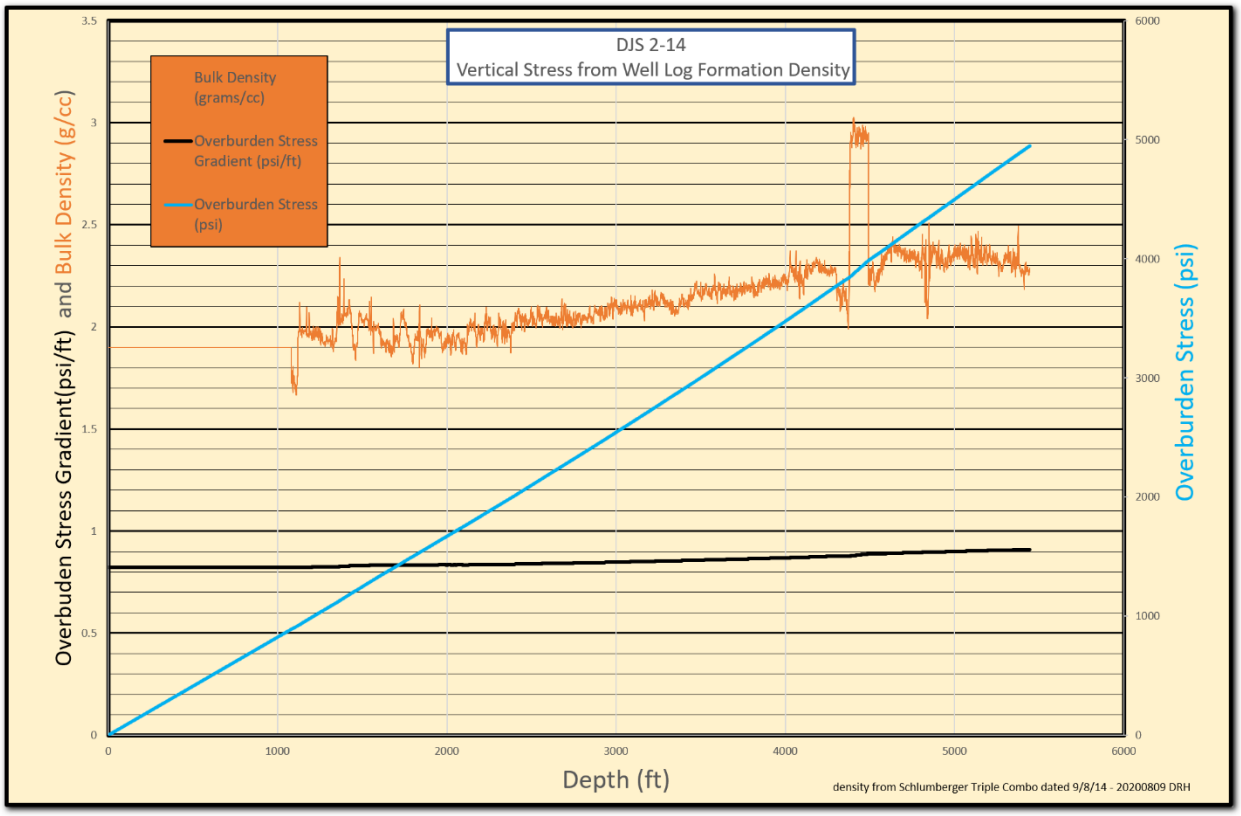

Exhibit 8-6 - Vertical Stress Gradient based on DJS 2-14 Well Log of Bulk Density

The Anderson A-phi Parameter of 0.75 was sourced from a recent publication that addresses the variation of the crustal stress field throughout North America (Jens-Erik Lund Snee, 2020). See **Exhibit 8-7** for a color-contoured map from this publication showing Idaho and the Relative Stress Magnitudes (A-phi or AF)

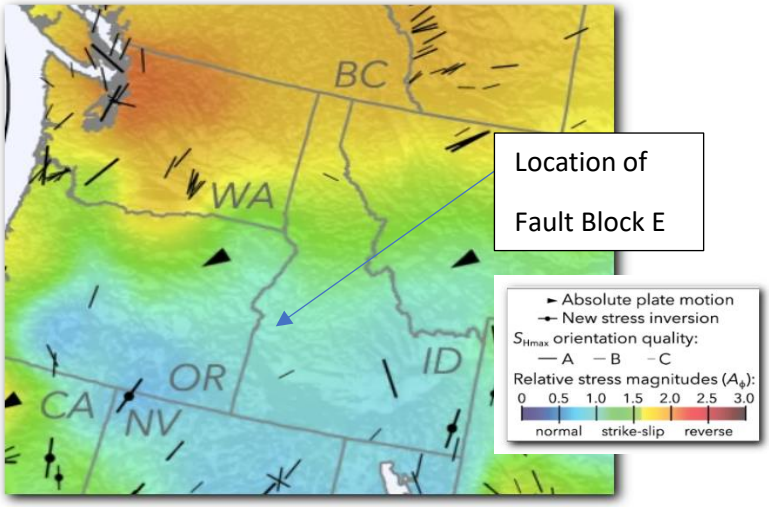

State of stress in North America

Exhibit 8-7 Color Coded Map Showing Variation of A-phi relative stress magnitude

Additional detail from this publication is also shown below in **Exhibit 8-8** that includes the southern portion of Idaho.

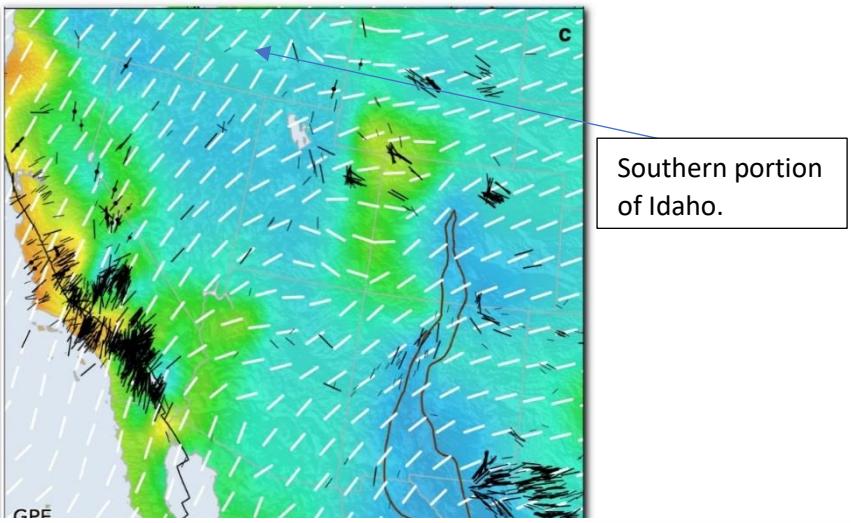

a–c Modeled S_{Hmax} orientations by Ghosh et al.[4] that account for **a** only gravitational potential energy (GPE), **b** basal tractions (BT) from modeled mantle flow, and **c** a combination of GPE and BT. **d** A model of S_{Hmax} orientations by Flesch et al.[47] that considered a smaller study area incorporated only GPE and plate boundary stresses (PBS), using simpler inputs and a smaller study area.

Exhibit 8-8 Detailed Hmax Stress Orientation Map Showing the Southern Portion of Idaho

The horizontal principal stress direction and relative stress magnitudes utilized for this analysis were determined from these maps, along with data from the relatively close geothermal exploration MH-2 Borehole (.A. Kessler, 2017), since no other direct information was available from the wellbores in this immediate vicinity. The MH-2 borehole was drilled in 2011 as part of an effort to examine the potential for the presence of commercial geothermal energy resources in the Snake River Plain. Borehole imaging identified borehole breakouts that indicated a maximum horizontal stress direction of N47E ±7°. This well is located at Mountain Home Airforce Base, approximately 80 miles southeast of the subject Fault Block E. Shown below in **Exhibit 8-9** is a locator map for the MH-2 well, along with the article citation and a link to the article.

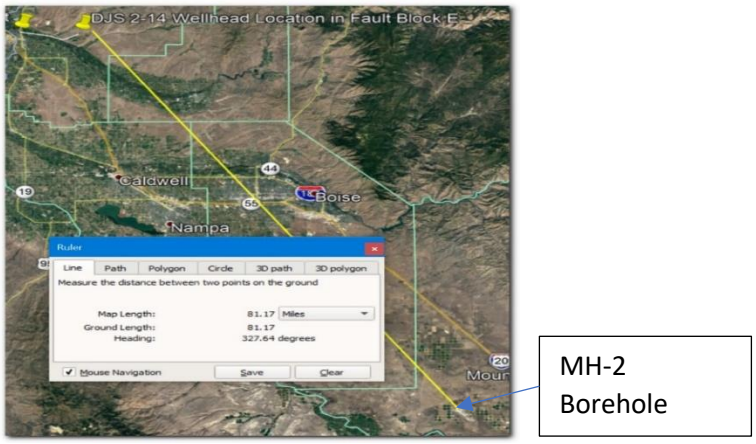

Exhibit 8-9 – MH-2 Borehole location, relative to Fault Block E, Idaho, USA

The minimum horizontal stress magnitude used in the analysis was estimated using the Zamora (Zamora, 1989)method. Shown below in **Exhibit 8-10** is the results from MI Swaco/Schlumberger's Mudware Program (M-I L.L.C - Mi SWACO - A Schlumberger Company, 2011). The resultant minimum horizontal stress or fracture gradient is 14.94 lb/gallon. This equates to 0.77688 psi/ft (14.94 lb/gal * 0.052 (gal*psi)/(ft*lb) = 0.77688 psi/ft). Note that this value is higher than the conservative 12.0 lb/gal value used in the injection capacity calculation

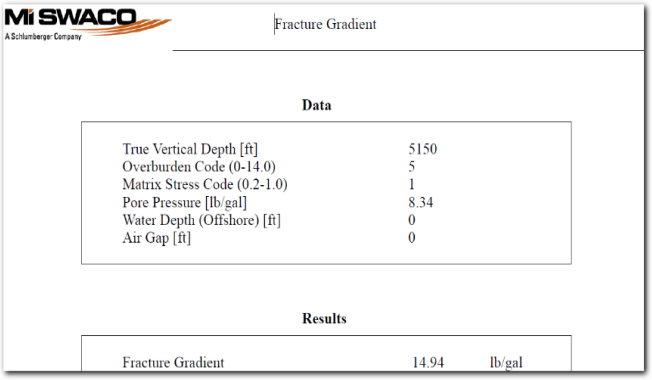
Mi SWACO
A Schlumberger Company

Fracture Gradient

Data

True Vertical Depth [ft]	5150
Overburden Code (0-14.0)	5
Matrix Stress Code (0.2-1.0)	1
Pore Pressure [lb/gal]	8.34
Water Depth (Offshore) [ft]	0
Air Gap [ft]	0

Results

Fracture Gradient	14.94	lb/gal

Exhibit 8-10 Minimum Horizontal Stress or Fracture Gradient Estimate from Mudware Output Report

as the upper limiting value for actual operational limits of injection, and indicates that the proposed injection capacity limitations are conservative.

The FSP program allows for the calculation of pressure increases based on a radial flow model in a uniform infinite radius layer. Using a height of 400' and a permeability of 300 md, along with an injection rate of 5000 BWPD generated a negligible pressure response in the modeled pressure increases over the lifetime of injecting water. In order to simulate the pressure increase created by this confined reservoir, pressures were entered to simulate the expected pressure increase. Based on the injection capacity calculation for Fault Block E, the proposed maximum pressure is 616 psi, which is based on limiting the reservoir pressure to 10% below a fracture gradient of 12 ppg. Two pressure increases were input for modeling purposes 308 psi and 616 psi. The pressure was set to be uniform over the entire area. **Exhibit 8-11** shows the entered pressure profiles.

Load External Hydrologic Model

Select to load a .csv file | Number of header lines: 1 | Load .csv File

	East km	North km	Change in PSI at 5150ft
1	0	20	0
2	20	20	0
3	20	0	0
4	0	0	308
5	0	20	308
6	20	20	308
7	20	0	308
8	0	0	616
9	0	20	616
10	20	20	616
11	20	0	616

Exhibit 8-11 Hydrologic Model Pressure Input Data Table

The results of the base geomechanical FSP analysis is shown below in **Exhibit 8-12** with a presentation that shows a map of the faults with the pore pressure to slip posted on each fault, along with a Mohr Circle and a stereonet with the fault normals. The pore pressures to slip range from 1624 – 2016 psi.

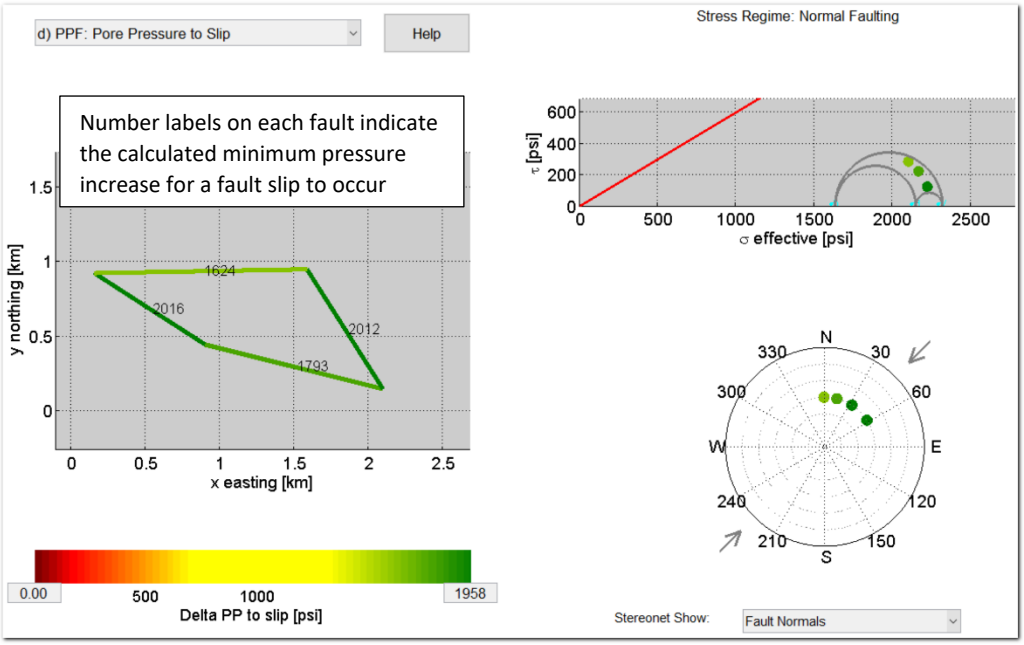

Exhibit 8-12 Base Case Geomechanical Fault Slip Analysis Results

A probabilistic Monte Carlo analysis was also performed, allowing for variation in the geomechanical stress model parameters. **Exhibit 8-13** shows the selections made for this model. These variations are expected to encompass the range of actual values that exist. The largest variations were assumed for maximum horizontal stress direction, the minimum horizontal gradient, and the minimum horizontal stress gradient.

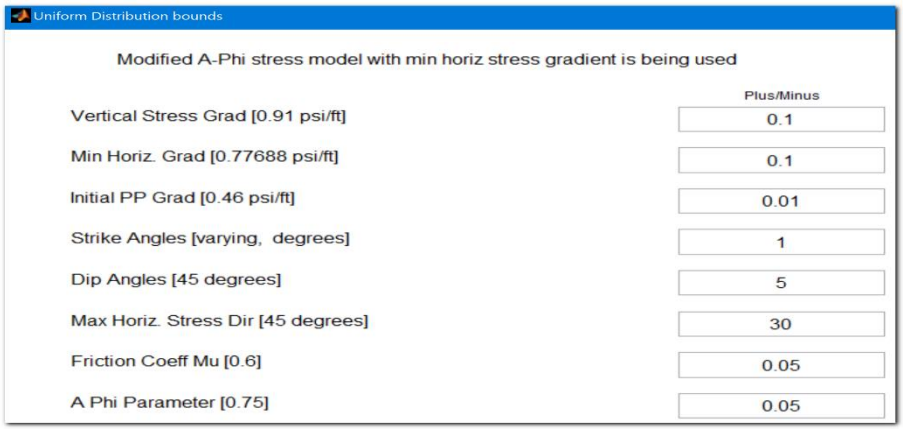

Exhibit 8-13 Parameter variation selections for probabilistic Monte Carlo analysis.

Shown below in **Exhibits 8-14 through 8-18** are displays of the probability of fault slip, along with the variability in inputs and the sensitivity analysis. The first exhibit shows all faults while the remainder 4 exhibits show individual faults with their sensitivity analysis.

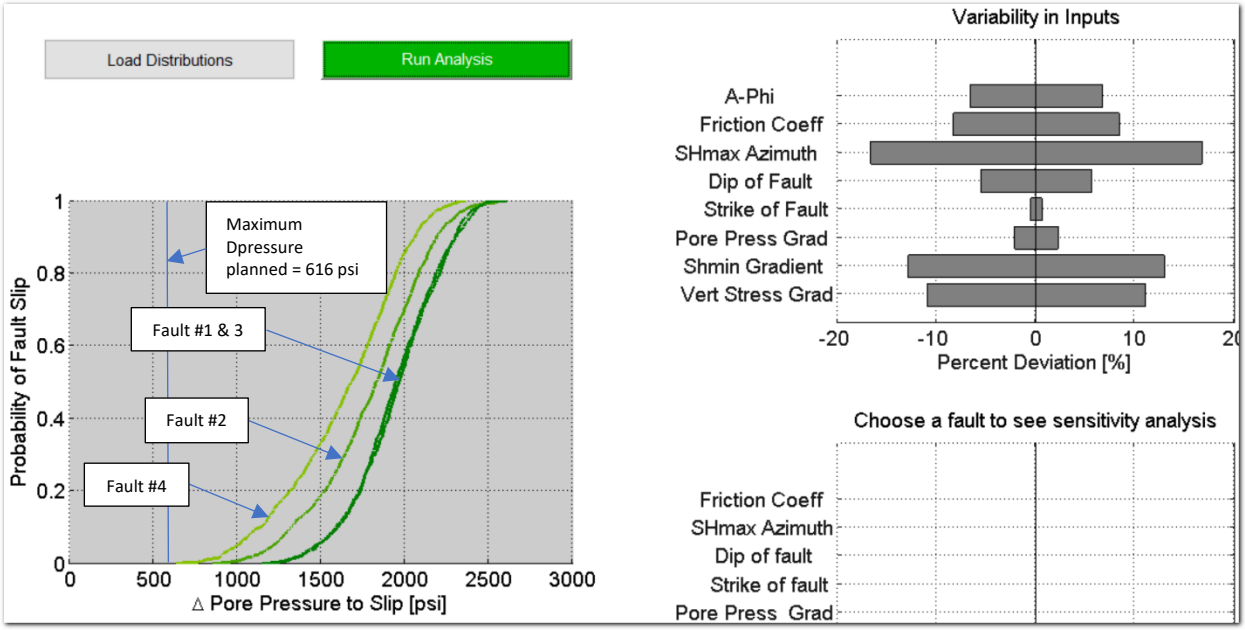

Exhibit 8-14 Summary plot of all faults showing Probability of Fault Slip versus DPore Pressure to Slip

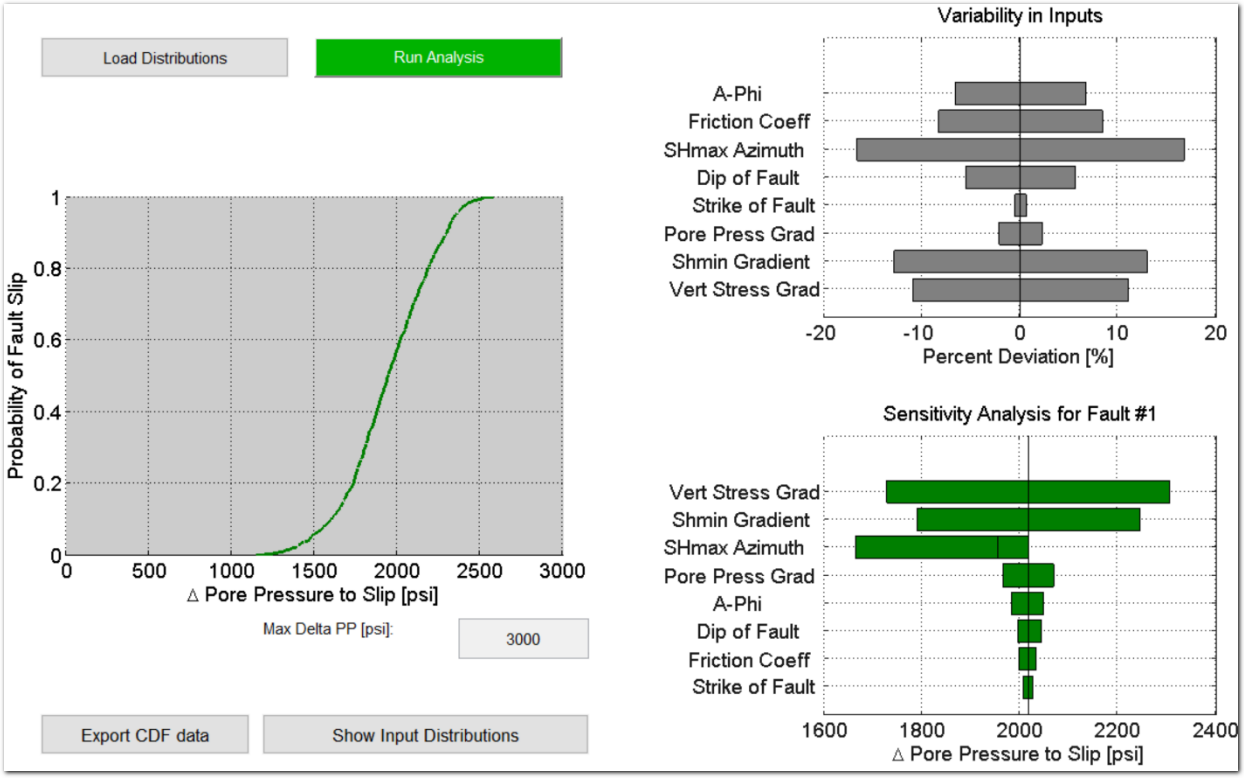

Exhibit 8-15 Fault #1 Probabilistic Fault Slip Analysis

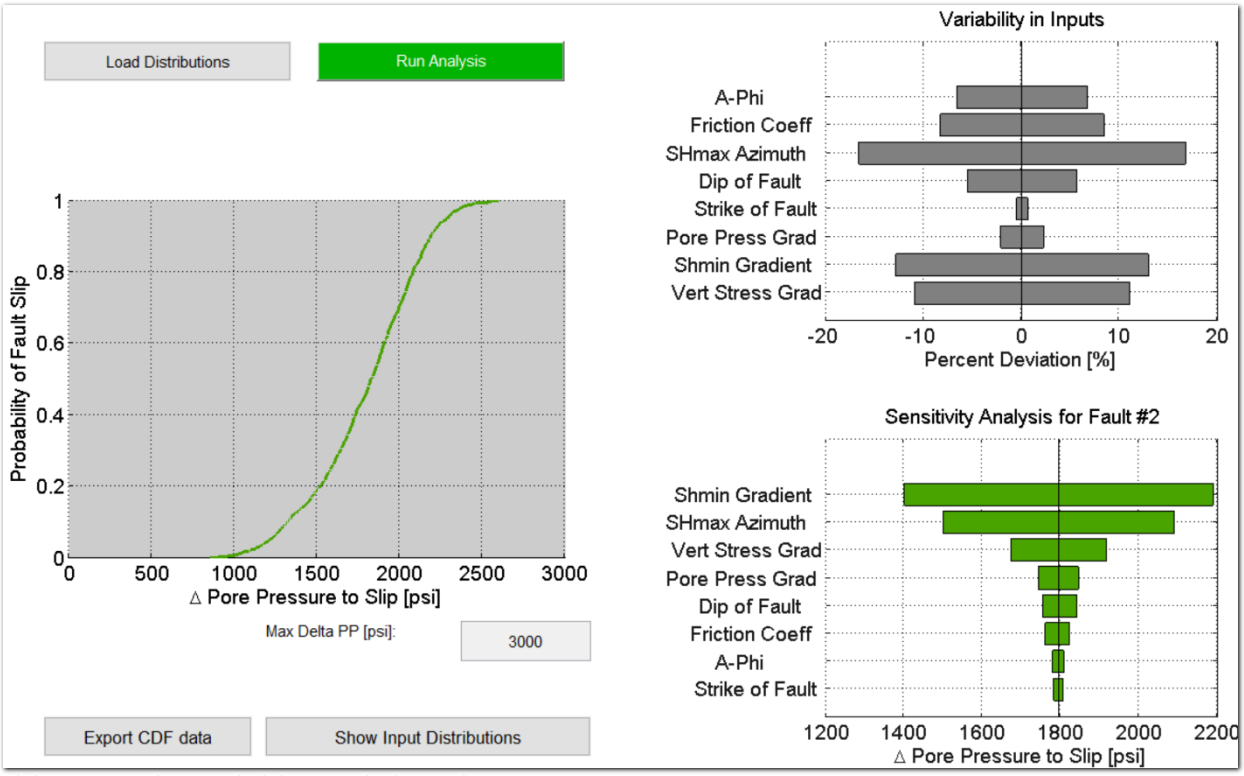

Exhibit 8-16 Fault #2 Probabilistic Fault Slip Analysis

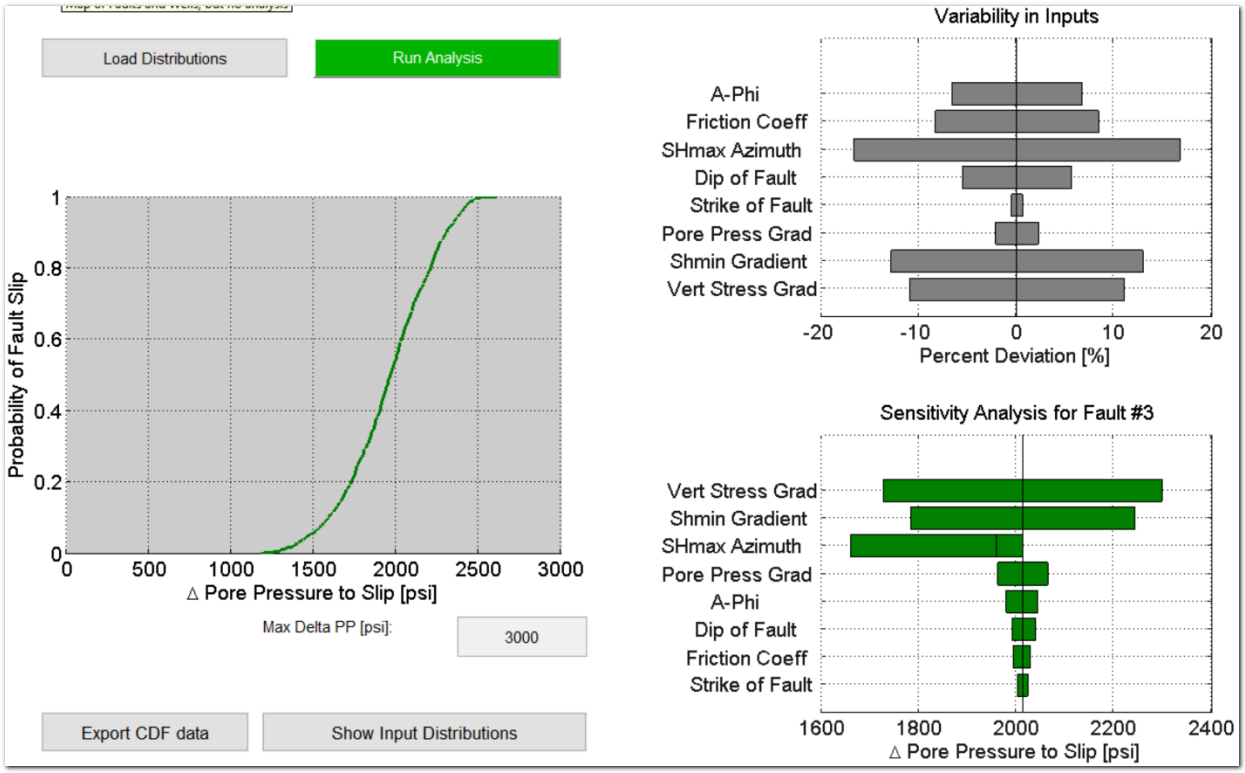

Exhibit 8-17 Fault #3 Probabilistic Fault Slip Analysis

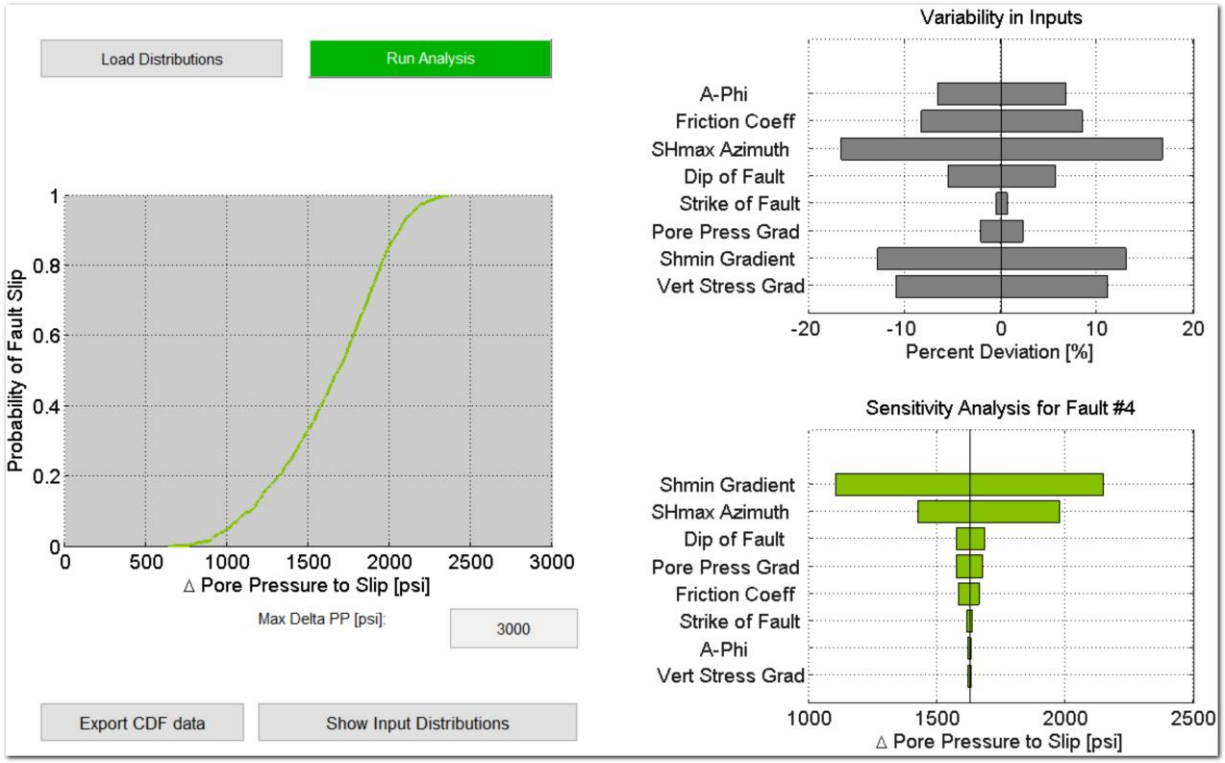

Exhibit 8-18 Fault #4 Probabilistic Fault Slip Analysis

Exhibit 8-19 that illustrates the pressure field that was used for the highest pressure increase. A uniform 616 psi is shown across the entire grid. As previously mentioned, this is the maximum planned pressure, based on the injection capacity calculation for Fault Block E. This assumes that the limiting pressure is below the assumed 12 ppg fracture gradient assumption in that calculation. The DJS 2-14 Well is shown by the numeral 1 in the lower left-hand side of the plot.

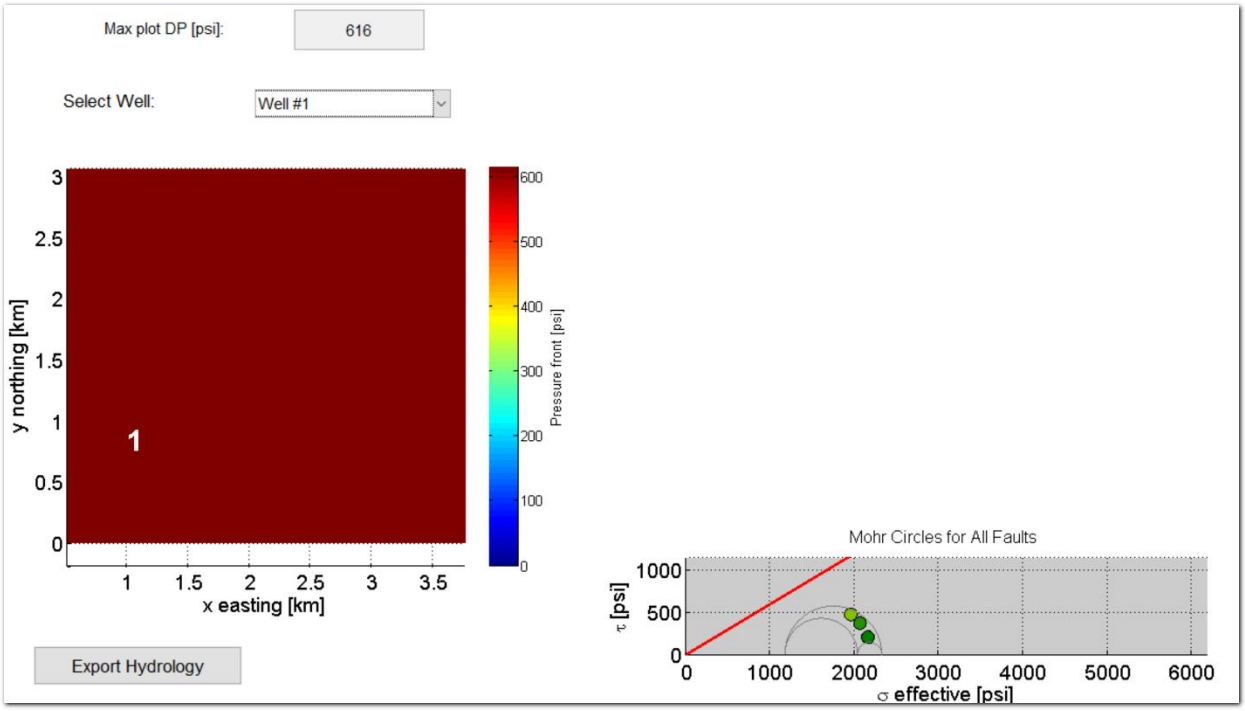

Exhibit 8-19 – Display of pressure profile in simulation grid illustrating 616 psi uniform DP across grid.

References

.A. Kessler, K. B. (2017). Geology and in situ stress of the MH-2 borehole, Idaho, USA: Insights into western Snake River Plain structure from geothermal exploration drilling. *The Geological Society of America, Lithosphere*, 476-498, Volume 9 Number 3.

Jens-Erik Lund Snee, M. D. (2020). Multiscale variations of the crustal stress field throughout North America. *Nature Communications - https://doi.org/10.1038/s41467-020-15841-5*.

M-I L.L.C - Mi SWACO - A Schlumberger Company. (2011). *Mudware - Pressures.* N/A: M-I L.L.C.

Walsh, Z. L. (2018). *FSP 2.0: A Program for Probabilistic Estimation of Fault Slip Potential Resulting From Fluid Injection.* Stanford, CA, USA: Stanford University - SCITS.stanford.edu/software.

Zamora, M. (1989, September). New Method Predicts Fracture Gradient. *Petroleum Engineer International*, pp. 38-43.

9. ***To supplement Attachment G, provide evidence that the geologic intervals with volcanic character below the proposed injection zone will act as a competent lower confining interval. This may include estimates of permeability and porosity, comparisons with like-formations from other locations, or other available information.***

Similar to the upper competent seals mentioned in attachment G, the confining interval below the proposed injection zone exhibits excellent sealing characteristics as well. This argument is best supported by reviewing the well history and log data from a well drilled in 1979 by Ore-Ida Food Incorporated. This well was spudded on 8/19/79 and is located 8.6 miles west of the DJS 2-14 (see Fig 10-1). The section from 5,500' and below, is stratigraphically equivalent to the section immediately below the Willow sands in the DJS 2-14.

The Ore-Ida #1 was drilled to 10,054' (ELOG) as a prospective geothermal project and was abandoned due to non-commercial performance. The log data and other well information obtained from the drilling of the well provides data on the deeper section in this area and provides a reliable analogous offset information to support the sealing capabilities of the lower sections below the proposed injection zone.

Proposed Injection Zone in DJS 2-14: 4,910' – 5,500' MD

Lower sections with impermeable beds in Ore-Ida #1: 5,500' – 10,000' MD

<u>Well Test Info – Prospective sands for Geo-Thermal project proved to have very low perm</u>

Before the Ore-Ida #1 reached its planned TD, an intermediate section of casing was run to 8,153' and an additional 1,901' of open hole was drilled to TD (10,054').

After drilling this section a slotted liner was run and hung off from 8153' – 10,054'. The slotted liner is essentially a steel casing with a series of slots cut out from top to bottom coupled with a 125 mesh screen for solids filtration. This allows reservoir fluids to communicate and flow into the well bore without the need to perforate the casing. With the exception of an open hole completion, a slotted liner is one of the most efficient ways to communicate to the reservoir and allow for minimal pressure drop near the sandface.

After the slotted liner was run into the well, the wellbore was displaced with freshwater (previously drilled with 11.0 ppg mud). This decreased the hydrostatic pressure exerted on the sandface from 8,153' - 10,054', creating a $\triangle$P of 1,410 psi. The well would not flow even after creating this lower pressure environment. The well was then jetted with nitrogen and all completion fluids were evacuated from the wellbore. This attempt was also unsuccessful as the well would not flow nor showed to have any fluid level movement indicating there was no feed in from the reservoir.

At this point, 260' of perforations were created in the liner using shaped-jet perforating guns over a gross interval 8,730' – 9,895'. After adding perforations and continually jetting the well with N2, there still was no indication of well flow or fluid level change.

An additional 240' of perforations were added from gross interval 5,980' – 8,340' and still proved to be unsuccessful with no flow or feed in from the reservoir.

The reasoning behind these failed attempts at making a commercial geo-thermal well can be contributed to very low permeability and by analogy further supports the impermeable nature of the thick volcanic beds that separate these sands between 5,500' - 10,000').

Log Data showing typical SP and Resistivity Character for impermeable beds between 5,500' – 10,000'.

In addition to the unsuccessful flow test data, log data indicates the presence of a series of thick impermeable beds between 5,500' – 10,000' that exhibit a rock quality with low – zero permeability. These sections show log responses that are typical for low-zero perm rock. Evaluating the SP and resistivity curves across these log sections provide the differentiation between permeable and impermeable beds between 5,550' – 10,000'.

Spontaneous Potential (SP) inflection (+) or deflection (-) signifies a difference in salinity between the mudfiltrate and adjacent reservoir water. Both negative and positive values are indicative of permeability due to ionic movement within the rock. Although the perm values could be relatively small, permeability is required to establish an SP curve with inflections or deflections. See log sections below identifying the SP character within the log sections mentioned (5,500' – 10,000'). See log sections Fig 9-1, 9-2, and 9-3

Another useful perm indicator that can be identified on the Ore-Ida #1 ELOG is the curve separation between the shallow and deep resistivity readings. This separation is indicative of mud filtrate flow into the adjacent rock. Due to the resistivities various depths of investigation (deep, shallow), the filtrate infiltration effects on the shallow (depth of investigation) in resistivity can be seen. See log sections below Fig 9-1, 9-2, and 9-3.

It is also important to note that during the drilling of the Ore-Ida #1 well, a lithology record of all drilling cuttings were tracked. Based on the cuttings report, these sections carried heavy portions of basalt, claystone, and siltstone, which all serve as excellent barriers.

See table below showing the lithology make up of each sealing section.

Depth	Thickness	Lithology makeup
5,700' – 5,830'	130'	Claystone, Siltstone, Basalt, Diabase
6,100 – 6,200'	100'	Basalt, Tuff
6,430' – 6,550'	120'	Claystone, Siltstone, Diabase, Basalt

See log Sections below with corresponding lithology descriptions from cuttings report (Log reference - Welex Dual Induction Guard Log 11/8/79):

Fig 9-1 Log Section 5,700' – 5,830' (Seal #1)

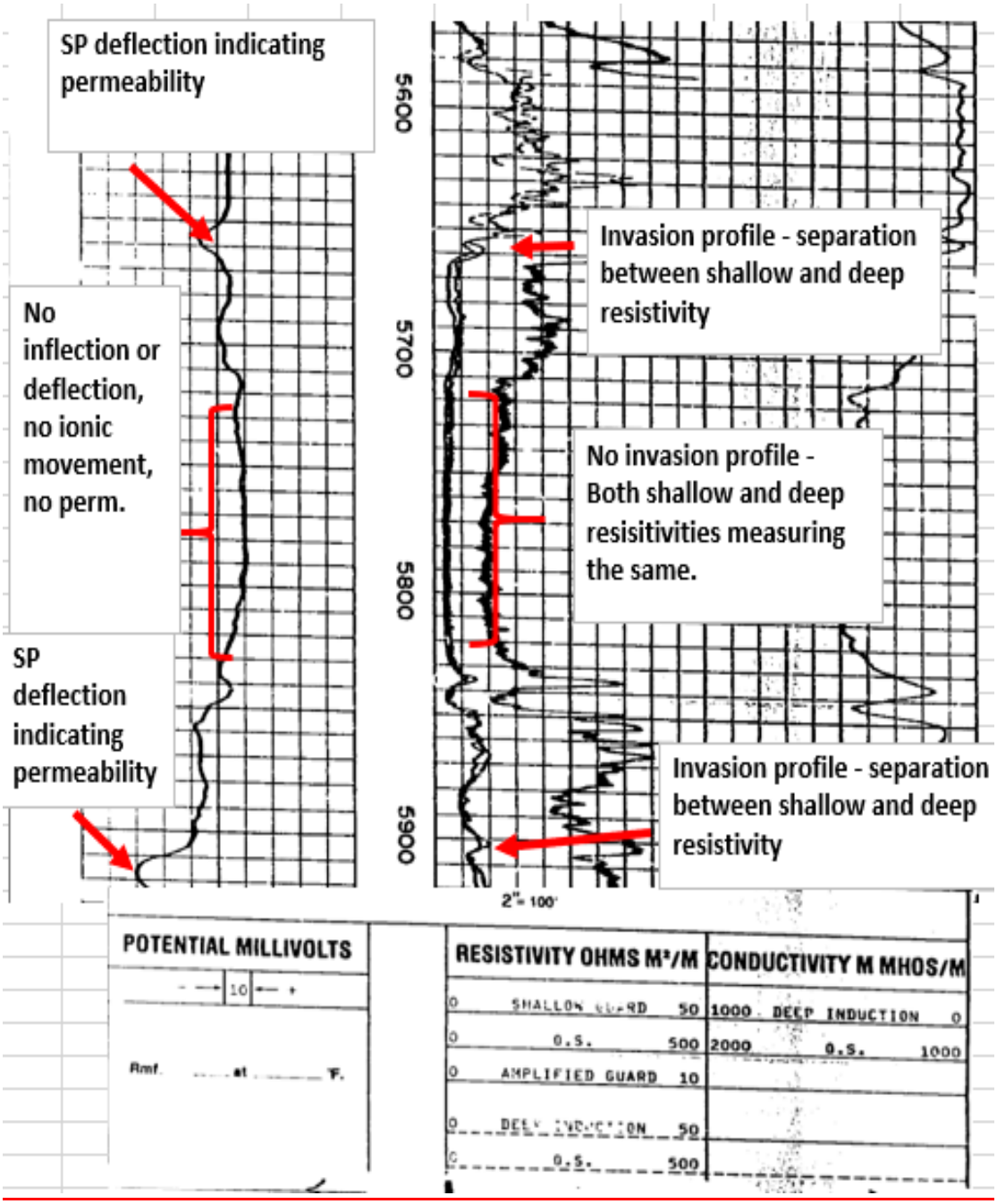

Depth and Lithology Description – Seal #1 (5,700' – 5,830')

5,700-5,720	80% Siltstone, as above, very light gray. 20% Basalt/Diabase, as above (caving). Trace of pyrite. Trace of Sandstone, medium grained, siliceous. Trace of Tuff, white, very fine grained, altered to clay.
5,720-5,730	80% Siltstone, as above. 20% Basalt/Diabase, as above (caving). Trace of pyrite.
5,730-5,740	70% Siltstone, light tan-gray, very tuffaceous, weakly to moderately indurated. 30% Basalt/Diabase, dark gray (plagioclase, pyroxene, abundant magnetite), (caving).
5,740-5,750	50% Claystone, light to medium gray, silty, tuffaceous. 40% Siltstone, light tan-gray, as above (% caving?). 10% Basalt/Diabase, as above (caving).
5,750-5,760	70% Claystone, silty, as above. 30% Siltstone, as above.
5,760-5,770	80% Claystone, as above. 20% Siltstone, as above.
5,770-5,780	90% Claystone, as above. 10% Siltstone, as above. Trace of Tuff, white, very fine grained, altered to clay.
5,780-5,790	90% Claystone, as above. 10% Siltstone, as above.
5,790-5,800	95% Claystone, as above, trace of disseminated pyrite. 5% Sandstone, light gray, fine grained, tuffaceous, weakly indurated.
5,800-5,810	60% Claystone, light to medium gray, as above. 40% Siltstone, as above. Trace of Sandstone, fine grained, tuffaceous. Trace of Sandstone, fine to medium grained (quartz, biotite), siliceous.
5,810-5,820	Poor sample--mostly caving. 100% Claystone(?), medium gray, micaceous.
5,820-5,830	90% Claystone, light to medium gray, silty, tuffaceous, disseminated pyrite. 10% Sandstone, fine to medium grained. Trace of coarse grained, light gray, tuffaceous Sandstone, angular to subrounded. Trace of Basalt/Diabase (caving). Trace of pyrite.

Fig 9-2 Log Section 6,100’ – 6,200’ (Seal #2)

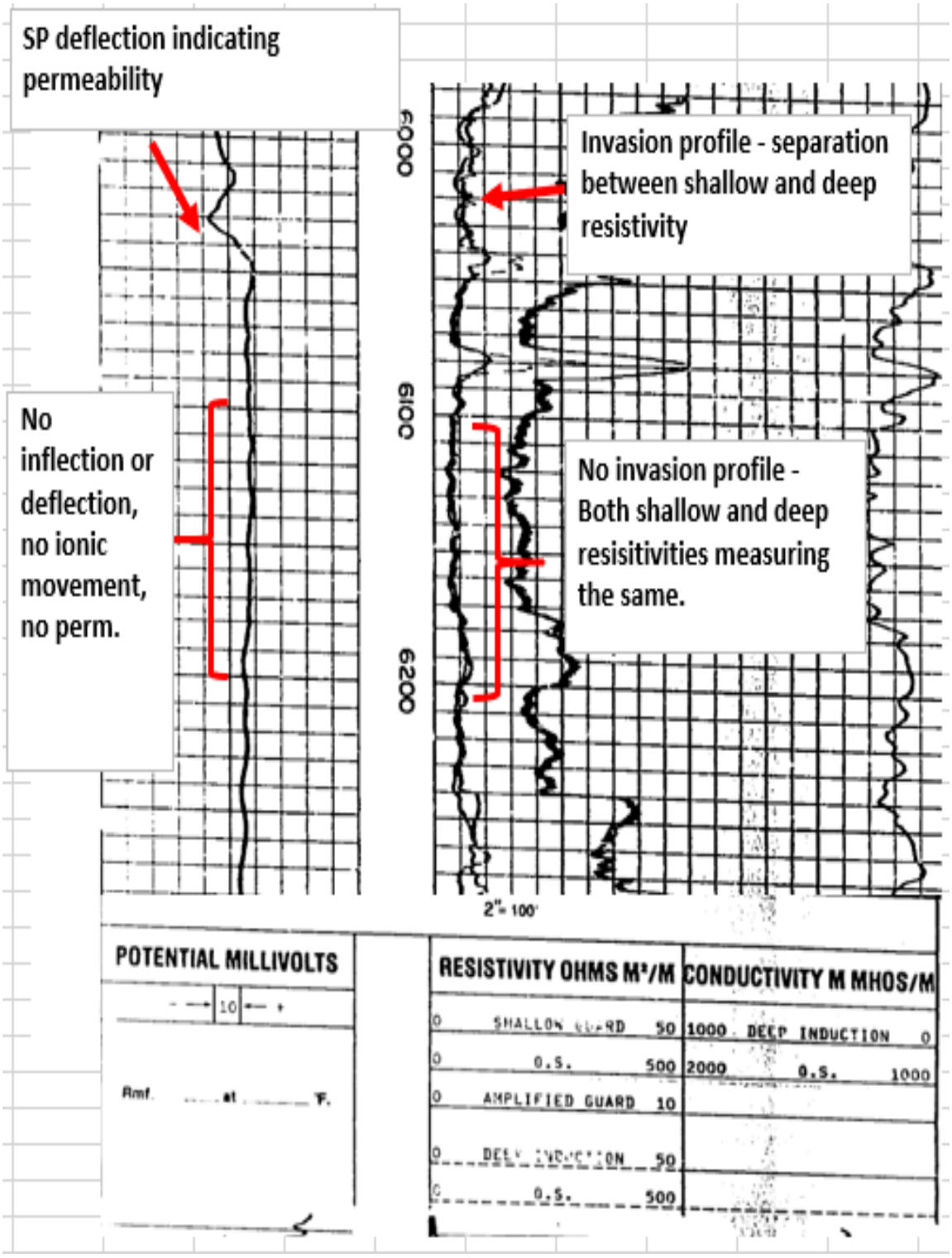

Depth and Lithology Description – Seal #2 (6,100' – 6,200')

6,100-6,110	95% Basalt, dark green-gray, as above. Some textures appear pyroclastic; some range to fine-grained diabasic. 5% Tuff, white, fine grained, altered.
6,110-6,120	95% Basalt, as above. Increasing diabasic texture. 5% Tuff, white, as above.
6,120-6,130	100% Basalt, as above, uncertain whether flow or intrusion. Matrix is very fine grained with a few phenocrysts of plagioclase and pyroxene. May contain clots of coarse crystals with more or less diabasic texture (glomeroporphyritic).
6,130-6,140	100% Basalt, as above.
6,140-6,150	100% Basalt, as above.
6,150-6,160	100% Basalt, as above.
6,160-6,170	100% Basalt, dark green-gray, fine-grained matrix, pyroxene and plagioclase phenocrysts, and abundant magnetite; pervasively altered, with feldspars saussuritized; patches of white clay-like alteration; texture is partly porphyritic, partly diabasic, and partly aphanitic.
6,170-6,180	100% Basalt, as above.
6,180-6,190	100% Basalt, as above.
6,190-6,200	100% Basalt, as above, trace of pyrite.

Fig 9-3 Log Section 6,430’ – 6,550’ (Seal #3)

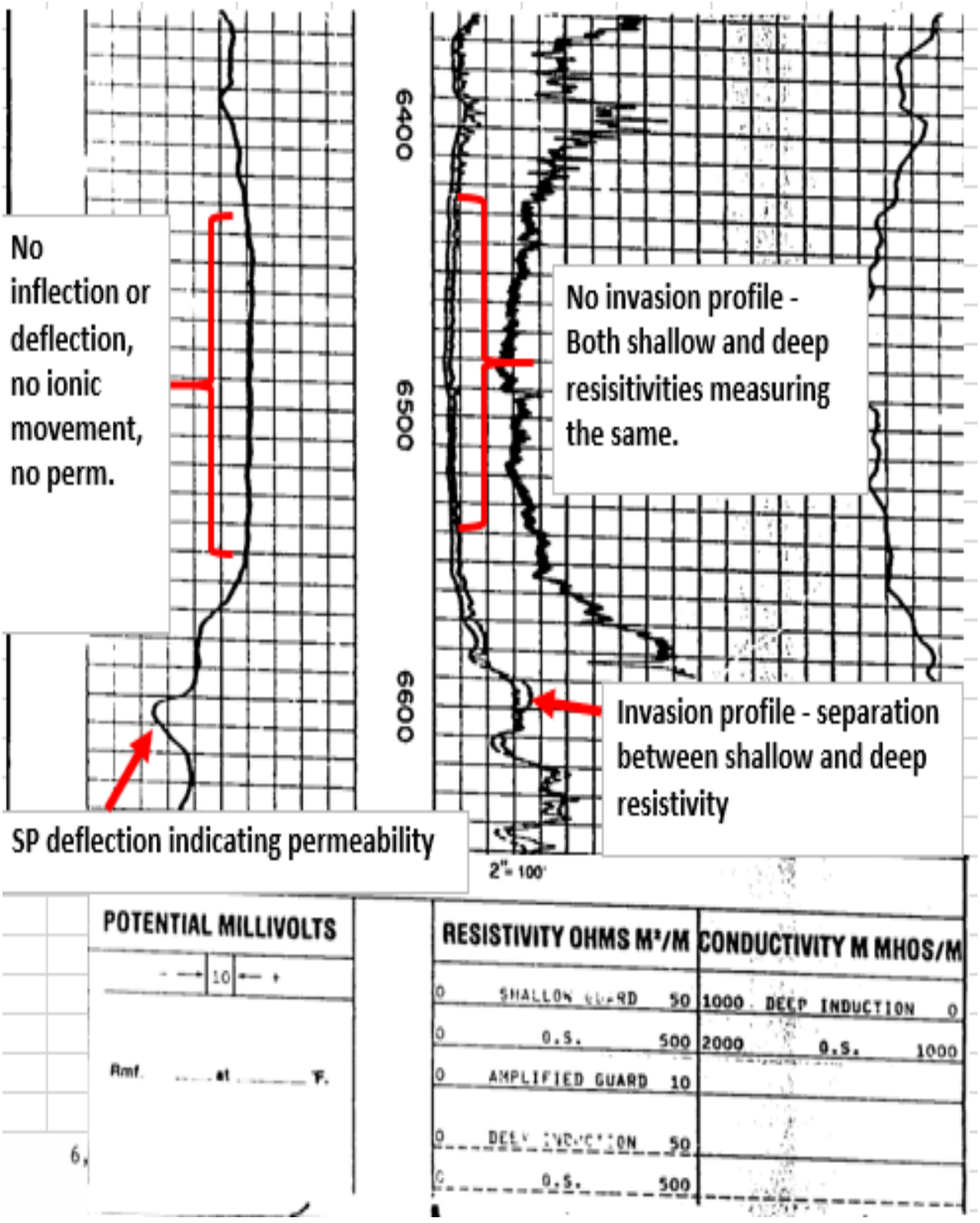

Depth and Lithology Description – Seal #3 (6,430' – 6,550')

6,430-6,440	40% Siltstone, as above. 30% Sandstone, as above. 30% Basalt, dark green-gray, fine to coarse crystalline (plagioclase, pyroxene, and abundant magnetite).
6,440-6,450	Poor sample. 80% Siltstone, as above. 10% Sandstone, as above. 10% diabase and fine-grained basic igneous rock.
6,450-6,460	50% Claystone, light to medium tan-gray. 20% Siltstone, light to medium tan-gray, siliceous, hard, pyritic. 30% Sandstone, light gray, fine grained, subangular to subrounded tuffaceous matrix. Weakly indurated. Trace of Tuff, white, fine grained, altered to clay. Trace of Basalt/Diabase.
6,460-6,470	50% Claystone, as above, micaceous. 40% Siltstone, as above, siliceous. 10% Sandstone, as above.
6,470-6,480	80% Claystone, as above, micaceous. 10% Sandstone, as above. 10% Siltstone, siliceous, as above.
6,480-6,490	80% Claystone, as above. 10% Sandstone, as above. 10% Siltstone, siliceous, as above.
6,500-6,510	40% Basalt, as above. 20% Claystone, as above. 20% Siltstone, as above. 20% Sandstone, as above.
6,510-6,520	Poor sample 40% Claystone, light to medium tan-gray. 40% Siltstone, light to medium tan-gray, siliceous, tuffaceous. 20% Basalt, as above.
6,520-6,530	90% Claystone, medium gray, as above. 10% Siltstone, light to medium gray, tuffaceous as above.
6,530-6,540	80% Claystone, as above. 20% Siltstone, as above.
6,540-6,550	40% Claystone, as above. 40% Siltstone, as above. 10% Sandstone, as above. 10% Basalt, as above.
6,550-6,560	60% Claystone, as above. 40% Siltstone, as above.

Below we evaluate the impermeable claystone beds that are present in the ML Investments #1-11 immediately below Willow sands 3, 4, and 5. These lacustrine claystones are very widespread in the field and therefore should be present downthrown in the DJS 2-14 well (see cross section Exhibit VI-F) . The ML Investments #1-11 is located 3,300' to the northwest of the DJS #2-14. There are multiple confining layers that can be seen in the structural cross section of the Willow Field that extend into fault block E and are logically present below the proposed injection zone in the DJS 2-14 (Willow Sands 3,4, & 5). Among the multiple barriers below the proposed injection zone, the description below highlights two (2) of the thicker confining layers that are immediately below the injection zone. See Fig 9-4 showing the structural cross section of the Willow Sands and associated confining layers.

Fig. 9-4 – Structural Cross section of the Willow Sands

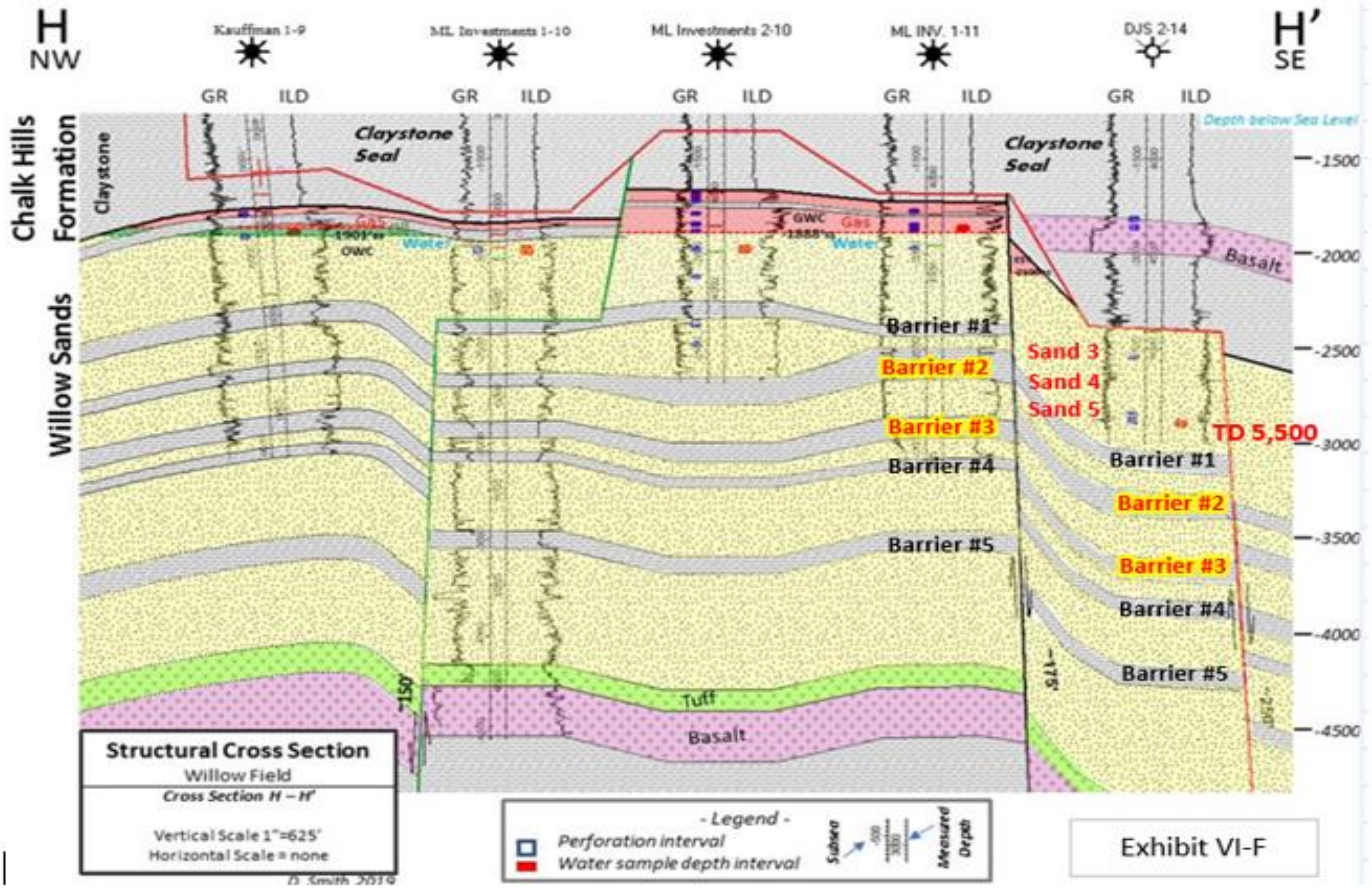

- **Barrier #2 – This confining layer is at 5,000' RKB in ML 1-11 and should be present in fault block E, below the base of the DJS 2-14 (TD 5,500').**

- **Barrier #3 – This confining layer is at 5,300' RKB in the ML 1-11 and should be present in Fault block E below the base of the DJS 2-14 (TD 5,500').**

Log Data

As with the Ore-Ida #1 confining layers, both barriers #2 and #3 are a thick section of claystone and siltstone which serve as excellent barriers. These confining layers straddle lower members of the Willow sands 7 & 8. See Fig 9-5 & 9-6 below illustrating these barriers.

Fig 9-5 – Open hole log showing Gamma Ray and Resistivity curves

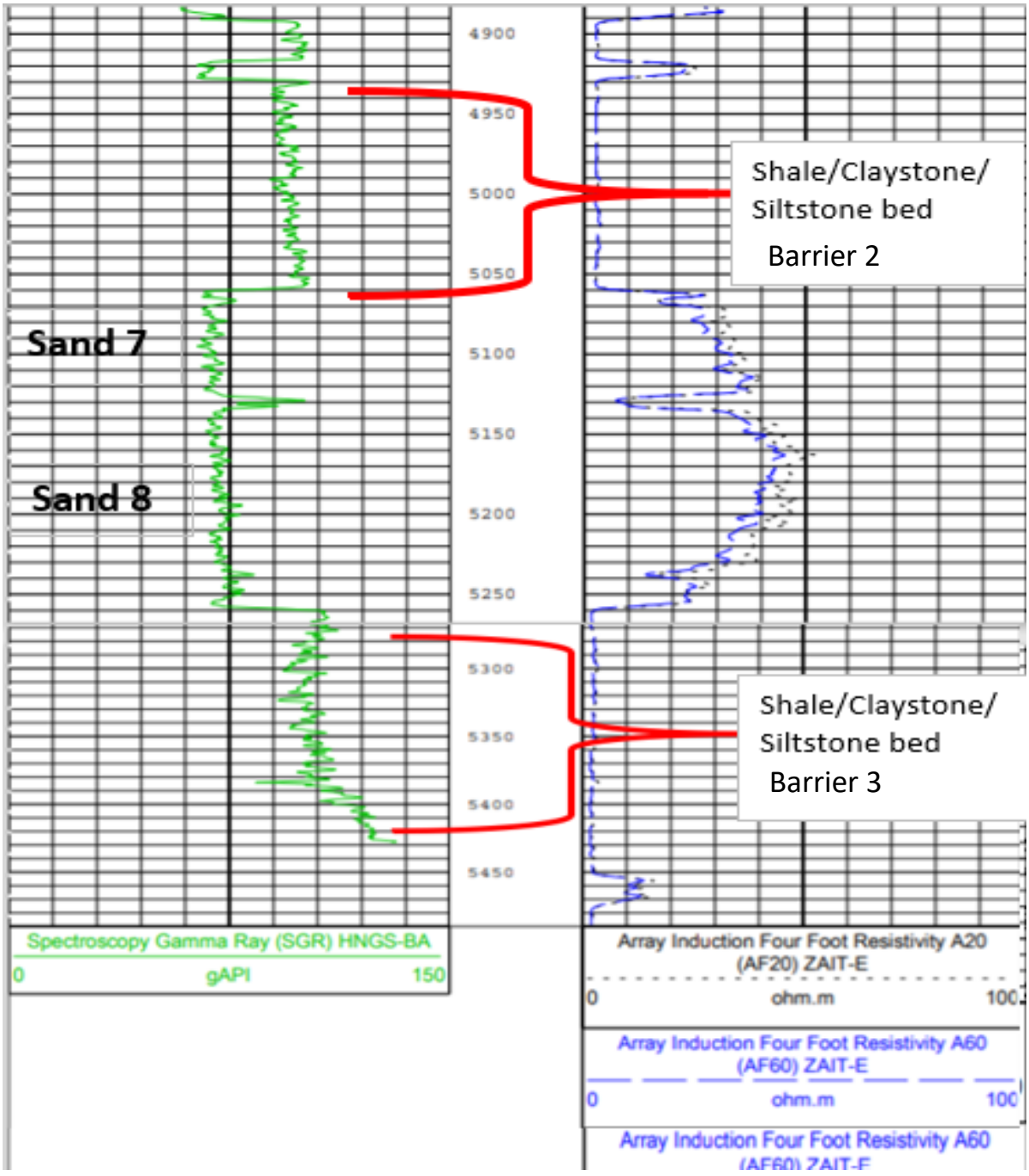

Fig 9-6 Processed log with permeability calculation (RT Scanner Log)

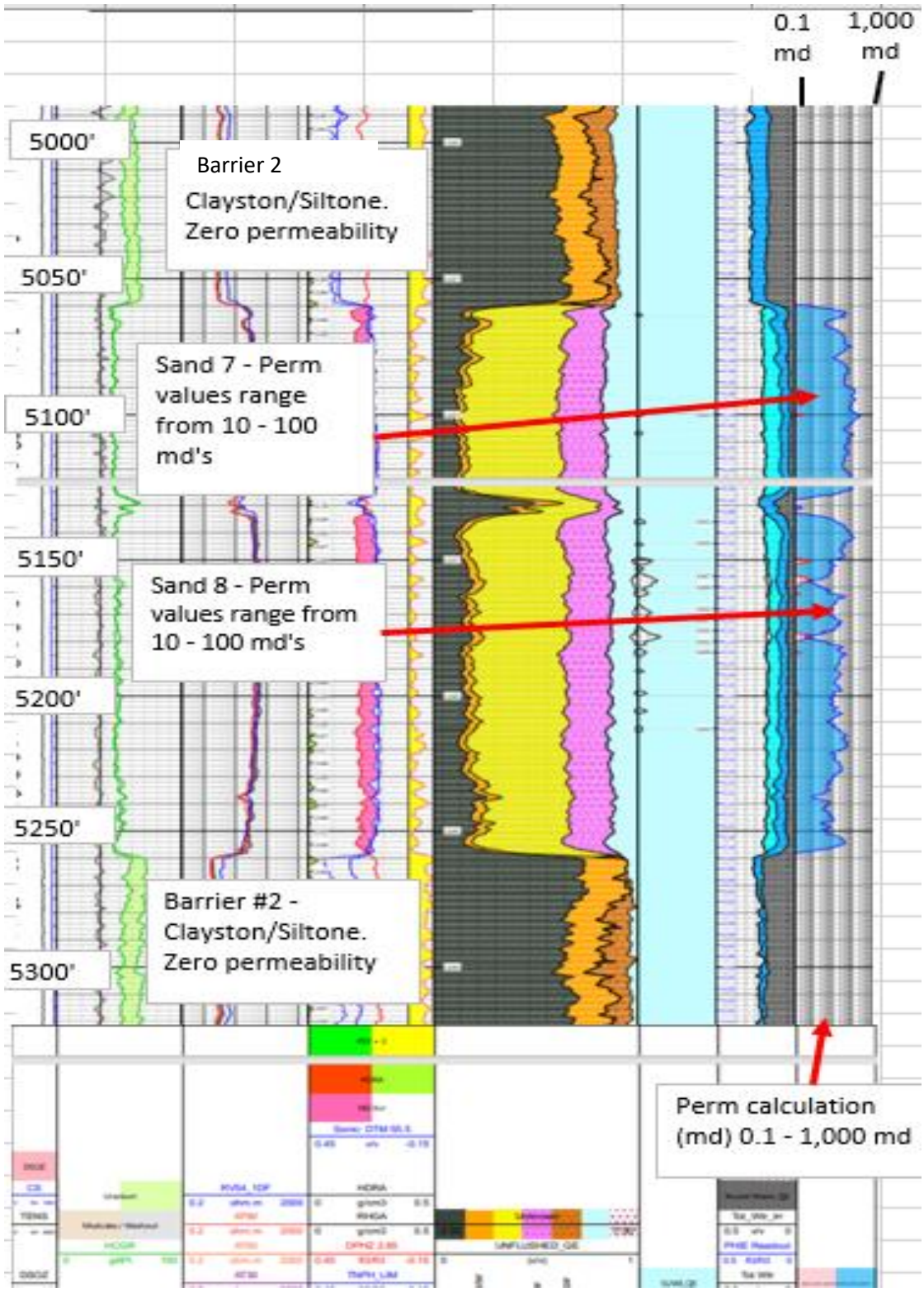

The log section in Fig 9-6 is a relatively new wireline technology with very reliable outputs focused on subsurface petrophysics. The RT scanner log is a data set that is generated from various wireline tools that measure both the vertical and horizontal resistivities of the adjacent formations. There are a plethora of data that is acquired by these tools including a permeability component. Focusing on the first track from the right, you can evaluate the permeability for each half foot logged. For this argument, it is evident that the two (2) barriers 2 & 3 both demonstrate shale/claystone sections that have virtually zero (0) permeability. In contrast to the straddling barriers, sand 7 & 8 are between the two barriers and exhibit permeabilities ranging between 10 – 100 md's. Note the low permeabilities calculated for the barrier intervals.

Evaluating the rock/cutting description in conjunction with the log data presented, barriers 2 & 3 can be viewed as competent confining layers.

References:

Koenig JB, Gardner MC, Technical Report for Deep Well Test and Exploration Program for Ore-Ida #1, 1980

Barrier 3

10. To supplement Attachment G, please provide a vertical distance between the injection zone and the nearest underlying instance of crystalline basement rock, if known and applicable. If not known and/or applicable, please provide the basis for SROG not obtaining this information and/or reaching this conclusion.

Multiple independent types of evidence indicate that the vertical distance between the injection zone and the nearest instance of crystalline basement rock is greater than 10,000 feet of separation. Evidence considered includes high quality 3-D and 2-D seismic data; the results of deep wells drilled in the area; surface geologic mapping and projections; and basin-scale gravity and magnetic studies incorporating the above types of evidence.

a. Surface Geologic Mapping: The nearest exposures of crystalline basement rock are 23 miles east of the injection well where the Idaho Batholith outcrops in a large area of central Idaho. (see fig 10-1 Geologic Map of Idaho, Idaho Geological Survey, 2012 – A digital copy of the map is in folder 10). The proposed injection well lies well out into the basin (WSRP), indicated by a red star. The location of significant deep wells in the basin are indicated by maroon triangles and will be discussed in 10 b. following. The Cretaceous aged granites of the Idaho Batholith are shown as the large pink areas to the east annotated in multiple areas as "Kg", "Ktg" and "Kog". A red dashed line has been added to the IGS map to highlight the contact between the underlying crystalline basement rock and the overlying Tertiary tuffs, basalts and lake sediments. The surfaces of the granites dip west and southwest at 15 to 20 degrees into the basin. Also added near the center of the map is a blue rectangle delineating the Squaw Butte Quadrangle, an area of recent extensive surface mapping by the IGS (Map in Digital folder 10 and presented as Fig. 10-3).

Fig. 10-1 Geologic Map of Idaho, Idaho Geological Survey, 2012

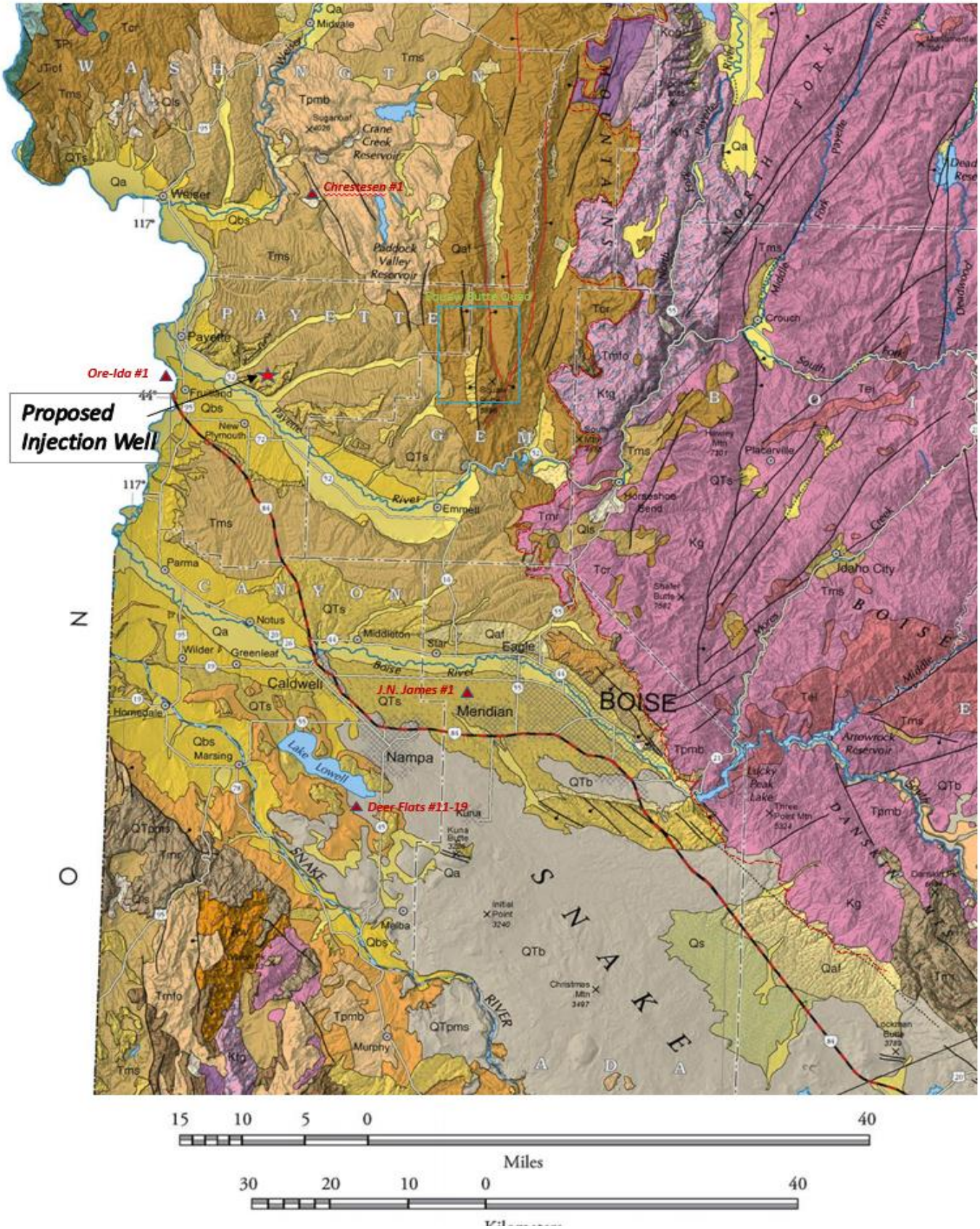

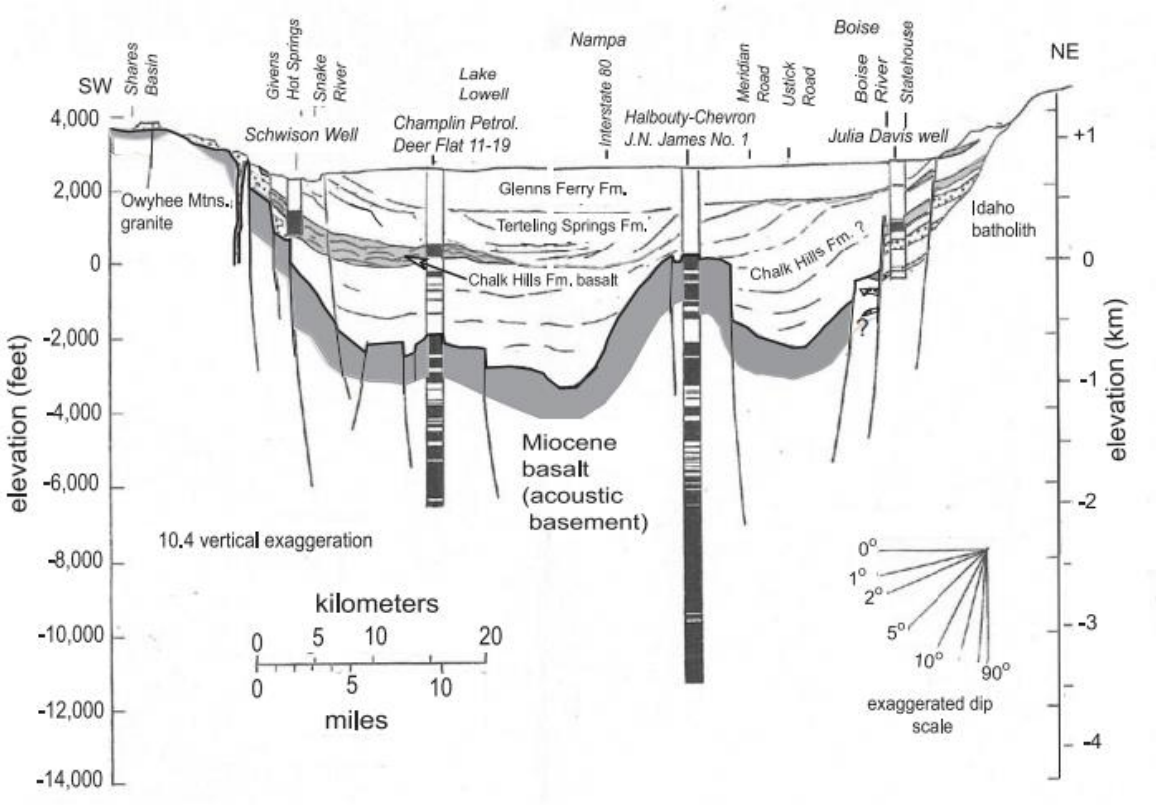

Figure 5. Section across the western plain showing the basalt occurrence (dark pattern) in the deep wells and the configuration of sedimentary fill and associated basalt from seismic reflection data. Shaded outline is the top of Miocene basalt. Stippled pattern is rhyolite that occurs in wells only at the margins of the plain.

Figure 10-2 (above fig. 5 from Wood, 2002) is a generalized SW to NE structural cross-section completely crossing the WSRP basin. Note Boise and the Idaho Batholith on the right, the J. N. James #1 and Deer Flat wells within the basin and the Owyhee Mountains granite on the southwest. None of the deep wells in the basin have encountered granite. The cross section is presented to show the stuctural style of the WSRP, with NW-SE trending extensional normal faults stepping into the basin. Note that the cross section has a vertical exaggeration of 10.4 X.

Figure 10-3 (following) is the IGS geologic map of the Squaw Butte Quadrangle, a multi-decade mapping effort by the IGS and numerous other academic and professional geologists. The map is in technical review by the IGS, but was cleared to be included in this application. A digital copy is in folder 10. The rocks exposed at the surface are several thousand feet of Columbia River Basalt, tuffs and lower Miocene sedimentary rocks.

Figure 10-3 (continued): On the map note cross sections B-B' and C-C', presented as Figure 10-4, following.

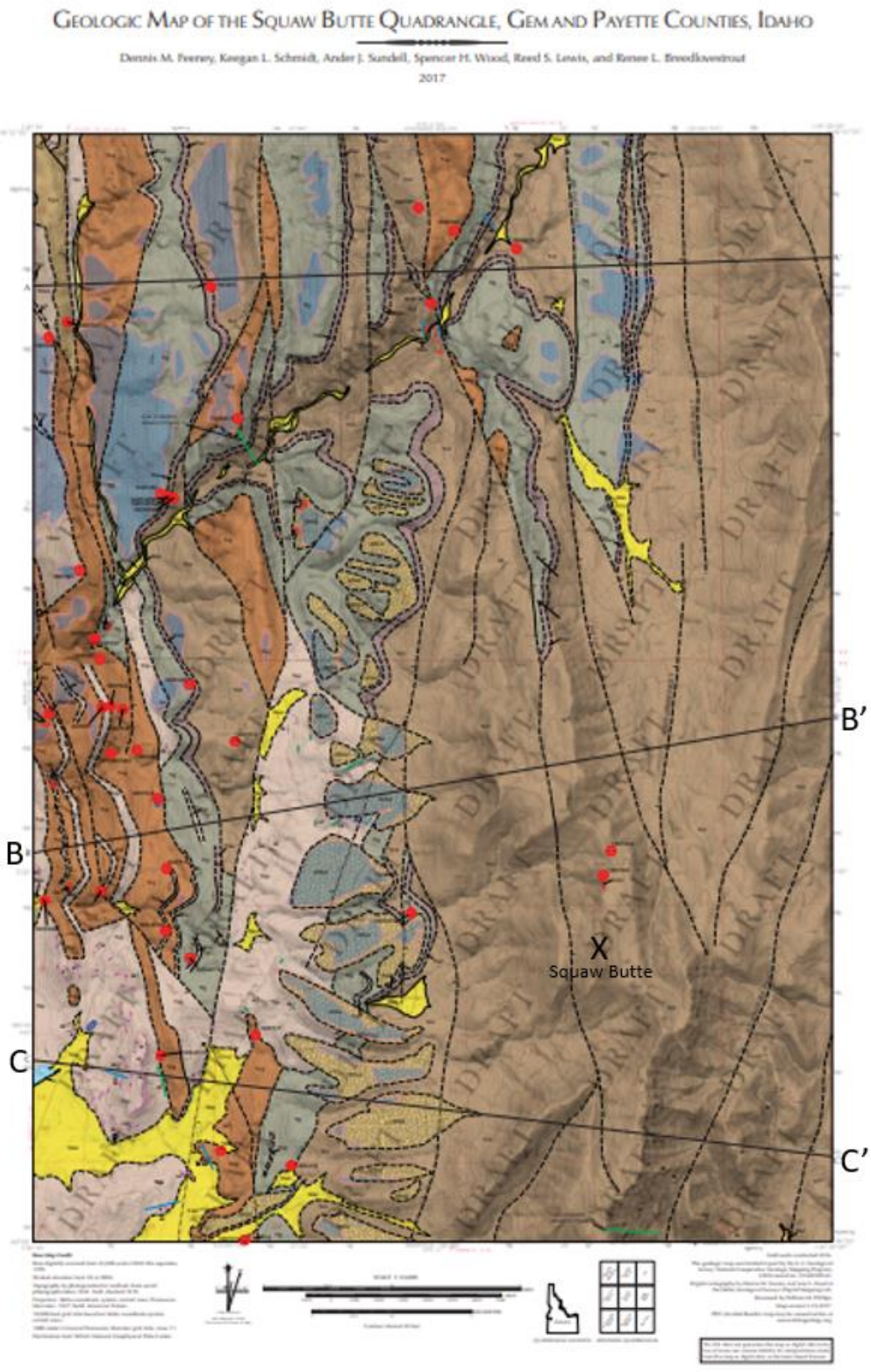

Fig. 10-4: Structural X-Sections (IGS)

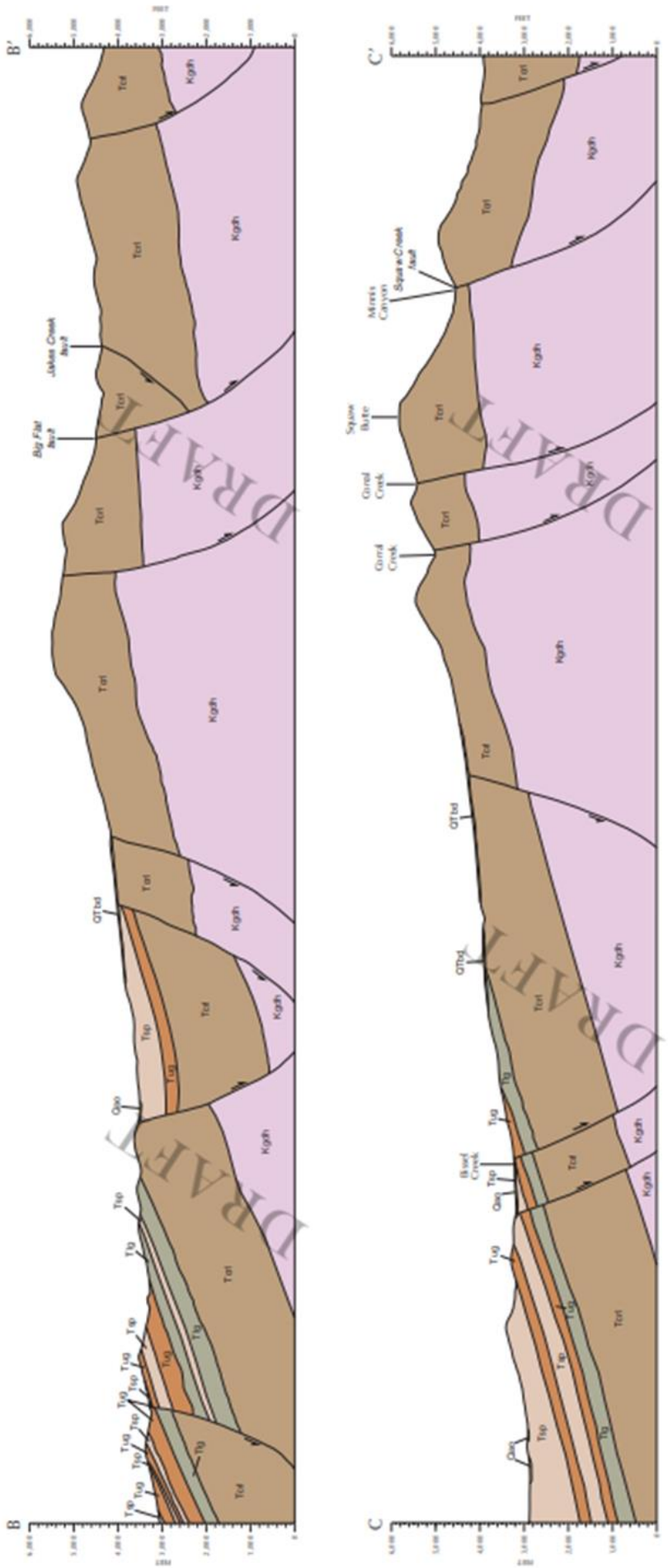

Figure 10-4 (preceding page): Two Structural Cross Sections from the Geologic Map of the Squaw Butte Quadrangle, IGS, in review.

The upper section B-B' is a true scale west to east cross section constructed by honoring the dips of the beds measured at the surface. Note the crystalline granitic basement dipping west at approximately 21 degrees (lower part of cross section, labelled "Kgdh" Horneblende-biotite-granodiorite (Cretaceous). The granite is projected to be at a depth of approximately 2000' subsea at the west end of the section. It is 14.1 miles due west to the proposed injection well from the west end of the section. Maintaining a constant dip of 21 degrees on the basement surface (2000'/mile) would project the top of crystalline basement to occur at -30,000' subsea at the injection well location. An exact depth projection is problematic, as dip rates change and there are a number of small down to the west and down to the east normal faults present to the west of Squaw Butte Quadrangle. Nonetheless, our 2-D and 3-D seismic data confirms the dominant westerly 10 to 20 degree dip into the WSRP in the region to the west, and that the majority of the normal faults present are down to the west, and into the basin.

The lower section C-C' is also a true scale west to east structural cross section. Surface dips here are more typically 15 degrees to the west. The Cretaceous granite surface is projected by the authors to be at approximately -2000' subsea at the west end of C-C'. Maintaining a constant west dip of 15 degrees would drop the granite surface at the rate of 1400'/mile going west. It is 14.2 miles west to the proposed injection well, which would project to a depth of approximately -22,000' subsea for the top of crystalline basement at the proposed injection well. As discussed above, this projection method is inexact due to variable dip rates and the presence of other faults in the region to the west. However, the seismic data which we have confirms the typical 10 to 20 degree westerly dip of the stratigraphic section into the basin (See figure 10-5).

The Willow Sands injection zone is found from -2200' to -3700' subsea at the proposed injection well. Using simple trigonometry and projecting the Cretaceous granite surface to the injection well location estimates it to be at a depth of approximately -22,000' subsea, a vertical distance of more than 18,000' between the injection zone and crystalline basement. This method of projecting the estimated depth should not be considered exact, because of the variability of dips and additive and subtractive errors of unknown faults. Error bars of this method are likely on the order of several thousand feet.

Figure 10-5: Seismic Data incorporated with Surface Geology

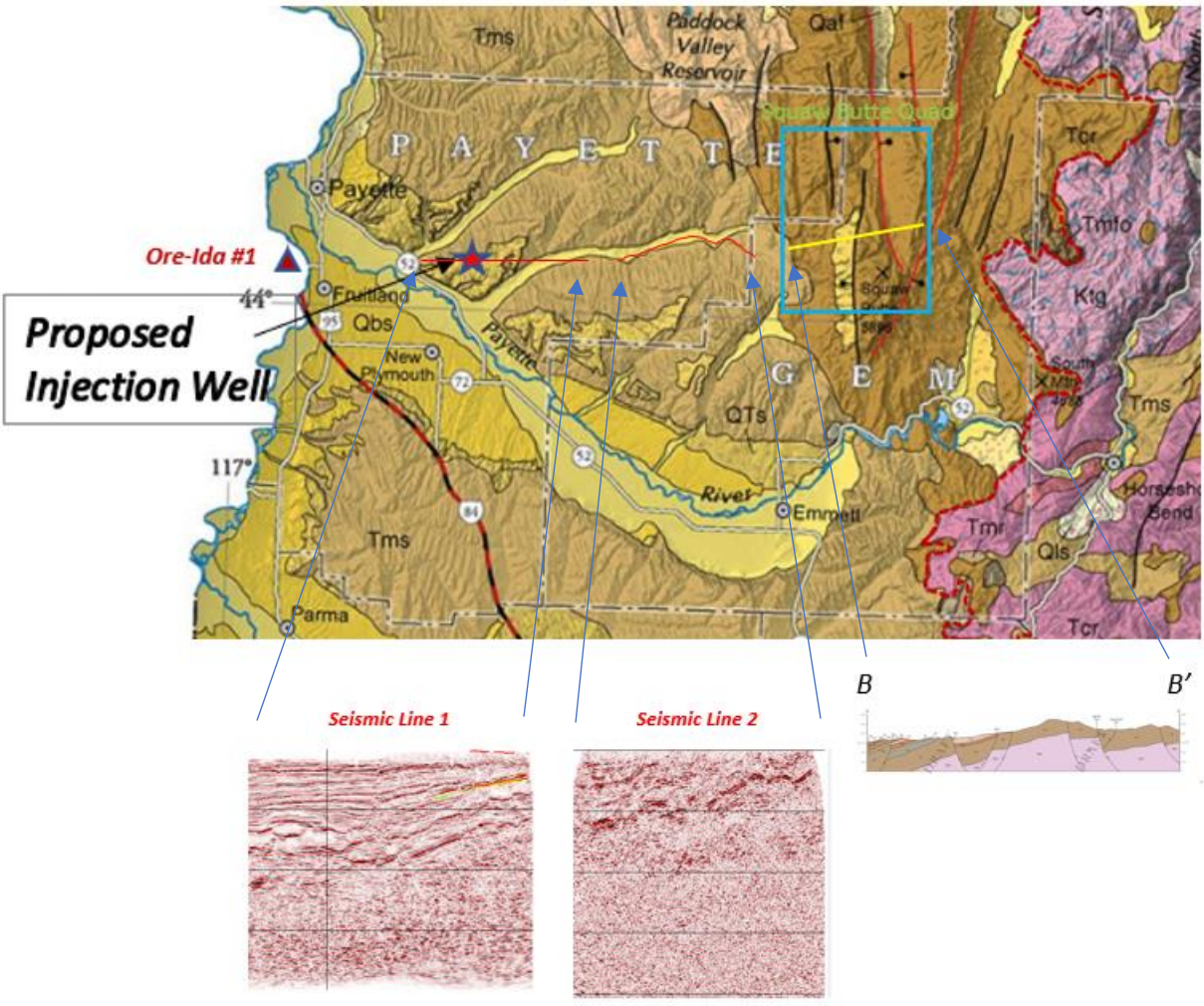

The above IGS Geologic Map of Idaho is annotated to show the Squaw Butte Quadrangle outline (blue) and the location of IGS structural cross section B-B' (yellow line). Seismic lines 1 and 2 locations are shown as red lines on the map and displayed above (in time). There is a data gap of 1.5 miles between the seismic lines, and a similar gap to the west end of structural cross section B-B'. The intent of this figure is to demonstrate that the stratigraphic section generally dips 10 to 20 degrees west into the basin, and that small-scale normal faults "step in" to the WSRP. Note that high amplitude west dipping reflections on the seismic data are basalt layers. These high impedance events reflect most of the seismic energy back to the surface, and therefore make seismic imaging of deeper beds below the basalts difficult.

b. ***Drilling results:*** ***The deepest well drilled in the area is the Chevron/Halbouty J.N James # 1, which was drilled to 14,006' in 1976. The location of the well is shown on the Fig. 10-1 map and the Fig. 10-2 cross section, it is 32 miles southeast of the proposed injection well. The James well was drilled on a structural high within the basin, yet was still drilling principally in basalts, with interbedded volcanic tuffs and claystones at total depth of 14,006'. A mud log and lithologic descriptions for the well are in folder 10.***

Figure 10-6: Idaho O & G Completion Report for J.N James #1 well

DETAIL OF FORMATIONS PENETRATED

Formation	Top	Bottom	Description*
Idaho	Surface	2270'	Predominately sand and comglomerate with streaks and zones of silt and siltstone.
Grassy Mountain Basalt	2270'	4108'	Predominately basalt with tuff, volcanic ash, and occasional streaks of siltstone.
Columbia River-Owyhee Basalt	4108'	±7600'	Basalts, sand, clay and tuff.
Sucker Creek	±7600'	Still in same at total depth	Principally basalt with varying amounts of tuff, ash, altered basalts with some clays and siltstone. Still in volcanics at total depth.

Of significance, this well establishes a Columbia River basalt/Sucker Creek section of nearly 10,000' (4108' to 14,006' MD), and this on a structural high within the WSRP. It is probable that there would be a greater total thickness of basalt, tuffs and sediment off of the high in a setting such as the injection well is found in. Crystalline basement rock was not reached by total depth of 14,006' MD (-11,455' subsea).

The Champlin Deer Flats #11-19 well was drilled to 9047' MD in 1981, it's location is noted on Figures 10-1 and 10-2, about 38 miles south of the injection well. The Deer Flats well was still drilling in basalts, and tuffs at its total depth. No granites were encountered in the well by 9047' MD (-6430' subsea). A mud log and completion report for the well is in folder 10.

The Ore-Ida #1 well was drilled to 10,054' MD in 1979. It is located 8.6 miles west of the proposed injection well and is shown on Figure 10-1. It encountered predominately lacustrine claystones and silty claystones from the surface to 4570' MD. This is the Glenns Ferry and Chalk Hills section. From 4570' to 8135' MD the well encountered interbedded basalts, tuffs, claystones, siltstones, sandstones and altered tuffs. This section is lower Chalk Hills and Payette formation, and the basalt intervals are

intrusives. From 8135' to total depth of 10,054' MD the well encountered predominately thickly bedded basalt flows, interbedded with numerous thin sedimentary layers. This 8135' MD is the top of the Columbia River Basalt interval. The sedimentary layers are white tuffs, tuffaceous sandstones, and light brown-gray siltstones. No crystalline basement was reached in the Ore-Ida well by 10,054' MD, equivalent to -7880' subsea. A significant deep test drilled to the northeast of the Ore-Ida well, the Phillips Chrestesen, encountered a 7100' thick interval of Columbia River basalts and tuffs prior to hitting granite. If the Columbia River basalt section at the Ore-Ida location is equivalent thickness to that seen in the Chrestesen well, then the Ore-Ida well would theoretically encounter crystalline basement at -13,061 subsea. The Chrestesen well (discussed below) was drilled in a shallower part of the basin on the east flank of the WSRP, and likely has a thinner CRB section than is present at the Ore-Ida location. The Ore-Ida well is the most proximal well of the deep wells in the basin to the proposed injection well. Logs and cuttings lithology description for the well are in folder 10. If the Ore-Ida location has a CRB/Sucker Creek section of equivalent thickness to that found in the James well, it would have basement at over -15,860' subsea. As the CRB and underlying tuff section are extremely widespread in the WSRP, the depth to crystalline basement estimated range of -13,061' to -15,860' subsea should be very comparable to the range estimated at the injection well site.

The Phillips Chrestesen "A" #1 well was drilled to 8000' in 1977. The location is shown on Figure 10-1 and 10-7, 15.8 miles north northeast of the proposed injection well. The mud log for the well is included in folder 10. The well encountered a thin, approximately 200' thick section of claystone, shale and sandstones at the surface (likely Payette Fm.) before drilling into the Columbia River basalt at 200' MD. The Chrestesen well then encountered a 7100' interval of predominately basalt to 7300' MD. Occasionally interbedded with the basalts are tuffs, sandstones and light gray claystones. From 7300' to total depth of 8000' the well drilled in Granite. As the well was drilled on the east flank of the WSRP, it is probable the CR basalt section would be thicker within the basin proper, in the location of the Ore-Ida well and the proposed injection well.

We have proprietary 3-D seismic which allows us to image the subsurface structure from the proposed injection well 8 miles north, halfway to the Chrestesen well (See Figure 10-7). This data shows consistent southwest dip into the basin from the Chrestesen well to the proposed injection well. The last 7.8 miles has no seismic data available, but previous workers have mapped down to the southwest normal faults dipping into the basin in the area of the Crane Creek-Paddock Valley fault system. Using the southwest dip rates shown on the seismic data would project the top of the Cretaceous granites (if present) at approximately -14,000' subsea.

Figure 10-7: Schematic Cross section- Chrestesen Well into the Basin

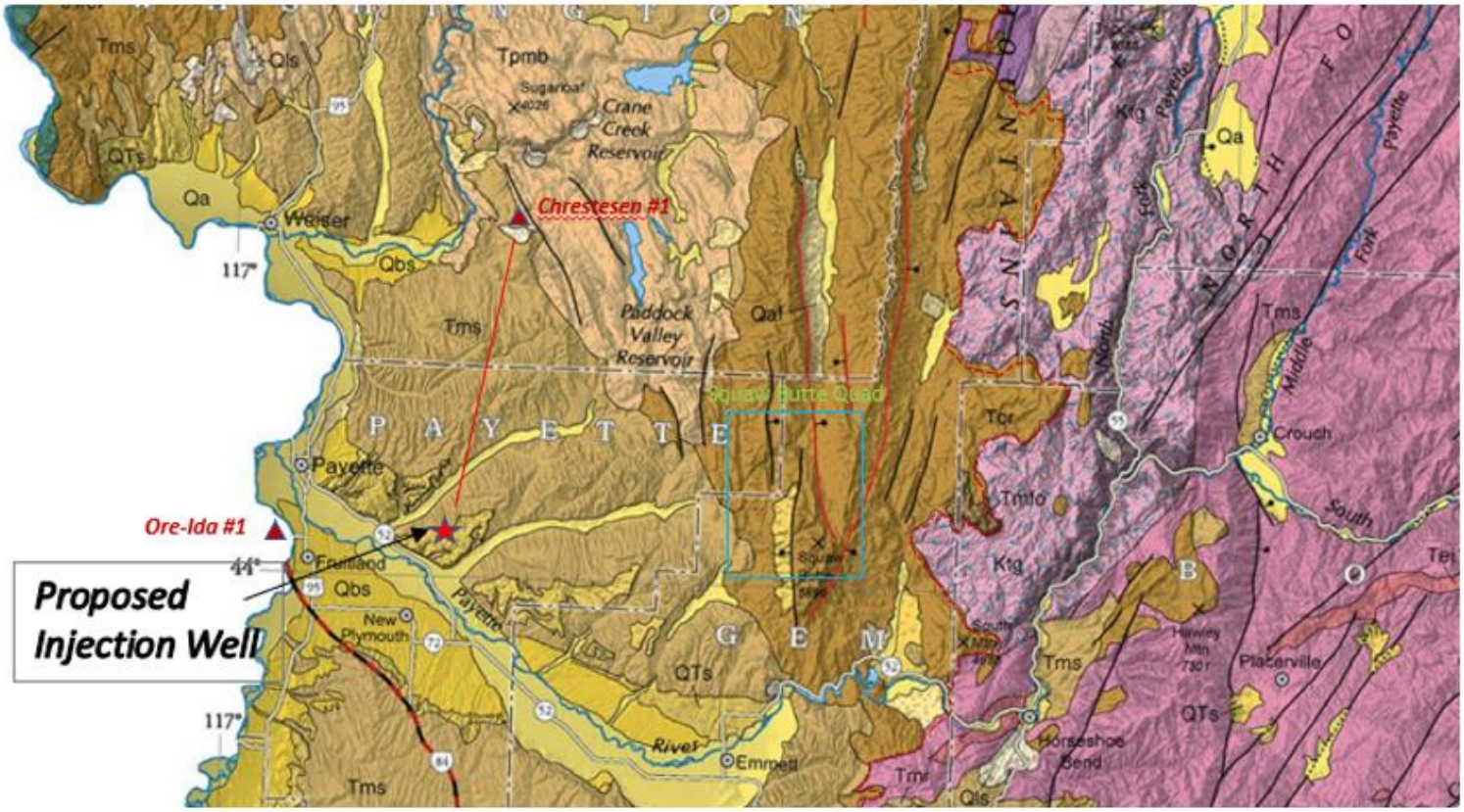

SSW

NNE

Prop. Inj. Well

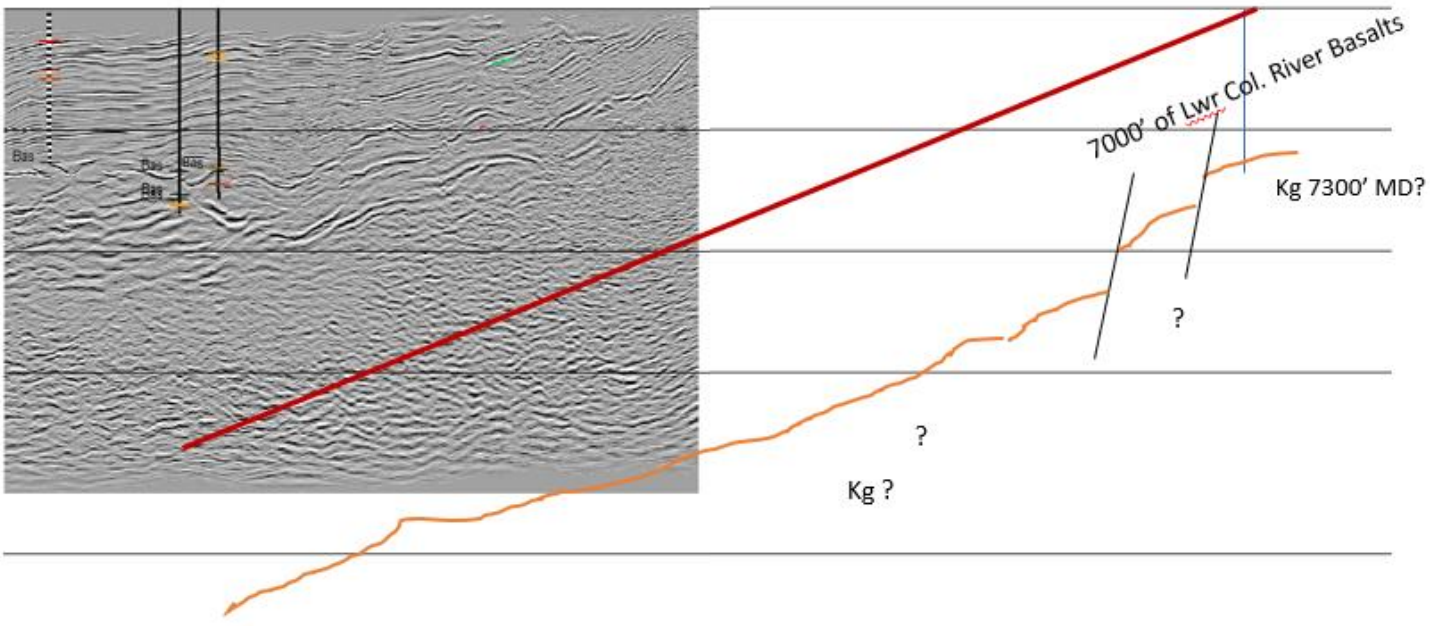

c. ***<u>Gravity and Magnetic Studies:</u> The deep structure of the WSRP has been studied by many geologists and geophysicists. Wood and Clemens (2002) did important work, and more recently Khatiwada and Keller (2017) furthered the study with new gravity, magnetic and field work. All of this work shows a very large gravity and magnetic anomaly in the WSRP. The anomalous area is due to the tremendous thickness of Miocene basalt filling the WSRP.***

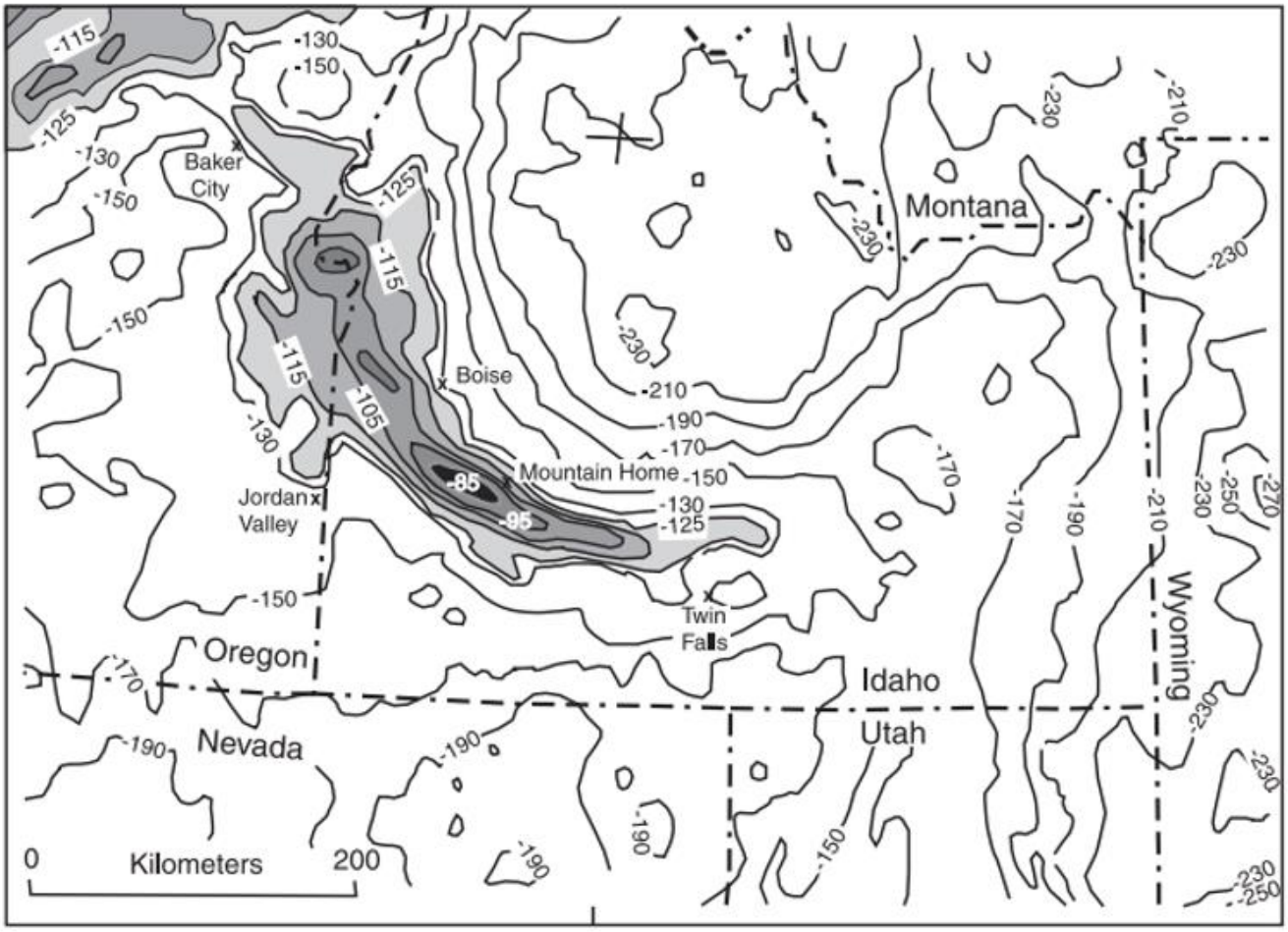

Figure 4. Map of Bouguer gravity anomalies of the western Snake River Plain region. Noteworthy is the high gravity anomaly of the western plain indicating rock of high density beneath the plain. Contour interval is 20 milligals, except for values more positive than -130 milligals. The areas of more than -125 milligals are shaded and contoured every 10 milligals. Map is from the Gravity Anomaly Map Committee (1987). Values are terrain corrected in areas of high relief. Bouguer anomalies are calculated by subtracting the theoretical attraction of rock mass above sea level using a standard crustal density of 2.670 g/cm^3. This attempts to remove the effects of varying topographic relief. Thus Bouguer anomalies result from masses above sea level with densities different from 2.67 g/cm^3, or from any lateral variation of density below sea level. In continental regions, the regional values are negative because topography is usually isostatically compensated by low density crust extending below sea level. Theoretically, corrected gravity will be zero only at sea-level measuring points.

Figure 10-8: Map of Bouger gravity anomalies of the Western Snake River Plain (Wood, 2002)

Figure 10-9: North-South Crustal Interpretation (Wood, 2002)

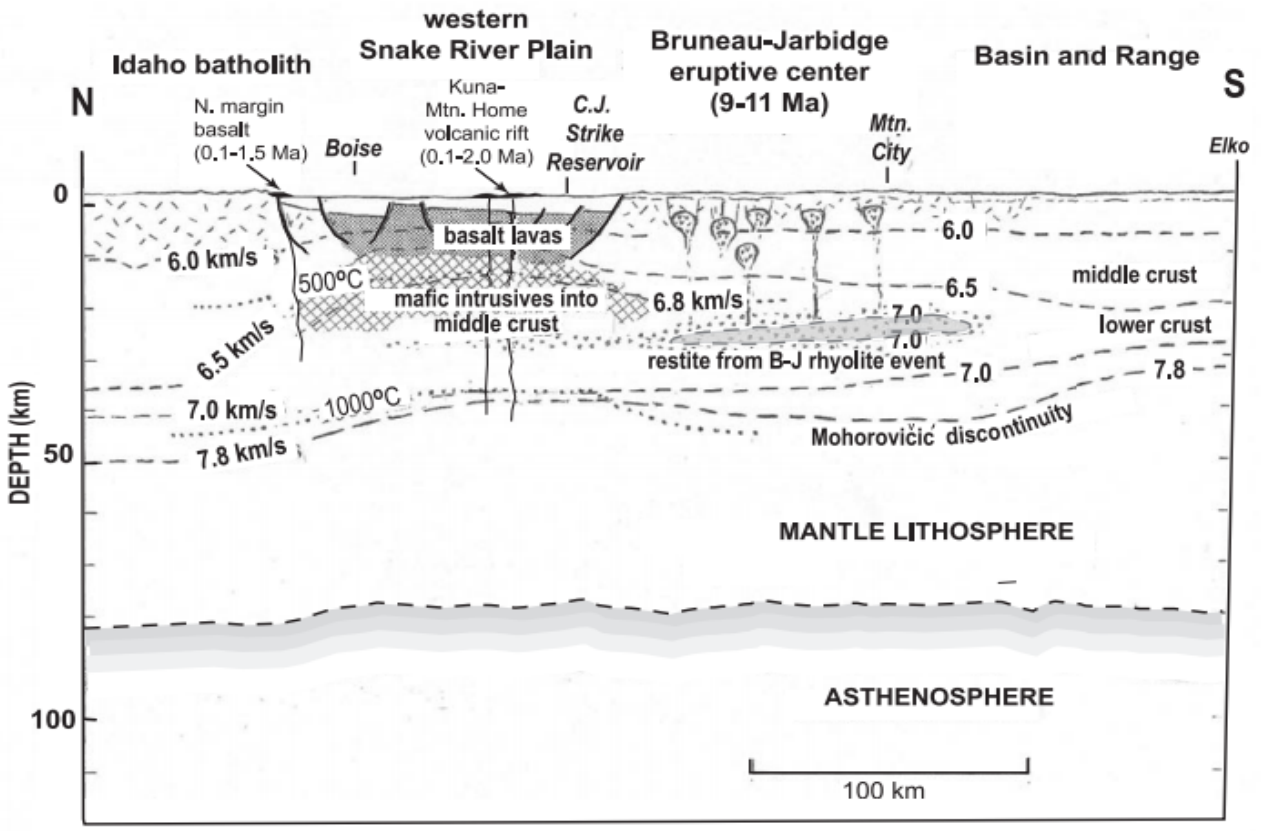

Figure 3 (A)

Figure 3. **(A)** Lithosphere structure interpreted principally from crustal structure beneath the western Snake River Plain and adjacent areas. Interpretation is based on the seismic refraction line of Hill and Pakiser (1967) and the reinterpretation by Prodehl (1979). Location of seismic line shown on map. Noteworthy is the upward bulge of material, with $V_p > 6.6$ km/s beneath the western plain believed to be mafic rock, and the overlying thin (~5 km) layer with velocity between 6.0 and 6.5, believed to be basalt flows or granite intruded by basalt. Prodehl's interpretation shows a high velocity layer ($V_p > 7.0$ km/s) that lies in the deep crust beneath what is now recognized as the Bruneau-Jarbidge rhyolite eruptive center along the track of the hot spot. We suggest the high-velocity layer might be restite remaining from the partial melt and extraction of rhyolite melt. It is important to realize that the crustal refraction velocities shown beneath the plain are obtained from arrivals into a string of detectors, south of Boise, and are an average of the crust between Boise and C.J. Strike. No experiments have explored structure beneath the Idaho batholith. The batholith structure shown is inferred from a section by Hyndman (1978) and Cowan and others (1986) and by analogy to the Sierra Nevada batholith shown by Fliedner and others (1996). Mafic intrusives in the intermediate crust were first suggested by Mabey (1976) from gravity data. Diagrammatic diapirs of silicic melts beneath the B-J area were suggested by Leeman (1989). Dotted-line isotherms are from heat-flow models of Brott and others (1978). One can only guess the depth of the asthenosphere at about 90 km (see Smith and Braile, 1993, Figure 35, for the eastern plain, and by analogy to the Rio Grande Rift, Baldridge and others, 1984, Figure 2).
(B) Prodehl's (1979) reinterpretation of refraction data and crustal structure from Boise to Elko.
(C) Map showing the location of the seismic refraction line. Labeled triangles are shot points, and circles are detector positions.

The section begins on the left with the Idaho Batholith, runs due south through Boise, crosses the WSRP and terminates at Elko, Nevada. The Creataceous granites of the Idaho batholith are shown on the left at an elevation of 2 km, in the WSRP they are downfaulted to a depth of 10 km, and overlain by 8 km of primarily basalt, topped by 2 km of lacustrine sediment. The gravity, magnetic and refraction velocity data strongly indicate that within the WSRP the basement rocks are heavily invaded by mafic intrusives, and found at a depth of 10 km below sea level.

Khatiwada and Keller (2017) carried Woods work forward with significant additional gravity, magnetic and crustal refraction velocity data collection and study.

Figure 10-10: Gravity Maps & Model of the WSRP (fig. 5 & 8 from Khatiwada, 2017)

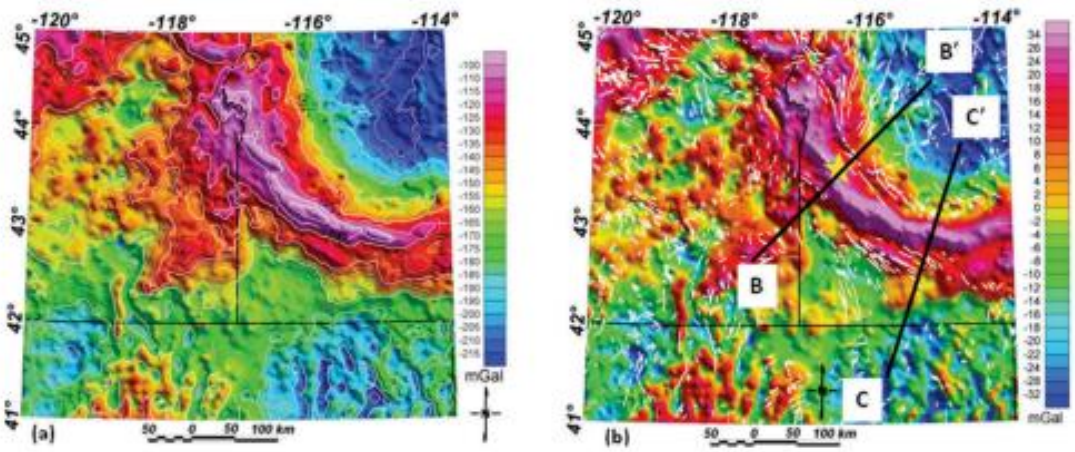

Figure 5. Gravity maps of the WSRP. (a) Complete Bouguer anomaly map of the area with major tectonic units and geographic features are identified and (b) Residual Bouguer anomaly map. B–B' and C–C' are two profiles along which gravity models were constructed in Figures 8–10. The yellow star is location of the J.N. James #1 exploratory well.

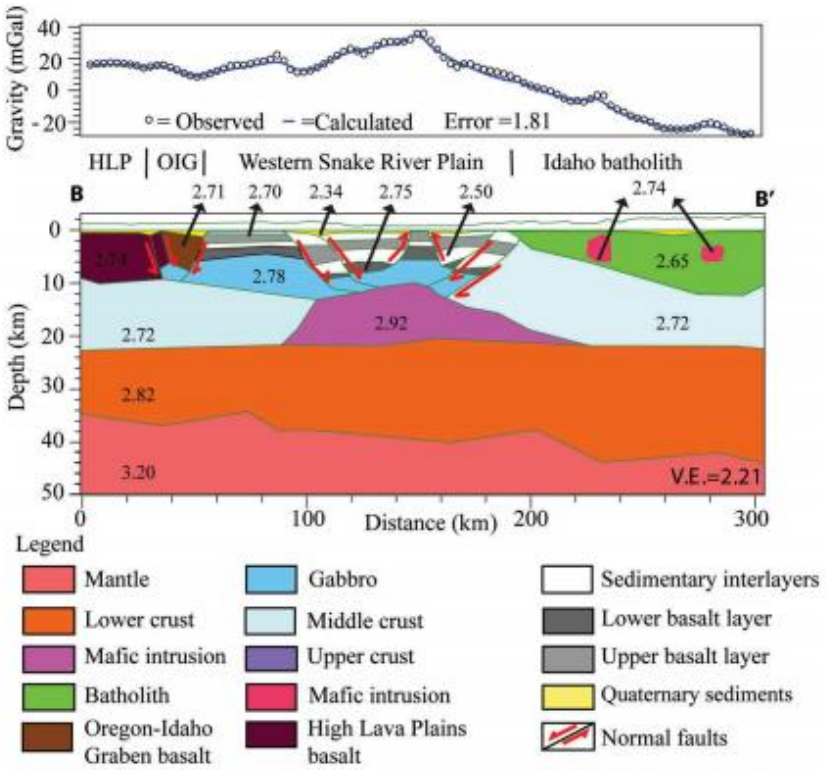

Figure 8. Gravity model across the WSRP starting from Owyhee Plateau (OwP) to the Idaho batholith along B–B' (Figure 5(b)). A mid-to-upper crustal mafic intrusive body was modelled as a major source for high gravity anomaly across the SRP. The density values are shown in g/cm^3.

The integrated crustal model presented in fig. 10-10 B-B' above was produced by integrating observed subsurface seismic velocities, gravity data, drilling results, surface geology, and a semi-iterative forward modelling technique. The methodologies employed are discussed in great detail in the Khatiwada 2017 paper, particularly on page 9. Both the Wood (2002) and Khatiwada (2017) papers are included in folder 10.

The model concludes that the crystalline basement in the WSRP is Gabbro and is typically found at a depth of 8 to 9 km (-26,000' to -30,000') below sea level. The intra-basin high that the James well was drilled on has basement interpreted to be at approximately 6 km (-19,000 subsea). Note that the James well was still in basalt at total depth of 14,006' MD (-11,455' subsea), and is on an intra-basin regional structure, which the proposed injection well is not. The proposed injection well is located north of the intra-basin high in a lower structural setting.

Khatiwada et al considered alternative solutions and another integrated crustal model is presented in the paper as figure 9, it is shown here as Figure 10-11, below:

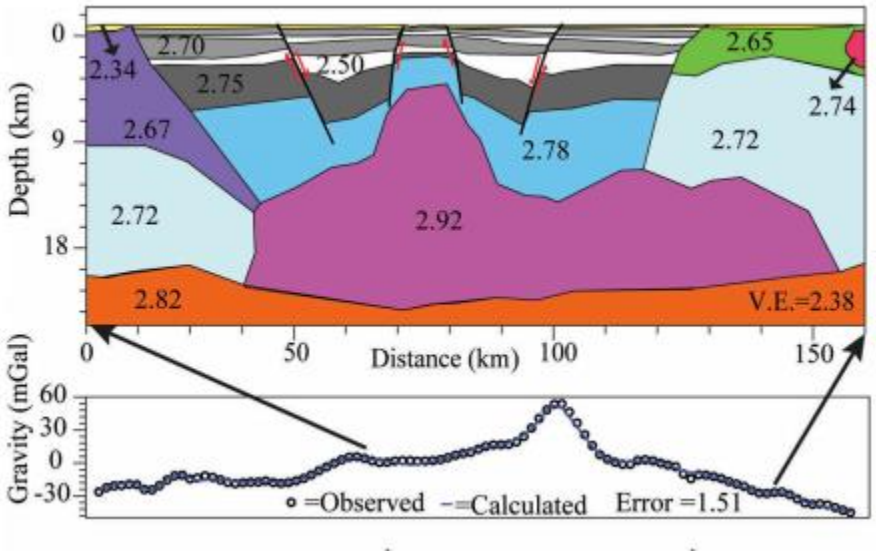

This solution interprets crystalline basement to be typically at 5 to 6 km subsea in the WSRP (-16,000' to -19,000' subsea).

The methods employed as discussed above to determine depth to crystalline basement each have their own inherent potential sources of error. Projecting the depth of crystalline granites into the basin with surface geologic mapping uses a tremendous number of data points collected at the surface, but the dip rates do change in the subsurface, leading to potentially large error. The deep well control can constrain the other methods, but the number of deep wells in the WSRP is few. Nonetheless, using the known thicknesses of the CRB/Sucker Ck. Sections in the Chrestesen and James wells, and projecting down from the top of the CRB in the Ore-Ida well gives a range of roughly -13,000 to -15,800'+ subsea for crystalline basement at the Ore-Ida well, which should be very similar to the depth of crystalline basement at the proposed injection well. The gravity/magnetic/refraction seismic velocity method utilizes an extremely large number of geophysical data points collected within and beyond the basin proper. The interpretation is constrained with surface geology, reflection seismic data, and the existing well control – however assumptions are made within the modelling process which can change the predicted depths to basement. Nonetheless, the methods consistently point to a predicted depth to basement at the injection well site to be between -14,000' to -20,000+' subsea. The estimated depth to crystalline basement at the proposed well site is conservatively stated to be -14,000' subsea. As the proposed injection zone is between -2200' and -3700' subsea, the vertical distance between the injection zone and the nearest underlying instance of crystalline basement rock is concluded to be over 10,000'.

References:

Feeney DM, Schmidt KL, Sundell AJ, Wood SH, Lewis RL, and Breedlovestrout, RL: 2017. Geologic Map of the Squaw Butte 7.5' Quadrangle, Gem and Payette Counties, Idaho: Deliverable to the U.S. Geological Survey for StateMap, scale 1:24,000, May 2017. Draft Map for Review-August, 2020.

Lewis Reed S., Link P.K., Stanford L. R., Long S. P. : 2012 Geologic Map of Idaho, Idaho Geological Survey.

Murari Khatiwada & G. Randy Keller (2017): A crustal-scale integrated geophysical and tectonic study of the Snake River Plain region, northwestern U.S.A., International Geology Review, DOI: 10.1080/00206814.2017.1303647

Wood, S.H., and D.M. Clemens, 2002, Geologic and tectonic history of the western Snake River Plain, Idaho and Oregon, in Bill Bonnichsen, C.M. White, and Michael McCurry, eds., Tectonic and Magmatic Evolution of the Snake River Plain Volcanic Province: Idaho Geological Survey Bulletin 30, p. 69-103.

11. ***To supplement Attachment G, detail whether there are any known fluid transmission routes between the Willow Sands and basement rock.***

There are no known fluid transmission routes between the Willow Sands and basement rock. Crystalline basement rock is estimated to be at or below -14,000' subsea at the location of the proposed injection well (Discussed in section 10). In order to communicate through 10,000' feet of underlying section there would need to be a transmissive fault or fractured section that communicates with basement rock. Neither of those conditions exist in this area.

The normal faults that are present in the area are small scale, syn-depositional faults that do not connect with basement rocks. They often terminate at depth into a parallel antithetic fault, or sole out at 90 degrees on a basalt surface. They typically have small throw of 50' to 200' or less, are short in length (typically a few thousand feet or less) and most are buried by younger section and do not reach the surface. These are all characteristic features of inactive depositional faults. It should be noted that applicants have an extensive 300 plus square mile proprietary 3-D seismic data set surrounding the Willow Field area. The excellent quality of the data allows very high confidence to the statements above and the subsurface interpretations that are made.

The observed declining pressure versus time data of the adjacent Willow Field oil and gas wells conclusively shows that the individual reservoirs are confined. For this to occur, the laterally adjacent faults must be sealing. Potential sealing mechanisms for the faults - clay smear and silica cementation – are common in the area and discussed in section 7. In order for the adjacent Willow Sand reservoirs to:

1. ***"pressure deplete" as they have,***
2. ***show different original gas/water contacts across the faults as they do,***
3. ***and have differing pressure versus time behavior across faults as they do, the adjacent faults must be non-transmissive.***

For the adjacent Willow Sand reservoirs to "pressure deplete" there must also be competent bottom seals or confining layers present below them. Otherwise water from deeper Willow Sands would recharge the pressure in the hydrocarbon reservoir that was being produced. The same lower confining layers exist below the Willow Sands in the proposed injection fault block. The lower confining layers in fault block E, as well as the deeper volcanic section below the fault block are discussed in section 9 in detail. The conclusion of extended testing of the lower volcanic section in the Ore-Ida well was that it is not sufficiently permeable to allow geothermal waters to flow through it. The Ore-Ida volcanic section tested is stratigraphically equivalent to the volcanic section underlying the Willow Sands in the area of the injection well. In summary, there appears to be a competent confining layer below the Willow Sands in

the volcanic section, as well as the interbedded claystone sections which separate the various Willow Sand members. This lower confining layer should provide a thick and competent barrier preventing communication to basement rock.

A separate type of evidence to consider in addressing the transmissibility question is empirical geothermal data. The Idaho Dept. of Water Resources has a long running Geothermal Investigations in Idaho series. The department studied the area of the proposed permit in Water Information Bulletin No. 30, Geothermal Investigations in Idaho Part 11, 1981. The report presents a cross section (Fig. 11-2) and map (Fig. 11-1) from the area of the Chrestesen well extending down to southeast of the proposed injection well. The report concludes that there is very little groundwater movement in the sediments of the Idaho Group (Chalk Hills and Glenns Ferry) in the area around the proposed injection well. This conclusion implies no upwelling fluids from basement rocks.

Figure 11-1

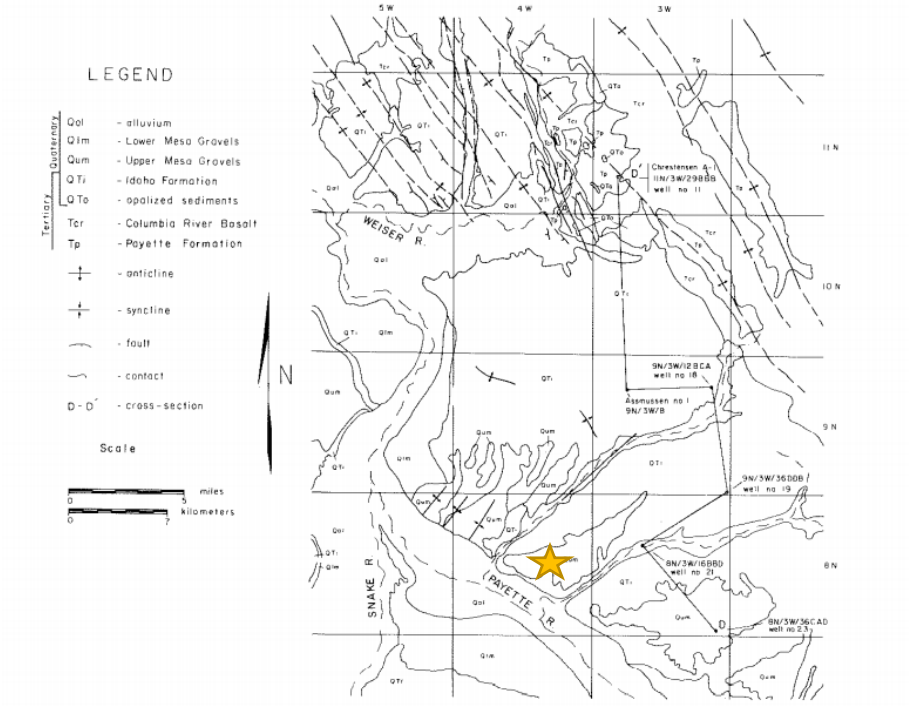

FIGURE 5-14. Generalized geologic map of the Weiser-Crane Creek area and location of D-D' section. Adapted from Kirkham (1931); Savage (1958); Young, et. al. (1977).

Figure 11-2

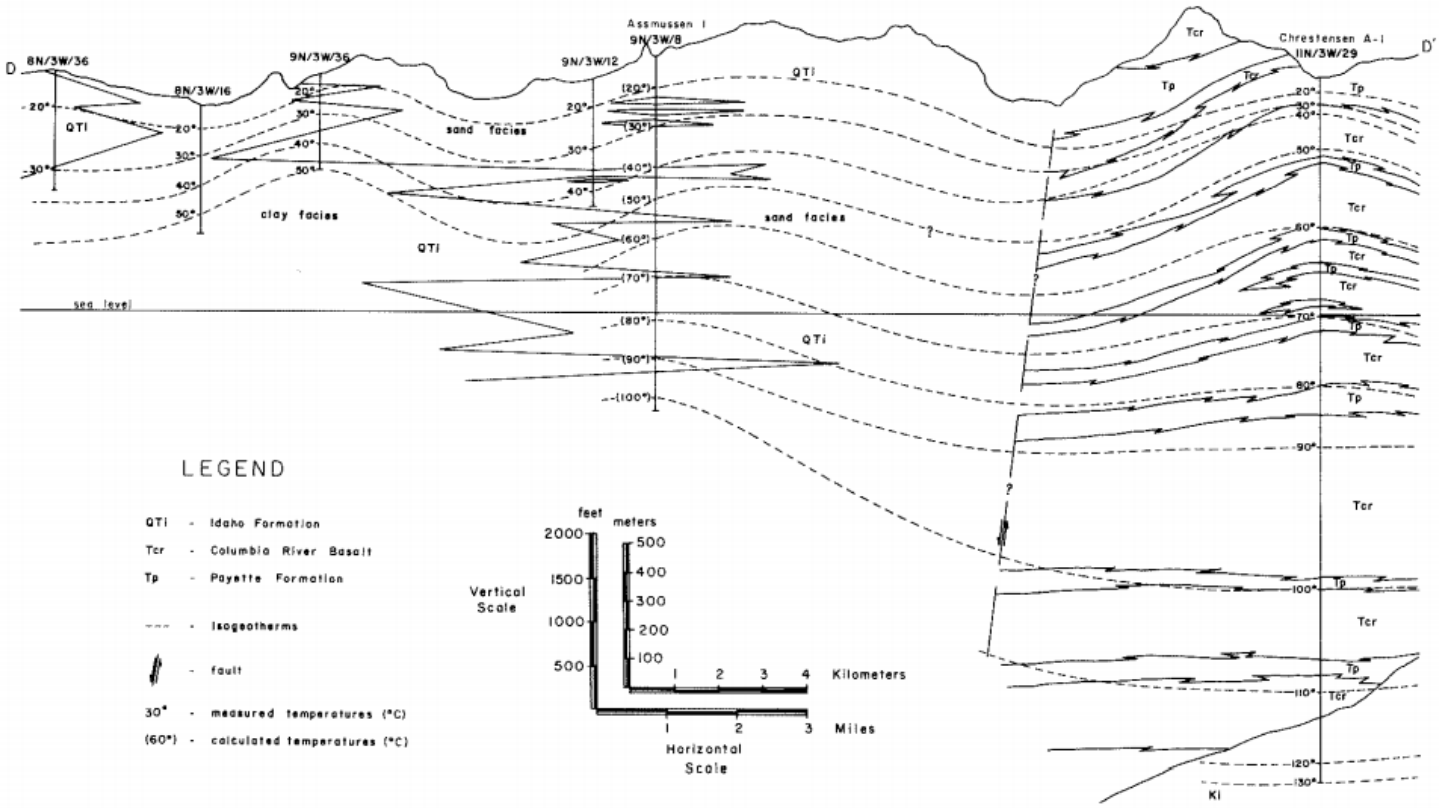

FIGURE 5-15. Cross section D-D' in the Weiser-Crane Creek area.

In figure 5-15, plotted isogeotherms show that near-surface topography affects the subsurface temperatures causing the isogeotherms to parallel the ground surface. In the Christensen A-1 well, No. 11, the isogeotherms appear to be crowded beneath the Payette Formation which overlies the basalts. This is interpreted to be an expression of upward-moving groundwater convecting deep temperatures toward the surface. Farther to the south, the temperatures of holes drilled in the Idaho Group indicate very little groundwater movement (linear temperature gradients) and the isogeotherms are evenly distributed.

References:

Mitchell JC,_WATER INFORMATION BULLETIN NO. 30, GEOTHERMAL INVESTIGATIONS IN IDAHO PART 11, Work performed under U.S. Department of Energy Contract No. DE-AS07-77ET28407 Modification No. A003 Designation DOE/ET /01834-3 Idaho Department of Water Resources, 1981

12. To supplement Attachment G, submit information on the seismic history of the area from available records, including the presence and depths of seismic sources.

While central Idaho has an active seismic history, the WSRP basin itself has been very quiet seismically for the last 120 years of recorded seismic measurements. Figure 12-1 below is the USGS map of all recorded seismic events for southwest Idaho since 1900. The proposed injection well site is indicated with an arrow and yellow star. The green outline is the -125 milligal gravity contour from Wood (2002), which indicates the outline of the WSRP basin. Note that all the 2800+ events are outside of the basin or on its margin except a few, discussed following.

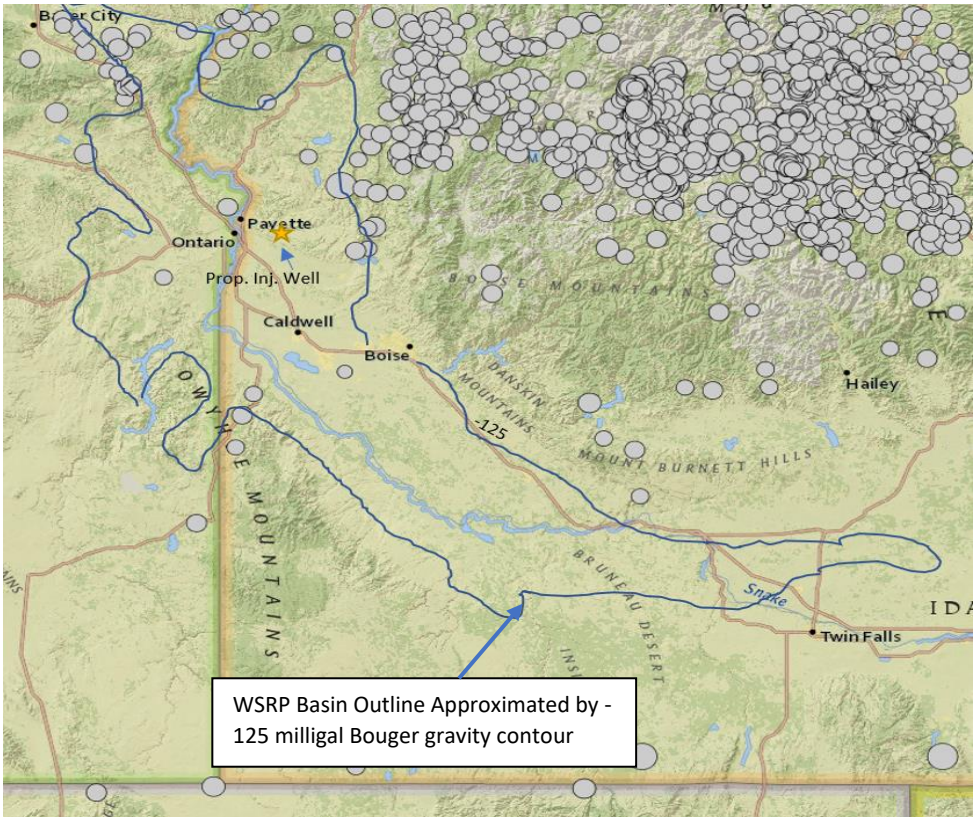

Figure 12-1: USGS Earthquake Map

The -125 milligal gravity contour placed on the map is significant, in that it shows the area of the extensively emplaced, several thousands of feet of Columbia River and later basalts which filled the WSRP. This emplacement largely occurred 17 to 14 million years ago. The active seismicity in Idaho can be seen on the previous map in central Idaho on the exposed basement rocks of the Idaho Batholith.

<u>Figure 12-2</u> below is the same Fig. 1 map but "zoomed in" to focus on the area around the proposed injection well, the circle is a radius of 10 miles, the map covers a 1200 square mile, 30 by 40 mile area. There has only been one event recorded in this entire area in the last 120 years (gray dot 13 mi. NW of well site, 7.5 mi. N of Ontario, OR.)

Figure 12-2: USGS Earthquake Map - focused on part of northern WSRP

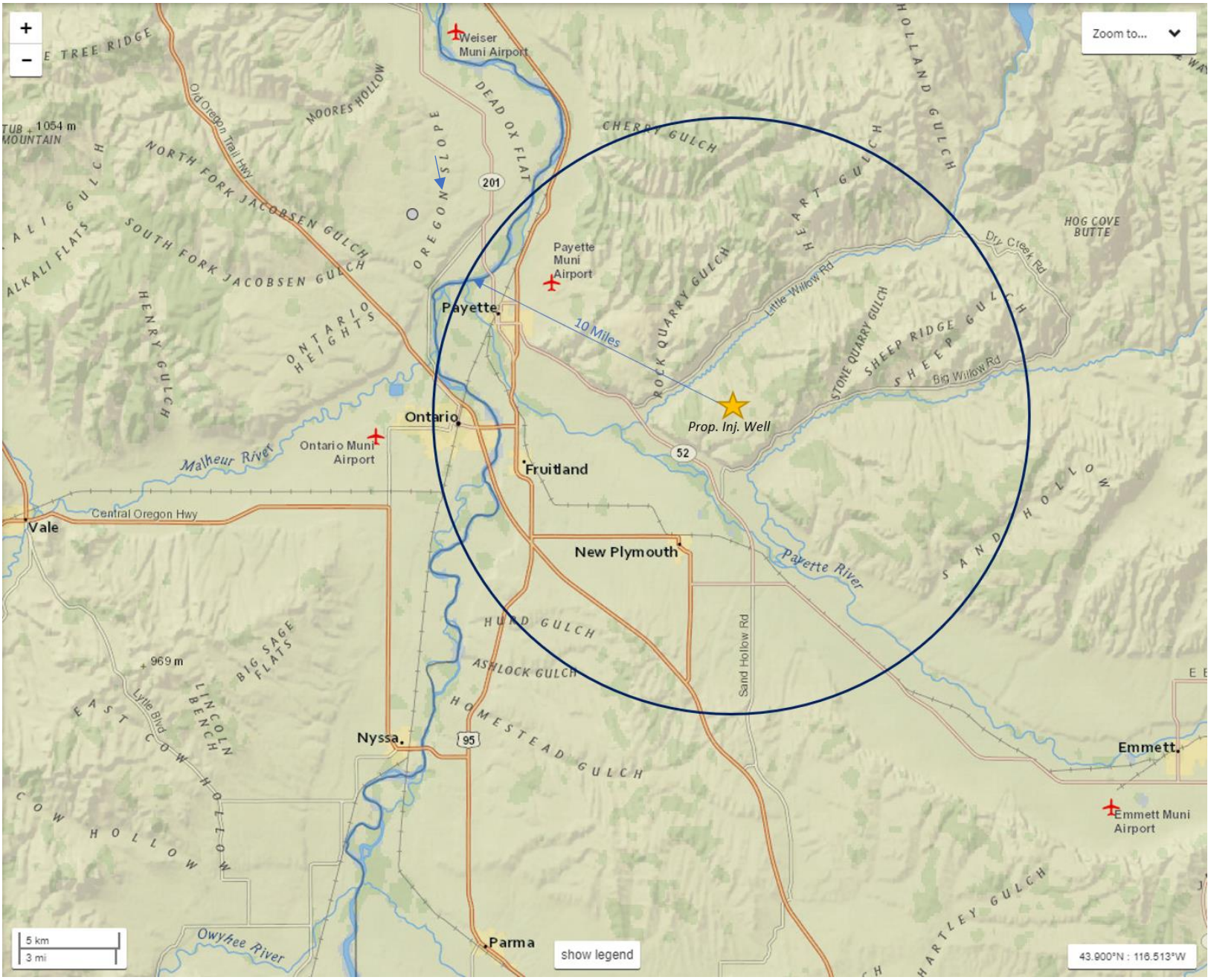

The event north of Ontario, OR was measured at M 2.9, occurred in 1989, and was calculated to occur at 0.8 km elevation above sea level, which is close to the ground elevation of that area. Events of this magnitude cause no damage, and are generally not felt by most people. The other seismic events recorded in the basin are shown on figure 12-3 below. They are very small magnitudes of 0.0, 0.0, 0.2, 1.4, and 2.3. The 2.3 event is at the southern end of an active fault system 25 miles east of the well site. The 1.4 event is on the southwest basin margin.

Figure 12-3: USGS Earthquake Map

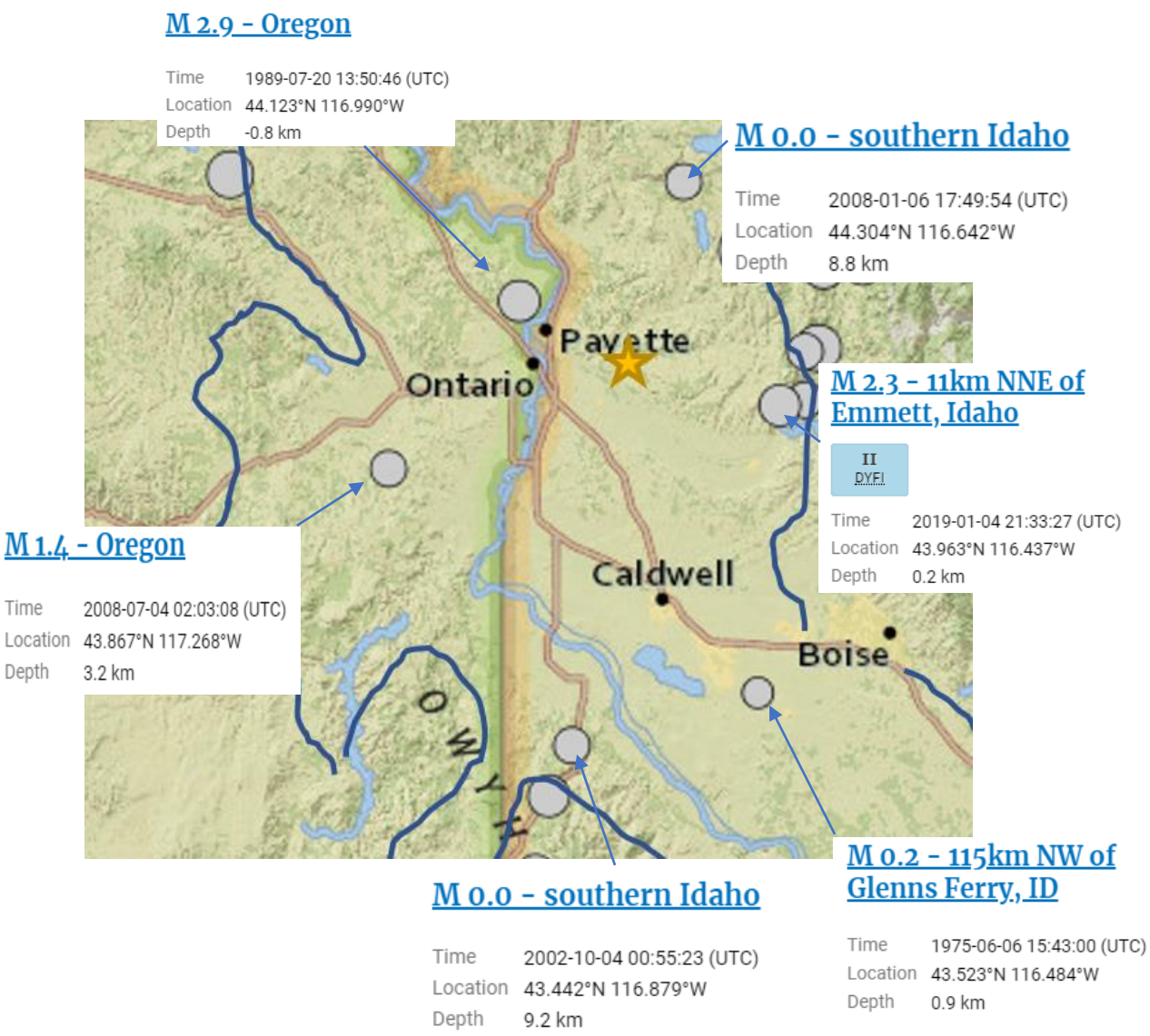

13. To clarify Attachment H, explain how the porosity of the injection zone was estimated and indicate how many data points were used to make this estimate?

a. The 23% porosity value was chosen by performing a general visual inspection of the Schlumberger Triple Combo Density-Neutron Porosity – Propagation Resistivity Log (open hole log 9/18/14). Density and Neutron curves were evaluated throughout the entire Willow sand section from 4910' – 5390' (proposed Inj zone). These curves suggest that the porosity, in general, range between 21% and 24%. Using a 23% value porosity is a reasonable measurement and provides a conservative approach when used in the volumetric calculations completed in the hydraulic model (Att H-1). See log section below Figure 13-1:

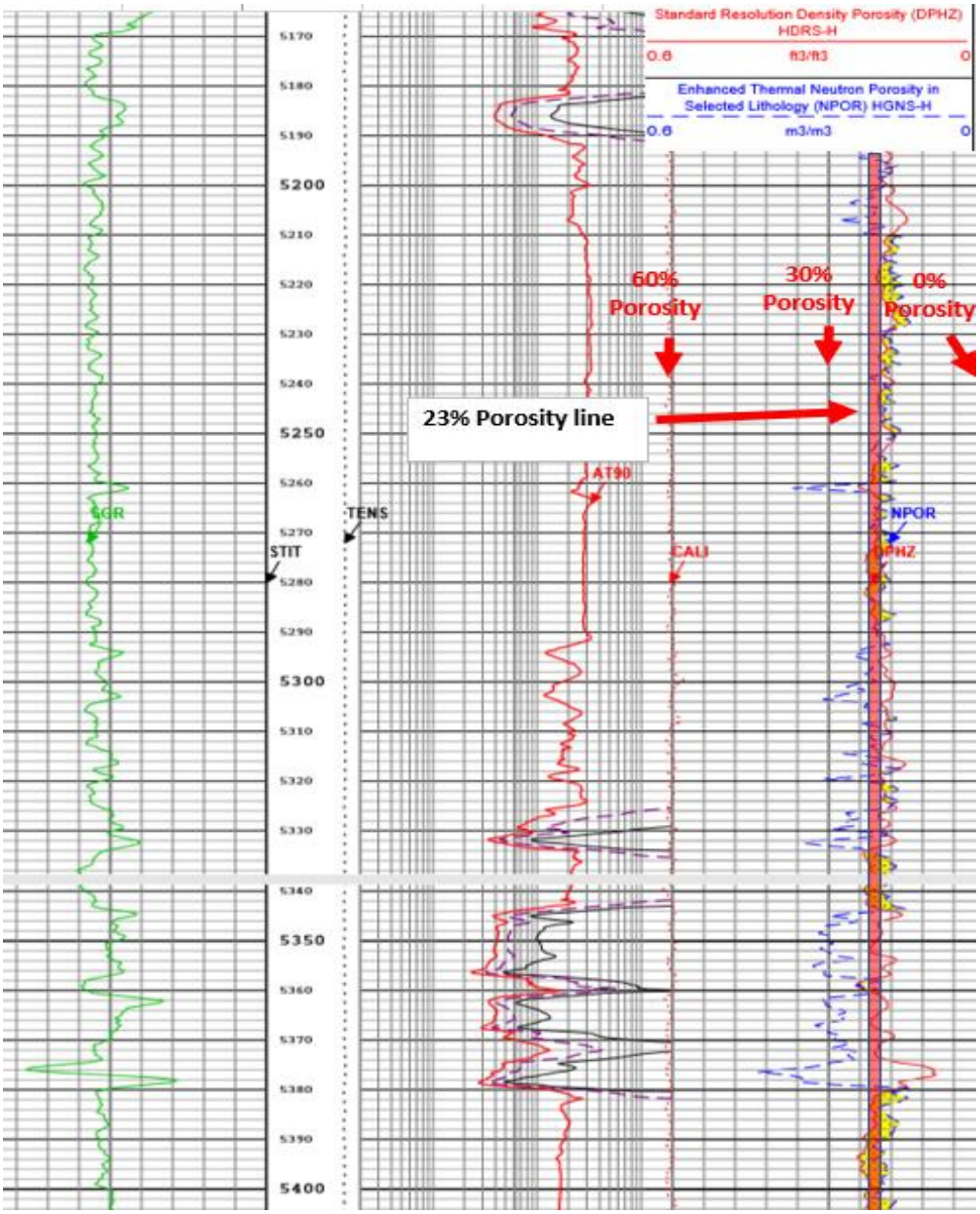

14. To clarify Attachment H, how was the water saturation value (80%) determined?

a. *The water saturation(Sw) for Attachment H was based on the assumption that the reservoir is a binary water / gas reservoir and that the residual gas exists due to prior movement of natural gas through this sand and subsequent movement of water, trapping gas and leaving behind a residual gas saturation. Production of a gas reservoir with a strong water drive is the analogy used for this model. Since 20% was assumed for the residual gas saturation Sgr, the Sw was determined to be the other 80% of the pore space.*

   The assumption of Sgr was utilized because direct calculation of Sw has been historically difficult because of the variation of salinity observed in the Willow Sands in this area. Most often the only practical way to prove that a zone was hydrocarbon productive was to perforate the interval and flow test the well. The DJS 2-14 Well was perforated and swab tested. During the completion attempt for this sand (5380-90') the zone did not flow naturally, and underwent swab testing for two (2) days. There were good gas shows observed during the swabbing operations indicating a reservoir with gas present (See Attachment 14 A-1). The water samples recovered also contained significant BTEX fractions, indicating the presence of natural gas, similar to the water samples from productive intervals elsewhere in this field.

   Calculations of Sw were made using a variety of Rw values and indicate a value in the 75 – 89% range. See Attachment 14 A-2 for details of this estimate.

   The residual gas saturation (Sgr) is often utilized in volumetric resource estimates and has been studied because this is a key factor in predicting and determining how much gas will be recovered from a reservoir. One of the most common and basic sources that is frequently referenced is a table (B.C. Craft and M.F. Hawkins, 1991) *of residual gas and water saturations as shown below in Figure 14 A-1 The section shown there of consolidated sandstones is most representative of the subject Willow Sands. This illustrates how fairly consistent the residual saturations appear to be for these consolidated conventional commercial production zones. In this area of focus (Willow sands), the sands can typically be characterized as clean and consolidated sandstones with high permeable beds and porosities ranging from 20% - 33%. According to Figure 14 A-1, this suggests that the residual gas saturation should range between 25% - 38%.*

Craft and Hawkins - Applied Reservoir Petroleum Engineering 2nd Edition 1991

The residual gas saturation can be measured in the laboratory on representative core samples. Table 3.3 gives the residual gas saturations that were measured on core samples from a number of producing horizons and on some synthetic laboratory samples. The values, which range from 16 to 50% and average near 30%, help to explain the disappointing recoveries obtained in some water-drive reservoirs. For example, a gas reservoir with an initial water saturation of 30% and a residual gas saturation of 35% has a recovery factor of only 50% if produced under an active water drive (i.e., where the reservoir pressure stabilizes near the initial pressure). When the reservoir permeability is uniform, this recovery factor should be representative, except for a correction to allow for the efficiency of the drainage pattern and water coning or cusping. When there are well-defined continuous beds of higher and lower permeability, the water will advance more rapidly through the more permeable beds so that when a gas well is abandoned owing to excessive water production, considerable unrecovered gas remains in the less permeable beds. Because of these factors, it may be concluded that generally gas recoveries by water drive are lower than by volumetric depletion; however, the same conclusion does not apply to oil recovery, which is discussed separately. Water-drive gas reservoirs do have the advantage of maintaining higher flowing wellhead pressures and higher well rates compared with depletion gas reservoirs. This is due, of course, to the maintenance of higher reservoir pressure as a result of the water influx.

TABLE 3.3.
Residual gas saturation after water flood as measured on core plugs
(After Geffen, Parish, Haynes, and Morse[5].)

Porous Material	*Formation*	*Residual Gas Saturation, Percentage of Pore Space*	*Remarks*
Unconsolidated sand		16	(13-ft Column)
Slightly consolidated sand (synthetic)		21	(1 Core)
Synthetic consolidated materials	Selas Porcelain	17	(1 Core)
	Norton Alundum	24	(1 Core)
Consolidated sandstones	Wilcox	25	(3 Cores)
	Frio	30	(1 Core)
	Nellie Bly	30–36	(12 Cores)
	Frontier	31–34	(3 Cores)
	Springer	33	(3 Cores)
	Frio	30–38	(14 Cores) (Average 34.6)
	Torpedo	34–37	(6 Cores)
	Tensleep	40–50	(4 Cores)
Limestone	Canyon Reef	50	(2 Cores)

Figure 14 A-1 – Residual Gas Saturation for water drive reservoirs

A conservative approach was used when assigning Sg to the injection capacity calculation (Attachment H in the Inj permit), where a Sg of only 20% was assigned. That left the Sw to be assigned an 80% value.

The accuracy of the injection capacity calculation is difficult to define because of the number of variables and the number of estimations required to generate variables in the capacity estimation. As is often the case with reservoir engineering and geologic problems, empirical correlations were used when calculating the reservoir capacity for Fault Block E. These include rock compressibility, water compressibility, and gas

compressibility. Each of these are based on basic criteria for each material/fluid and are subject to varying from the true values. The estimated reservoir bulk volume from planimetering the gross isopach map of Fault Block E is based on the seismic interpretation and should not have too much error, unless there are some small unseen faults that also seal and create a barrier to flow in the fault block. The question of heterogeneity also could come into play for porosity and the saturations assumed. Also, the limiting final reservoir pressure was based on a fracture gradient of 12 ppg, which is believed to be conservative but could be higher by 2-3 ppg or lower by 1 ppg. The gas saturation is a sensitive variable, because of the significantly larger compressibility of gas over the compressibilities of water and the rock matrix. One could do a Monte Carlo type assessment of the sensitivities and variability of the estimate, but it is doubtful that would add any real value to this application. Based on our experience and the given data, it is believed that the current estimated reservoir capacity is conservative.

References

B.C. Craft and M.F. Hawkins, R. b. (1991). *Applied Petroleum Reservoir Engineering.* Englewood Cliffs, N.J., United States of America: Prentice Hall.

Attachment 14 A-1 Work Reports documenting gas blows

WELL:	DJS Properties 2-14		
Oct 19 2014	RIG SUPERVISOR:	Jeff Janik	
	OPERATIONS AT REPORT TIME:	Drill out cmt	
	Ru rig x equipment. Remove blind flange on top of frac valve. Install BOP's. Test to 3000#; OK. PU x GIH x 6" bit x csg scraper x 135 jts 2 7/8" tbg. SWIFN.		
	24 HR FORECAST:	Drill cmt. run logs	
	DAILY JOB COST:	$16,400	TOTAL JOB COST: $584,927
	TOTAL WELL COST:	$1,568,476	
Oct 20 2014	RIG SUPERVISOR:	Jeff Janik	
	OPERATIONS AT REPORT TIME:	POH x tbg	
	Move testers from 1-11 to location. RU same. PU 2 jts tbg x tag top of fill at 5082'. Drl hard cmt for 2 jts. Got gas to surface. Circ out gas for 20 min. continue in hole. Washed sand down 9 jts to top of float collar. Circ well clean. Test csg to 1500#. OK. Lay down 11 jts tbg. SWIFN		
	24 HR FORECAST:	PLH; log well	
	DAILY JOB COST:	$21,940	TOTAL JOB COST: $606,867
	TOTAL WELL COST:	$1,590,416	
Oct 21 2014	RIG SUPERVISOR:	Jeff Janik	
	OPERATIONS AT REPORT TIME:	GIH x tbg to swab	
	SIP - 0. POH x 2 7/8" tbg. Load well w/12 BW. RU Warrior Wireline. GIH x CBL. Log from 5408' to surface. Indicates TOC at 4300'. Pump into surface csg ARO 2 BPM at 300#. Notified IDL of top job on surface tomorrow. GIH x PNN tool x log from 5408-4200'. POH x tools. SWIFN		
	24 HR FORECAST:	Swab well, perf, test	
	DAILY JOB COST:	$36,750	TOTAL JOB COST: $643,617
	TOTAL WELL COST:	$1,627,166	
Oct 22 2014	RIG SUPERVISOR:	Jeff Janik	
	OPERATIONS AT REPORT TIME:	Swabbing	
	SIP - 0. RU Cementers. Pump 9 cu yds cmt down surface csg for top job. Pump in ARO 2 BPM at 300#. RD cementers. GIH x tbg to 2800'. Swab well to 1000'; recovered 32.4 BW. Cl - 25,454, 8.7 ppm. RU E line. GIH 3 1/8" csg gun x perf 5380-90' ELM w/4 JSPF x 90 deg ph. No psi after perf. RD wireline. GIH x 2 7/8" tbg to 5100'. RU swab. Tag fluid at 550'. Made 11 runs with fluid staying at 1500'. Recovered 37 BW x no show of oil. Had good gas blow after each swab run. Cl on last run was 31,515 ppm. SWIFN.		
	24 HR FORECAST:	Swab well, flowback	
	DAILY JOB COST:	$25,900	TOTAL JOB COST: $669,517
	TOTAL WELL COST:	$1,653,066	
Oct 23 2014	RIG SUPERVISOR:	Jeff Janik	
	OPERATIONS AT REPORT TIME:	JSA	
	SITP - 25#. SICP - 25#. Took gas samples x bled to 0. GIH x swab x tag fluid at 900'. Swabbed well. Made 27 runs x recovered 158 BW. 1st run had Cl - 24,200. Final run Cl - 601. Had gas blow with each swab run. Saw some gas vapors with swab runs. Will catch gas samples in the AM. SWIFN		
	24 HR FORECAST:	Set retainer to isolate perfs and perf new zone at 5358-60.	
	DAILY JOB COST:	$15,670	TOTAL JOB COST: $685,187
	TOTAL WELL COST:	$1,668,736	

Attachment 14 A-2

Calculation of Sw, using various sources for Rw

Using Archie's equation for determining water saturation (Sw)

Archie's Equationn: $Sw = \sqrt{Ro/Rt}$

Where:

*Ro = F*Rw*
F = Formation Factor
Rw = Resistivity of water
Rt = True Resistivity

Rw values used in the calculation of Sw for the DJS 2-14:

1. Avg Rw across multiple wells: Used water analysis data from samples taken from Willow sands from five (5) different wells (inclusive of DJS 2-14). All Rw values from analysis reports were corrected to reservoir temperature and averaged. The average Rw value was then included into the Sw calculation. *Average Rw = 0.97 Ohm* m*

2. Rw from a single well (DJS 2-14): Used water analysis data from samples taken from the Willow sand within the DJS 2-14 well only. The Rw value reported in the analysis was corrected to reservoir temperature and included into the Sw calculation as well. Rw = 1.37 Ohm*m

The following data set shows the various Rw values and their average for five (5) different wells within the Willow area. Also included are the corresponding Sw and Sg calculations.

Well Name	Rw (surf) Ohm*m	Rw (corr) Ohm*m	Sw %	Sg % (1 – Sw)
DJS 1-15	3.05	0.79		
DJS 2-14	5.32	1.37	0.89 ~ 89%	0.11 ~ 89%
ML 1-11	3.42	0.88		
ML 2-10	2.56	0.66		
ML 1-10	4.42	1.14		
Average Across All Wells	Avg	Avg		
Average:	3.75	0.97	0.75 ~ 75%	0.25 ~ 25%

**Due to the variations in Rw, Sw ranges between 75% - 89% when inserting an Rw of 0.97 and 1.37 into the Sw equation respectively.*

In should be noted that the Formation Factor and True Resistivity were kept constant when calculating the Sw in both scenarios. It is key to note that any increase in the porosity value within Archie's equation, will result in a significant decrease in Sw and an increase in Sg. As stated, the porosity value of 23% has been used throughout the application, and is believed to be a conservative measure relative to sidewall core data as well as sonic log data for the DJS 2-14.

15. To clarify Attachment H, what log characteristics were used to determine the net reservoir thickness?

Multiple independently measured log characteristics and other types of evidence were used to determine the net reservoir thickness:

a. The "Mud Log" is a record of the physical descriptions of samples of the rock being drilled displayed versus depth. These samples are analyzed under a microscope in real time, on the drilling location in a portable laboratory trailer. A copy of the mud log for this well is available in sub-folder 15 in the electronic files, as well as at the following link:

https://ogcc.idaho.gov/wp-content/uploads/sites/88/2017/12/1107520023_DJS2-14_MUD_20140916_PTS.pdf

The Willow Sand section is shown to be typically 90% to 100% quartz sandstone from 4910' to total depth of 5500' MD, a 590' thick gross interval. Also present in this dominately massive sand section are thin claystones and tuffs (ash beds). Subtracting out the thin claystones, tuffs and low-permeability sands from the 590' thick gross interval results in an approximate 500' thick net reservoir thickness.

b. The open-hole "Triple Combo" log provides other independently measured physical properties that are used to determine net reservoir thickness. A digital copy of the Triple Combo log is included in sub-folder 15 in the electronic files and also available at the following link:

https://ogcc.idaho.gov/wp-content/uploads/sites/88/2017/12/1107520023_DJS2-14_TriCombo_1in5in_20140918_PTS.pdf

1.) The Gamma Ray log passively measures the natural emission of gamma rays by the formation versus depth as the tool is slowly pulled back to the surface from total depth. The sands here typically have values of 60 to 70 API units, shales and claystones read higher values of 80 to 115 API units due to the higher occurrence of radioactive elements in the shales/claystones.

2.) The Induction Logs measure the resistivity of the formation to an induced electric current at varying depths of investigation (10", 30" 60" and 90"). These logs are an excellent indicator of permeability. Porous and permeable sandstones near the wellbore are flushed of their native water and invaded to a depth of several inches by filtrate from the drilling fluid, the same sands are not flushed or affected by the filtrate chemistry farther away from the wellbore. This results in different resistivity readings from the shallow (10" curves) to the deepest (90" curves) if the sands are flushed, thus providing an excellent qualitative indicator of formation permeability.

3.) The Neutron/Density porosity logs measure the porosity of the formation versus depth using 2 independent methods. The Neutron tool primarily measures the presence of Hydrogen. In a clean, water saturated sandstone it typically reads very accurately and the same

porosity values as the Density log. Claystones have high levels of hydrogen bound in the mineral structure of the clays, and thus the Neutron log will read anomalously higher porosity values than reality. Cross checking with the Gamma Ray log avoids a false interpretation. The Density log reads the bulk density of the formation. The known matrix density is an input (here 2.65 g/cm3), the departure from that value is assumed to be water filled porosity and is displayed as such.

16. ***To clarify or modify Attachment H, why were two depths (5,150 ft. and 5,390 ft.) used to estimate a fracture pressure of 3,214 psi?***
    a. *The frac pressure estimate of 3,214 psi is associated with the mid-point of the Willow sand package [(5,390' – 4,910') / 2] + 4,910 = 5,150'). The frac pressure referenced at 5,390' on page 39 is a misnomer and to be consistent, it should read "The Frac pressure in the Willow Sand package at 5,150' (MP) has been estimated to be 3,214 psi". <u>Note:</u> Regardless of the frac pressure estimate, a step-rate-test will be performed which will define the actual operating limits.*

17. ***To supplement Attachment H, describe how the industry-standard correlations for water, gas, and pore space compressibility were chosen.***
    a. *Water Compressibility – Osif's correlation for water compressibility (Cw) was chosen as it is one of the most common correlations to use for determining water compressibility. Osif's Correlation Conditions include: Pressures between 1,000 psi – 20,000 psi, Temperatures between 200 – 270 deg F, and NaCl concentrations up to 200 g/L. All three (3) parameters are applicable to the Willow sand in terms of reservoir characteristics.*
    b. *Gas Compressibility – Meehan et al are constituents who created a simple calculator (Excel based) method for determining various PVT data including gas compressibility. Originally, a module was created by Hewlett-Packard called The Petroleum Fluids Pack, in which Meehan et al assisted in developing (circa 1980's). One of the most important factors that is built into the modular PVT calculation mentioned above, is the Standing & Katz correlations for determining the gas deviation factor (Z-factor). This widely used correlation is prominent in virtually all applied reservoir engineering calculations for understanding gas behavior in gas reservoirs.*
    c. *Rock Pore Volume Compressibility – A correlation developed by Hall, in which it is the most well known and widely used correlation for determining rock compressibility. The correlation is a function of porosity and is an adequate measure of rock compressibility within a sandstone that is normally pressured.*
18. ***To supplement Attachment M, submit any cement bond logs performed on well DJS 2-14.***

A cement bond log was run in the DJS #2-14 well and filed with the State of Idaho. It is available at the following link:

https://ogcc.idaho.gov/wp-content/uploads/sites/88/2017/12/1107520023_DJS2-14_CBL_20141020_PTS.pdf

A digital copy of the cement bond log is also located in the electronic files folder submitted along with these responses.

19. ***To clarify Attachment M, please explain any directional deviation of the DJS 2-14 wellbore. If necessary, clarify depth identifiers (e.g. MD vs. TVD) in the application.***
    a. ***A directional survey was run in the DJS #2-14 well using gyroscopic tools. The well was drilled as a "straight hole", but due to the nature of rotary drilling the bit and drill pipe are rarely exactly vertical (0 degrees), but are often very slightly inclined 0.1 to 2 degrees from the vertical axis. There is typically a very slight helical path described by the bit around the intended vertical axis of the wellbore. The directional survey measures the location of the well bore every 100 feet, from the surface to total depth of the well (5497' Measured Depth "MD" in this case).***
    b. ***The directional survey taken in the DJS #2-14 was filed with the State of Idaho and can be seen at the following link:***

https://ogcc.idaho.gov/wp-content/uploads/sites/88/2017/12/1107520023_DJS2-14_DIR_20140917_PTS.pdf

    c. ***The directional survey is also available in the electronic files folder submitted with these responses, in folder 19.***
    d. ***The data acquired during the survey are presented in a table format. All depths are presented "RKB", or "Relative to Kelly Bushing". This is a bushing on the floor of the drilling rig, and is a solid reference point to measure from. "Measured Depth FT" is the wireline depth of the gyro tool lowered in the well below the Kelly Bushing, expressed in feet. "TVD FT" is the calculated True Vertical Depth (TVD) in feet of the tool below the Kelly Bushing. If the wellbore was perfectly vertical, MD and TVD values would be exactly the same. In this case, as the wellbore has very slight occasional deviation, the TVD of the well is approximately 2 feet shorter than MD (i.e. 5494.989' TVD at 5497.000' MD).***

20. ***In Exhibit M-4, a comment indicates that the surface casing was cemented to surface, and a top-job cementing operation was performed. To clarify Attachment M, please provide an explanation for why a top-job procedure was needed.***

a. *Per IDAPA 20.07.02.05 d. "All surface casing shall be cemented solid to the surface by pump and plug, displacement, or other approved method. When surface samples are cured, additional drilling activities may commence."*
Based on drilling reports, the top out/top job was performed to ensure that the 9 5/8" surface casing had adequate cement to surface as well cement coverage across the conductor shoe depth at 80'. During the cementing of the surface casing, there were some fluid losses, however, a total of 4 bbls of cement was observed in the returns during cementing indicating there was cement in all annular space between conductor and surface casing as well as the open hole and the surface casing. A redundant measure was taken in order to ensure proper cement placement per the rule above. The PVC piping that was run to 85' (drilling rpt) provided a way to convey (circulate) cement directly to the conductor shoe depth which would ensure that cement was, at minimum, covering the conductor shoe as well as circulated back to surface. An additional 4 bbls of cement was observed in the returns during the top out/top job.

21. In Exhibit Q-3, in Attachment Q, the plugging and abandonment cost estimate, prepared by HTI services, LLC, states that the cost to plug DJS 2-14 is projected to be $66,000 "based on what was required on the past abandonment work." To clarify Attachment Q, please demonstrate that the method for plugging this well meets the criteria to be used in the Plugging and abandonment of DJS 2-14 (and that, therefore, a comparison of cost estimates is appropriate).

a. ***The proposed WBS that was included in the Permit application was created prior to the recent plugging operations done in the Payette area. To supplement this attachment, a revised proposed WBS and EPA form 7520-14 has been included. The plugging method for the recently plugged wells was performed without a workover rig (rigless) and when applicable, the entire wellbore was filled with cement covering any and all potential fresh water source sands. This method proved to be the most economic and was preferred by the IDL during the P&A planning discussions. A revised quote from HTI Services LLC has been included, reflective of the rigless P&A procedure.***

22. To modify or clarify Attachment Q, please confirm that the upper proposed plug in the plugging and abandonment plan will isolate the turbidite sands in the Upper Glenn's Ferry Formation.

a. ***Per the revised P&A plan mentioned in question #21, the entire well bore will be filled with cement at plugging and abandonment, thus the turbidite sands in the Upper Glenn's Ferry Formation will be isolated.***